Zinc Acquisition Mechanisms Differ Between Environmental and Virulent *Francisella* Species

Gregory Brett Moreau
Alexandria, Louisiana

B. S. Louisiana State University, 2011

A Dissertation presented to the Graduate Faculty
of the University of Virginia in Candidacy for the Degree of
Doctor of Philosophy

Department of Microbiology, Immunology, and Cancer Biology

University of Virginia
May 2018

Abstract

Francisella tularensis is a Tier 1 Select Agent with a high potential for lethality and no approved vaccine. A better understanding of *Francisella* nutritional requirements and virulence factors is required for the development of therapeutics. Zinc is an essential nutrient for bacterial growth. Because host cells can restrict pathogen access to zinc as an antimicrobial defense mechanism, intracellular pathogens such as *Francisella* must sense their environment and acquire zinc in response. While acquisition of zinc has been shown to be required for virulence of numerous intracellular pathogens, zinc uptake has not been characterized in *Francisella*. RNA sequencing of both *Francisella novicida* U112 and the virulent *Francisella tularensis* ssp. *tularensis* Schu S4 strains grown under zinc limitation identified a limited number of genes predicted to contribute to zinc uptake and homeostasis. In many bacteria, the conserved transcription factor Zur is a key regulator of zinc acquisition. An *F. novicida zur* homolog was identified and a transposon mutant in this gene was used to identify mechanisms of zinc uptake by RNA sequencing. Only five genes were identified by RNA sequencing, of which three were confirmed by quantitative RT-PCR as regulated by Zur and zinc limitation. One of these genes, FTN_0879, is predicted to encode a protein with similarity to the *zupT* family of zinc transporters, which are not typically regulated by Zur. Although a putative *znuACB* operon encoding a high affinity zinc transporter was identified in U112 and Schu S4, expression of this operon was not controlled by Zur or zinc concentration. Disruption of *zupT* but not *znuA* in

U112 impaired growth under zinc limitation, suggesting that ZupT is the primary mechanism for zinc acquisition in these conditions.

Subsequent investigation in the virulent *F. tularensis* subsp. *tularensis* Schu S4 strain identified genetic differences that affect the importance of these genes in zinc uptake. In Schu S4, *zupT* is a pseudogene and attempts to delete *znuA* were unsuccessful, suggesting that it is essential in this strain. A reverse TetR repression system was utilized to knockdown expression of *znuA* in Schu S4, revealing that *znuA* is required for growth under zinc limitation and contributes to intracellular growth within macrophages. Despite growth defects in the *znuA* mutant strain, zinc-dependent immune responses were not induced during infection with wild-type Schu S4, and neither zinc sequestration nor supplementation decreased bacterial burden during infection. Overall, this work identifies genes necessary for adapting to zinc limitation and highlights nutritional differences between environmental and virulent *Francisella* strains.

Acknowledgements

I would never have been able to accomplish this dissertation without the guidance of my committee members, the help of my friends and lab mates, and the support of my family. First and foremost, I would not have been able to accomplish this work without the advice and support of my faculty mentor, Barbara Mann. Her advice and words of wisdom encouraged me to persevere through the trials of research. I have grown tremendously as both a scientist and a person due to her guidance, and I'm thankful that I've been able to learn from her over these last six years.

I would also like to thank my friends and lab mates who have provided advice and helped me grow into the scientist I am today. In particular, I would like to thank Matt Brown and Emily McMains, who gave me a shot at my first lab jobs and "valuable work experience" that really did open my eyes to the reality of a field I knew nothing about. Thanks to Melinda Clark for mentoring me on the ins and outs of basic bacteriology when I knew almost nothing and listening to my questions with the utmost patience. Thanks also to Aiping Qin, who served as an invaluable source of knowledge and was always able to figure things out when the problem was too much for me to handle. Thanks to Girija Ramakrishnan, Yan Zhang, and Natalie Perez for their friendship and commiseration, as well as my fellow grad students, especially Amber Woods, Krystal Haley, and Margaret Grant.

I would never be where I am today without my family. First, I'd like to thank my grandmother, who planted the seeds of a career in science by keeping the TV on PBS when I was a kid, exposing me to a world I never knew existed. I'd also like to thank my brother Gary and my sisters Karen and Susan, who have always shown an interest in my work. And of course, my parents, Garrison and Tammy Moreau, who have supported me through everything, even when neither of us really knew where this path would lead. Throughout all of the trials and tribulations of this process, they have always been there, willing to listen to my failures and triumphs as well as providing advice and never letting me give up. Thanks for always believing in me, even when I didn't believe in myself.

Finally, I have to give special thanks to Samantha Alleman. Graduate school is a trying time filled with long nights and many failed experiments. I feel very lucky that I've had her by my side through all the struggles to keep me grounded and focused on what's important. Over the years she has sacrificed so much of her time and effort to help me succeed and has had the utmost patience in dealing with the constant demands of lab. I truly couldn't have done it without you.

Table of Contents

Table of Figures

Chapter 1: *Francisella tularensis* is the Causative Agent of Tularemia

1.1: *Francisella tularensis* causes a severe disease with potential use as a biological weapon

Francisella tularensis is a Gram-negative bacterium and the causative agent of tularemia. Clinical manifestations of the disease depend on the route of entry, but tularemia is generally associated with abrupt onset of flu-like symptoms such as fever, chills, and general malaise approximately 3-5 days post-infection [1]. Disease can be acquired through a number of different mechanisms [1, 2] but ulceroglandular tularemia, which results in subcutaneous infection due to vectorborne transmission or direct contact with an infected animal, is the most common clinical presentation of the disease. The hallmark of ulceroglandular tularemia is the development of an ulcer at the site of infection, followed by enlargement of the draining lymph nodes after several days [3]. Other rarer presentations of tularemia can result from direct infection of the eye, which is associated with conjunctivitis and purulent secretion, or ingestion of contaminated food or water [3, 4]. Inhalation of infectious particles can result in pneumonic presentation of the disease, which is associated with fever, malaise, and chills accompanied by a dry cough or prominent pneumonitis [1, 2], ultimately leading to systematic disease. Despite the diverse routes of infection, human to human

transmission has not been reported, and standard precautions are recommended for infected individuals [2].

While most cases of tularemia are acquired through subcutaneous infection [1], the severity of the respiratory form of the disease makes *F. tularensis* a primary candidate for use as a bioweapon. *F. tularensis* ssp. *tularensis* has also been classified as a Tier 1 select agent by the United States Centers for Disease Control [5], signifying that it poses a severe health threat if deliberately misused. The bacteria has a low infectious dose, with as few as 10 colony forming units (CFUs) being capable of causing disease in humans [6]. They can also be easily aerosolized, and the resulting respiratory infection leads to an up to 30% mortality rate if untreated [7]. *F. tularensis* was previously developed as a biological warfare agent by the Japanese during World War II [8] as well as by the United States and Soviet Union during the Cold War [9], where it is rumored that the Soviet Union developed an antibiotic resistant strain [2]. A World Health Organization committee calculated that an aerosol dispersal of *F. tularensis* in a metropolitan area of 5 million inhabitants would result in 250,000 incapacitating casualties and 19,000 deaths [10]. Based on this analysis, the CDC calculated that an *F. tularensis* attack would have a cost of $5.4 billion for every 100,000 persons exposed [11]. Due to the potential of *F. tularensis* for use as a bioweapon, efforts to develop a vaccine are critical. Although a live attenuated vaccine strain (LVS) was engineered in the Soviet Union through repeated passages of an *F. tularensis* ssp. *holarctica* strain, it offers incomplete protection and the mechanism of attenuation is unknown [12]. Because of this, there is currently no approved vaccine for *F.*

tularensis [2]. Better understanding of critical bacterial virulence factors is necessary for the development of antimicrobial therapies and the identification of vaccine targets.

1.2: *Francisella* species and subspecies

Francisella belongs to the γ subclass of proteobacteria. Based on 16S sequencing data, *Francisella* is a deeply diverging lineage of γ-proteobacteria, with only limited similarity to human pathogens such as *Coxiella burnetii* and *Legionella pneumophilia* [13]. While *Francisella* is most closely related to the intracellular symbiont *Wolbachia persica*, reclassification of this species into the *Francisellaceae* family has recently been proposed [14]. *F. tularensis* can infect a wide variety of organisms, with cases of tularemia being reported in at least 250 species of mammals, birds, reptiles, and fish [15]. There are three *F. tularensis* subspecies that are distinguished by differences in geography and severity of human disease: *tularensis*, *holarctica*, and *mediasiatica*. In this dissertation, "*Francisella*" will be used to refer to features that are associated with all members of the genus, while more specific naming will be provided for features specific to a particular species or subspecies. *Francisella tularensis* ssp. *tularensis* is found exclusively in North America and causes the most severe form of the disease [16]. *F. tularensis* ssp. *tularensis* infection is most commonly associated with hares and rabbits, from which tularemia derives the colloquial name "rabbit fever" [1, 15, 16]. However, this subspecies also survives within ticks and biting flies, which serve as an arthropod vector for transmission [17]. Schu S4, a strain isolated from an infected

individual [18, 19], is the most commonly studied *F. tularensis* ssp. *tularensis* experimental strain and must be manipulated under Biosafety level 3 (BSL3) conditions. *Francisella tularensis* ssp. *holarctica* is spread throughout the northern hemisphere but is primarily found in northern Europe. This subspecies causes a milder form of the disease with slower dissemination [1]. It is more commonly associated with aquatic rodents, such as muskrats, beavers, as well as hares and other rodents [16]. The live vaccine strain (LVS) is an attenuated *F. tularensis* ssp. *holarctica* strain that is useful for experimental models because it can be manipulated under Biosafety level 2 (BSL2) conditions and, although attenuated in humans, is still capable of causing disease in mice [16]. *F. tularensis* ssp. *mediasiatica* is limited to the Central Asian republics of the former USSR, and human disease with this strain has not been documented in the literature [16, 20].

Francisella novicida is a closely related bacterial species that is used as a laboratory model for *F. tularensis* disease. While *F. novicida* does not cause disease in immunocompetent humans, cases have been observed in immunocompromised individuals [21]. The model *F. novicida* strain is U112, which was isolated from a salt water lake in Utah [22]. *F. novicida* is used as a surrogate for virulent *Francisella* species because it shares a high degree of genome sequence similarity with the virulent species and, although it causes a similar disease in mice, can be manipulated under BSL2 conditions [16]. A transposon mutagenesis library with single transposon disruptions of all non-essential genes has also been generated in U112 [23], allowing for identification of phenotypes of specific gene knockouts. A proposal to reclassify *F. novicida* as a *F. tularensis* subspecies has been published

[24], but this proposal met formal objection because it was based purely on sequence similarity without taking phenotypic differences into account [25]. There are a number of differences between *F. novicida* and the more virulent *F. tularensis* subspecies that lead to concerns that *F. novicida* may not be a useful model for investigating all aspects of *F. tularensis* virulence [20, 26, 27]. Unlike *F. tularensis*, which replicate in nature through a cycle of arthropod vectors and amplifying hosts, *F. novicida* has only been isolated from salt water environments [20, 28]. The absence of evidence of animal infection in the wild suggests that *F. novicida* is not a zoonotic bacterium. This is reflected in the genome: although *F. tularensis* and *F. novicida* are ~98% identical, virulent strains have nearly 20% fewer protein encoding genes [29]. Over 10% of protein coding sequences in *F. tularensis* subspecies are disrupted by insertional elements, with many of these genes encoding proteins involved in transport, DNA metabolism, or amino acid biosynthesis [29, 30]. Phylogeny of *Francisella* species has determined that *F. novicida* is evolutionarily the oldest [31], suggesting that genomic reduction in *F. tularensis* subspecies may represent an adaptations to the host niche after *F. tularensis* and *F. novicida* diverged. Differences in the immune response as well as in nutritional requirements, which will be discussed below, also argue that results obtained in studies with *F. novicida* may not be applicable to *F. tularensis* subspecies.

1.3: Course of Infection with *Francisella tularensis*

F. tularensis disease progression has been heavily studied in the mouse model. After aerosol infection of mice with *F. tularensis* ssp. *tularensis,* bacteria reside within the lungs before dissemination to the liver and spleen on day 2 [32, 33]. A hallmark of this early stage of infection is a delayed host response to the bacteria. In a murine respiratory model of infection, nearly 25% of cells infected by *F. novicida* U112 one day post-infection were neutrophils, while neutrophils were not detected on day 1 with the virulent *F. tularensis* ssp. *tularensis* Schu S4 strain [26], indicating that infection with virulent strains is not initially detected by the host. By four days post-infection, burdens up to 10^{7}-10^{8} in the lungs, liver, and spleen as well as pronounced bacteremia were observed in *F. tularensis*-infected mice [33]. Although proinflammatory cytokines such as TNF-α and IFN-γ are markedly increased at this point in the infection [32, 34], the immune response is either too late to contain bacterial growth or inflammation is so pronounced that it contributes to death at day 5-6 [32, 35]. Although *F. tularensis* is not detected during the early stages of infection, the immune response is still important for bacterial clearance, as mouse knockout strains in TLR2-/- or MyD88 -/-, or neutropenic mice have decreased survival when challenged with *F. tularensis* [36, 37].

F. tularensis is primarily an intracellular infection. While there is evidence for an extracellular phase of infection [38], the intracellular phase is thought to be

dominant, as mutants that are unable to survive and replicate intracellularly are attenuated for virulence [39-41]. *Francisella* can replicate within a variety of cell types, including phagocytic cells such as macrophages, neutrophils, and dendritic cells [42, 43], as well as non-professional phagocytes such as murine [44] and human lung epithelial cell lines [45, 46], hepatocyte cell lines [40, 47], and fibroblasts [33]. Survival within non-professional phagocytes may be sufficient for virulence, as a mutant in *F. tularensis* that was unable to replicate within macrophages maintained the ability to replicate within epithelial cells *in vitro* and cause virulence in a mouse respiratory model [33]. Uptake into non-professional phagocytes is thought to be mediated non-specifically through micropinocytosis. In contrast, uptake into professional phagocytes is mediated through a variety of receptors, including the Fc receptor, the Complement receptor 3 (CR3), the Class A Scavenger receptor, and the Mannose receptor [48, 49]. Entry through these routes results in differences between bacterial survival once intracellular as well as in cytokine responses to the pathogen [50].

As macrophages are the primary cell type infected by *Francisella*, the intracellular life cycle within macrophages has been well characterized. After uptake into the host cell, bacteria are enclosed in a phagosome that acquires markers of early (EEA1) and late (LAMP1-2) endosome maturation [51, 52] but does not acquire lysosomal hydrolases [53], suggesting that lysosomal fusion does not occur. Phagosomal escape occurs within 30-120 minutes after internalization, depending on the route of entry [54]. While *F. tularensis* has been shown to prevent acidification of the phagosome [53], some level of phagosomal acidification seems

to be important for optimal phagosomal escape, as this process was delayed in host cells treated with acidification inhibitors [52, 55]. After phagosomal disruption, bacteria escape into the host cell cytosol, where rapid replication begins between six and eight hours post-infection [52]. Between 16 and 24 hours post-infection, a majority of bacteria are also enclosed within a LAMP1-positive *Francisella*-containing vacuole (FCV) [51], suggesting that autophagy may be induced during infection. This process may depend on the host and cell type, as it was observed within murine bone marrow-derived macrophages but not human monocyte derived macrophages [56]. Although FCVs fuse with lysosomes, bacterial degradation was not observed [51], indicating that this process may not be detrimental to the bacteria. After 24-36 hours of growth, host cells undergo programmed cell death, releasing the bacteria to infect other cells. Cell to cell transfer of *Francisella* by a trogocytosis-like mechanism has also been observed [57], suggesting additional mechanisms of *Francisella* dissemination during infection.

1.4: The Cellular Immune Response to *Francisella* infection

The ability of the host to detect and initiate an immune response against invading pathogens is critical for pathogen clearance. Detection of bacterial pathogens by the innate immune system is accomplished by specific pattern recognition receptors (PRRs) that recognize conserved bacterial ligands, known as pathogen associated molecular patterns (PAMPs). The most well characterized PRRs are the Toll-like receptor (TLR) family, membrane receptors with lumenal

domains that recognize conserved pathogen ligands and cytoplasmic protein-protein interaction domains that initiate downstream signaling cascades [58]. Signaling through these receptors converges on the signaling molecule MyD88, ultimately leading to activation of the transcription factors NF-κB and AP-1 and transcription of proinflammatory cytokines [59]. TLR2 and TLR4 are major PRRs that detect bacterial pathogens, primarily detecting bacterial lipoproteins and lipopolysaccharide (LPS), respectively [58]. While TLR2 and TLR4 can detect both extracellular and vacuolar bacterial ligands, detection of cytosolic pathogens relies on Nod-like receptors (NLRs), cytoplasmic sensor proteins that are capable of recognizing bacterial products or danger signals initiated by infection [60, 61]. Activation of these cytosolic sensors initiates assembly of an immune complex called the inflammasome [60], ultimately leading to the cleavage and activation of the host protease Caspase 1 as well as activation and release of the proinflammatory cytokines IL-1β and IL-18. Release of these cytokines requires convergence of TLR and inflammasome signaling: An initial signal via TLR activation is required for transcription and production of pro-IL-1β and pro-IL-18, but inflammasome activation and active Caspase 1 are required to process these cytokines into their active forms [62]. Cleavage of Caspase 1 is also associated with pyroptosis, a form of proinflammatory programmed cell death allowing for further propagation of the immune response [63, 64].

The ability of *F. tularensis* to cause infection without immune detection is a major determinant of its virulence and differentiates these virulent subspecies

from environmental *F. novicida* isolates. The immune response to *Francisella* infection is primarily mediated by TLR2, as decreased survival to infection is observed in MyD88-/- and TRL2-/- but not TLR4-/- mice [65, 66]. The absence of a TLR4-mediated immune response to *Francisella* is due to modification of LPS. The lipid A moiety of *Francisella* LPS has fewer acyl chains and lacks the phosphate groups found in *Escherichia coli* LPS, resulting in an LPS molecule that is undetected by TLR4 [67, 68]. Mutant strains that are unable to modify LPS are attenuated for virulence [68-70]. Despite similar structures, LPS derived from *F. novicida* U112 stimulates a stronger immune response than that from *F. tularensis* LVS [71], echoing a pattern of higher immune stimulation observed in environmental *F. novicida* strains compared to more host-adapted *F. tularensis* strains.

While both *F. tularensis* and *F. novicida* avoid TLR4 stimulation, *F. novicida* infection is associated with increased production of proinflammatory cytokines [27, 72, 73] and earlier recruitment of neutrophils to the site of infection [26]. Greater activation of TLR2 and inflammasome dependent signaling pathways is partially responsible for increased immune detection in *F. novicida*-infected animals, as *F. tularensis* is capable of reducing TLR2 detection through a number of different mechanisms. Serum-opsonized *F. tularensis* ssp. *tularensis* Schu S4 is capable of suppressing TLR2 activation in a CR3-dependent manner, whereas *F. novicida* U112 is incapable of this suppression [50]. Additionally, *F. novicida* stimulates expression of the microRNA miR-155, which downregulates expression of the PI3K-Akt negative regulator SHIP, ultimately resulting in increased

proinflammatory cytokine expression [27]. Upregulated miR-155 is not observed during Schu S4 infection.

A stronger immune response in *F. novicida* is also associated with greater activation of the inflammasome compared to *F. tularensis*. Inflammasome activation is critical for clearance of *F. novicida*, as mice deficient in the inflammasome component AIM2 are unable to control *F. novicida* U112 bacterial replication and are more susceptible to infection than wild-type mice [74]. Cytosolic bacteria are required for inflammasome activation and host cell death, as mutants that are unable to escape the phagosome fail to stimulate the inflammasome [75, 76]. *F. novicida* is detected upon bacterial escape from the phagosome and emergence into the cytosol [77, 78] and this results in high levels of IL-1β and IL-18 [79] as well as Caspase 1 dependent proinflammatory cell death [77, 80]. In contrast, *F. tularensis* strains LVS and Schu S4 elicit lower levels of active IL-1β and IL-18 compared to U112 [79]. Inflammasome priming is similar between *Francisella* species [76], suggesting that the impaired cytokine production observed in *F. tularensis* subspecies is due to impaired inflammasome triggering after phagosomal escape. Infection with virulent *F. tularensis* subspecies also results in Caspase 3 dependent, Caspase 1 independent cell death [81, 82], which is not associated with proinflammatory cytokine production. These data suggest that virulent *F. tularensis* strains stimulate a different, less inflammatory infection that minimizes immune detection.

1.5: Intracellular growth relies on scavenging host-derived nutrients.

As the ability to replicate intracellularly is critical for *Francisella* virulence, factors required for phagosomal escape have been identified. One of most important virulence determinants for *Francisella* is a 34kb region of the genome known as the *Francisella* Pathogenicity Island (FPI). The FPI encodes a Type VI-like secretion system (T6SS) that is essential for intracellular growth and virulence, as single mutations in T6SS components are unable to escape the phagosome and attenuated in virulence [39, 41, 83]. The exact mechanism by which the T6SS facilitates escape from the phagosome is unknown, but data implicate T6SS effectors in phagosome rupture. Proper folding of the T6SS is also critical for virulence, as mutants in genes required for T6SS folding show similar growth defects to T6SS mutants [84, 85]. T6SS genes may not be necessary for intracellular replication once the bacteria have escaped from the phagosome, as mutants in genes encoding T6SS components grow similarly to wildtype when microinjected into the cytosol of host macrophages [86]. While the FPI is highly conserved between *F. tularensis* and *F. novicida*, *F. tularensis* strains have a duplicated copy of the FPI [87]. Gene duplication of the Shiga toxin genes in *Shigella dysenteriae* led to increased gene expression [88], suggesting that FPI duplication may represent a mechanism of increased T6SS expression necessary for adaptation of *F. tularensis* strains to the intracellular environment.

Once *Francisella* has escaped from the phagosome into the host cell cytosol, the bacteria must be able to scavenge nutrients from the host to serve as carbon

and energy sources. Of particular importance is acquisition of host-derived amino acids, as a number of amino acid biosynthesis pathways are absent in *Francisella*. This is particularly critical in the more virulent *F. tularensis* subspecies, where over 40% of genes involved in amino acid biosynthesis are disrupted compared to *F. novicida* [29]. In lieu of amino acid biosynthesis, *F. tularensis* strains utilize amino acid transporters to acquire these nutrients from the host. Genes involved in amino acid transport are highly upregulated during growth of *F. tularensis* Schu S4 within macrophages [89], and genetic deletion of annotated amino acid transporters in *F. tularensis* spp. *holarctica* LVS results in impaired intracellular growth within macrophages and attenuated virulence in the mouse model [90, 91]. *F. tularensis* can also hijack host mechanisms such as autophagy to enhance bacterial amino acid uptake. Inhibition of autophagy results in decreased bacterial growth after 24 hours, and this growth defect was rescued with the supplementation of amino acids [92]. In addition to their necessity in the absence of biosynthesis pathways, amino acids may also serve as an energy source for *F. tularensis*. Gluconeogenesis, the generation of glucose from non-sugar compounds such as amino acids, is critical for *Francisella* growth, as mutation of genes in the gluconeogenesis pathway results in impaired growth intracellularly and attenuation during murine infection [93]. Supplementation of autophagy-inhibited macrophages with serine or pyruvate, which cannot be converted into all 13 amino acids required for *F. tularensis* growth, was sufficient to rescue bacterial growth to levels observed with total amino acids [92], suggesting that amino acids acquired from autophagy are primarily utilized as an energy source. Transcriptional data identifying genes

required for amino acid catabolism are highly upregulated during intracellular growth also implicates amino acids as gluconeogenesis substrates [89].

Trace metals such as iron represent another nutritional requirement for *Francisella* intracellular growth. Genes required for iron acquisition are highly upregulated during intracellular growth [89, 94], highlighting the importance of this metal to bacterial replication. *Francisella* utilizes two distinct iron acquisition systems: a siderophore for ferric (Fe(III)) iron uptake as well as a ferrous (Fe(II)) iron transport system [95]. The *fslABCDE* operon encodes genes required for assembly, release, and reuptake of siderophore [96], a small molecule with a high metal affinity that can scavenge iron from the environment. Expression of this operon is regulated by the ferric uptake regulator (Fur) [97, 98], a transcriptional repressor that blocks expression of genes under high iron conditions. A mutant in *feoB*, which encodes an inner membrane ferrous iron transporter, was still capable of producing a siderophore but was unable to grow on ferrous iron [99]. Individual mutants in genes of the *fslA* operon or in *feoB* are not attenuated intracellularly compared to wild-type, but double mutants in both iron acquisition systems are unable to grow intracellularly and attenuated in virulence [95, 99]. Although the role of iron acquisition in *Francisella* virulence has been thoroughly investigated, the contribution of other trace metals has not been well characterized. Although two potential magnesium transporters were upregulated in Schu S4 grown in magnesium limiting-media, single deletion mutants grew similarly to wild-type under magnesium limitation [100].

The importance of zinc for *Francisella* growth and virulence is not well understood. Most of the current understanding of the role of zinc during *Francisella* infection pertains to effects on the host. Serum zinc levels are significantly decreased in *F. tularensis* Schu S4-infected rabbits over the course of infection [101], which likely represents an acute phase response to infection [102]. Induction of host zinc-sequestering genes such as metallothioneins was detected at 16-24 hours post-infection in LVS-infected peripheral blood monocytes [103], indicating that a zinc-dependent immune response may be mounted during *Francisella* infection. Zinc also contributes to an effective immune response against *Francisella*, as rats that were fed a zinc-deficient diet were more susceptible to *F. tularensis* LVS challenge after immunization than pair fed controls [104]. It is unclear whether this impaired immune response under zinc deficiency is due to effects of zinc limitation on the immune response or inhibition of bacterial growth due to nutrient depletion. While not much has been reported about the nutritional requirements for zinc in *Francisella*, analysis of *F. tularensis* genes predicted to associate with zinc based on GO categories and InterPro motifs predict that zinc is associated with a number of enzymes implicated in fundamental biological processes, such as DNA replication, translation, and amino acid metabolism (Fig. 1). Some identified genes encode potential virulence factors, such as the copper-zinc-dependent superoxide dismutase SodC. A *ΔsodC* mutant strain in LVS was inhibited in intracellular growth and attenuated in a mouse model [105]. Based on the importance of zinc-dependent proteins for bacterial survival and virulence, a better understanding of zinc acquisition mechanisms and regulation has the potential to identify targets for antimicrobials or potential vaccine candidates.

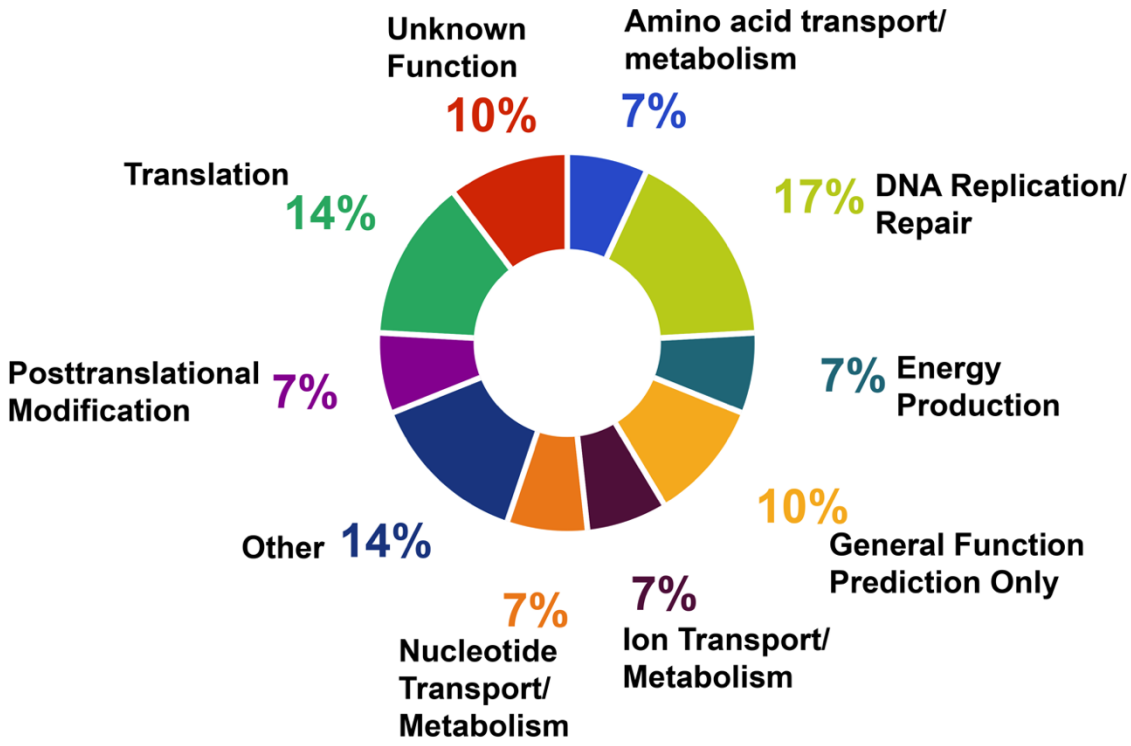
Unknown Function
10%
Amino acid transport/ metabolism
7%
Translation
14%
17%
DNA Replication/ Repair
Posttranslational Modification
7%
7%
Energy Production
10%
General Function Prediction Only
Other
14%
7%
Nucleotide Transport/ Metabolism
7%
Ion Transport/ Metabolism

Figure 1: Predicted *Francisella* zinc-binding proteins participate in a variety of cellular processes. The PEDANT gene database was utilized to investigate the *F. tularensis* ssp. *tularensis* Schu S4 genome for genes involved in zinc binding or transport. Genes with Gene Ontology (GO) categories predicting function involving zinc or InterPro motifs predicting zinc binding were selected. Predicted functions of selected genes were organized according to Cluster of Orthologous Groups (COG) Category.

Chapter 2: Zinc is an Essential Nutrient for Prokaryotes and Eukaryotes

2.1: Zinc is required for essential biological functions

Zinc is an essential nutrient for both prokaryotes and eukaryotes. The role of zinc in proteins can be categorized into three major functions: structural, catalytic, and regulatory. Zinc that acts as a structural component of enzymes is required for coordination of amino acid residues in an enzyme but does not directly interact with the substrate during the reaction [106]. In contrast, zinc acting in a catalytic function directly participates in the reaction performed by the enzyme, interacting with glutamate, aspartate, or histidine residues on the substrate [107]. Zinc can also act on proteins in a regulatory role, such as transcription factors where direct binding to zinc changes their ability to enhance or repress gene expression [108, 109].

Around 4-8% of all bacterial proteins require zinc, usually as a cofactor for enzymes that are required for a variety of fundamental cellular processes [110]. This includes proteins that are required for DNA replication, transcription, and translation, such as the DNA primase [111] and multiple ribosomal proteins [112]. Metabolism and ATP generation are also dependent on zinc, as several dehydrogenases and peptidases necessary for breakdown of substrates are metalloproteins [112, 113]. In addition, zinc-binding enzymes contribute to regulatory functions in bacteria, with binding of zinc to transcription factors such

as Fur and Zur being critical for their functions [114, 115]. Beyond basic biological processes, a number of virulence factors also require zinc for their function, including β-lactamases that degrade antibiotics such as penicillin [116], zinc-containing superoxide dismutases that mitigate damage from oxide radicals [117], and metalloproteinases that facilitate invasion into host tissue [118]. The variety of different functions performed by bacterial zinc-binding proteins is supported by investigation in *F. tularensis*, where these proteins fit into over 10 distinct COG categories, including DNA repair, amino acid metabolism, energy production, and translation (Fig. 1).

In eukaryotes, transcription factors make up a much larger proportion of zinc-dependent proteins, consisting of nearly 50% of all proteins that bind zinc [119]. The human zinc proteome is estimated to include around 3000 proteins [120], including proteins with zinc-finger domains that make up around 3% of genes in the human genome [121]. In addition to being necessary for proper function of individual proteins, zinc plays a key role in cellular signaling. Zinc can facilitate cell-to-cell communications as a neurotransmitter, where it is released at synapses to signal between neurons [122]. It can also act as an intracellular signaling molecule in response to extracellular stimuli [123]. Intracellular zinc signaling can be divided into two schemes. An early, rapid zinc signaling cascade called the "zinc wave" can be produced through the release of zinc from the endoplasmic reticulum [124]. A less rapid zinc signaling cascade can also occur, but this cascade is dependent on transcriptional changes in expression of cellular

zinc transporters to facilitate changes in cytosolic zinc [123, 125]. Once intracellular free zinc levels have increased by either mechanism, zinc can interact with downstream transcription factors such as NF-κB to facilitate changes in gene expression, potentially by altering transcription factor binding affinity for DNA [126].

Although zinc is a necessary nutrient, excess zinc can have detrimental effects on survival. Zinc is a highly competitive metal that outcompetes other metals for binding to transport proteins and enzymes. In bacteria, this competition for metal binding can result in deficiency of other trace metals, impairing growth and making bacteria more susceptible to host immune mechanisms [127]. In eukaryotes, elevated zinc levels can induce programmed cell death associated with the loss of mitochondrial membrane potential and DNA fragmentation [128]. To minimize the potential for zinc toxicity, free zinc ions are kept at minimal levels within the host. Zinc is primarily distributed in the muscles, bones, and liver, with only 0.1% of zinc circulating in plasma [129]. Of the zinc circulating in the blood, around 70% is inaccessible, bound to proteins such as serum albumin [130]. On an intracellular level, both prokaryotes and eukaryotes tightly control the levels of free zinc, with concentrations of free zinc in the picomolar range despite total cellular zinc concentrations being in the micromolar range [131, 132].

2.2: Eukaryotic zinc homeostasis is controlled by zinc transport and chaperone proteins

Eukaryotic cells employ a number of strategies to control intracellular free zinc levels. The availability of free zinc within the cytosol is controlled by metallothioneins (MTs), small proteins that scavenge and sequester metals [133]. Two major MT isoforms (MT-1 and MT-2) are expressed in most mammalian cell types in response to zinc limitation [134]. While metallothioneins bind to up to seven zinc molecules per protein, the affinities of different zinc binding sites differ by four orders of magnitude, with four binding sites exhibiting strong zinc affinity, two exhibiting intermediate affinity, and one exhibiting low affinity [135]. Differences in binding affinity allow MT to act as a buffer, providing labile zinc for use by proteins that require it for their function [136]. Data also suggests that MTs are capable of direct transfer of zinc to zinc-dependent proteins [137].

Complementary to MT regulation of free cytosolic zinc, import and export proteins regulate the total amount of zinc within the cell as well as its distribution within different intracellular compartments. Eukaryotic zinc transporters come from two major families, the SLC39A (ZIP) family which facilitates zinc transport into the host cell cytosol from either the extracellular environment or intracellular compartments and the SLC30A (ZnT) family which facilitates transport in the opposite direction. There are a large number of isoforms for each family in mammals (14 ZIP isoforms and 10 ZnT isoforms) which vary in expression, cell tropism, and intracellular localization [138]. Localization of transporters to

organelle membranes allows not only movement of zinc in and out of the cell but also distribution of zinc into intracellular compartments, which can act as a storage mechanism for zinc without altering cytosolic zinc levels. Both ZIP and ZnT family proteins typically contain 6-8 transmembrane domains, as well as a conserved histidine-rich loop that is involved in zinc binding [139]. Both ZIP and ZnT proteins require dimerization for efficient zinc transport [140, 141], but the mechanism of action for these transporters has not been fully characterized. Transport in ZIP and ZnT homologs is dependent on the proton gradient [142], and neither protein family appears to have an ATP hydrolysis domain, suggesting that levels of zinc import and export relies less on the affinity of these transporters for zinc and more on the level of transporter expression.

These genes must be responsive to changes in intracellular zinc concentration to maintain homeostasis. Gene expression is controlled by MTF-1, a transcription factor which, when bound to zinc, translocates to the nucleus and binds to metal response elements (MREs) upstream of regulated genes to affect their transcription [143]. MTF-1 has a relatively low binding affinity for zinc, ensuring that binding only occurs in the presence of excess zinc [144]. Binding of MTF-1 typically increases expression of MTs and ZnT family transporters [145], allowing for either export or sequestration of zinc under conditions of excess zinc. However, MTF-1 can also repress expression of genes required for zinc import, as binding of MTF-1 to MREs downstream of the ZIP10 gene strongly reduced gene expression [146, 147]. While MTF-1 provides a mechanism for transcriptional control of these genes in response to changes in intracellular zinc homeostasis,

they can also be regulated post-translationally. For example, ZIP1 and ZIP3 are endocytosed from the plasma membrane at a higher rate in the presence of excess zinc, preventing intracellular zinc levels from getting too high [148]. Overall, these mechanisms ensure that eukaryotic cells are able to not only acquire sufficient zinc for proper function, but also able maintain zinc homeostasis under changing conditions.

2.3: Zinc is required for proper immune development and responses

Due to the wide range of functions performed by zinc-requiring proteins, zinc deficiency has a debilitating effect on growth and development. In humans, deficiencies in zinc has been shown to be a major risk factor for malnutrition, which is responsible for over one third of all childhood deaths in emerging nations [149]. It is estimated that more than 25% of people are zinc deficient, and zinc deficiency ranks fifth among most important health risk factors in developing countries and 11th worldwide [150]. Zinc deficiency is also associated with increased risk of infections [151, 152], implicating zinc as vital for a competent immune response.

Zinc is required for a number of basic functions utilized by innate immune cells to mediate pathogen clearance. Innate cells mount the immediate host response against infection, migrating to the site of infection where they minimize pathogen burden through phagocytosis of pathogens, destruction of pathogens through the release of antimicrobial mediators, and production of

proinflammatory cytokines in response to PAMP detection [153]. Zinc plays a fundamental role in all of these functions. For example, zinc deficient neutrophils display impaired chemotaxis [154], preventing them from reaching the site of infection. Impaired chemotaxis may be due to zinc acting as a chemoattractant, as neutrophils will migrate towards a gradient of excess zinc [155]. Zinc limitation also impairs neutrophil and macrophage effector functions including phagocytosis [156] and reactive oxygen species (ROS) production [157]. This phenotype appears to be cell specific, as monocytes cultured under zinc limitation were more active in phagocytosis and ROS production but were impaired in their ability to produce proinflammatory cytokines [158]. Zinc is also critical for the induction of "NETosis", a specialized form of cell death in which neutrophils release neutrophil extracellular traps (NETs), a matrix of DNA, chromatin, and nuclear proteins that can entrap and kill bacteria [159]. NETosis can be induced by 12-myristate 13-acetate (PMA), which is associated with an influx in intracellular zinc, and inhibited by sequestration of zinc using a cell permeable chelator [160]. Overall, insufficient zinc levels impair the ability of innate immune cells to mediate effector functions necessary for the clearance of pathogens.

Development and differentiation of immune cells is also mediated by zinc-dependent intracellular signaling. Stimulation of TLR4 on dendritic cells (DC) results in host-mediated sequestration of intracellular zinc, which is critical for DC maturation [123]. Addition of the zinc chelator TPEN is able to mimic TLR4 stimulation and initiate DC maturation, while zinc supplementation can block maturation. Zinc signaling is required for TLR4 activation in macrophages as well,

as chelation of zinc after stimulation with LPS results in dampened expression of proinflammatory cytokines [161]. Zinc is also critical for proper development and activation of adaptive immune cells. The effects of zinc deficiency on T cell development are particularly dramatic, as insufficient zinc results in significant thymus atrophy accompanied by a 60% increase in apoptosis of pre-T-cells [162]. Zinc signaling contributes to T cell activation, with knockdown cells in the ZIP8 zinc importer displaying reduced secretion of the activation markers IFN-γ and perforin [125]. Skewing of T cells towards a Th1 response is also impaired during zinc deficiency, as production of Th1 cytokines, such as IFN-γ and IL-2 is decreased, while production of Th2 cytokines such as IL-4 and IL-10 is unaffected [163]. Supplementation of zinc in zinc deficient mice can restore Th1 cytokine production to normal levels [164]. Th1 skewing is critical for clearance of a number of bacterial and fungal pathogens [165, 166], making this deficiency particularly damaging for the immune response to infections.

2.4: Host mechanisms of zinc sequestration in response to infection

Although zinc is of critical importance in eukaryotes for proper cellular function and immune responses, maintaining necessary levels of zinc is complicated during infection. Pathogens also require zinc for many essential functions, and free zinc in the host can be scavenged by bacteria to enhance their growth and virulence (mechanisms used by bacteria to scavenge host zinc will be discussed below). In order to combat these pathogens, the host can sequester necessary nutrients as a means of preventing pathogen growth. This process,

termed nutritional immunity, is best characterized with respect to host sequestration of iron, but its role in the limitation of other trace metals such as zinc and manganese has recently become more appreciated [167]. Even during homeostatic conditions, circulating zinc only represents 0.1% of total body zinc to prevent zinc toxicity and limit access from extracellular pathogens. Inflammatory signals during infection lead to further reduction of circulating zinc. Release of IL-6 leads to upregulation of the zinc importer ZIP14 on hepatocytes [102], resulting in transport of zinc from blood into the liver and significantly reducing the amount of circulating zinc. On a more local level, innate immune cells can produce and secrete S100 family proteins that bind and scavenge metals [168]. These proteins have two binding sites for zinc at high affinity [169, 170], allowing for zinc sequestration that limits pathogen growth. For example, the protein S100A7 is produced in response to proinflammatory cytokines in the skin and is capable of killing *E. coli* due to zinc sequestration [171]. The most well characterized members of the S100 family are S100A8 and S100A9, which form a heterodimer commonly known as calprotectin [172]. Calprotectin is a major component of the innate antimicrobial repertoire, making up nearly 50% on neutrophil protein during infection [167]. Calprotectin has been shown to significantly reduce the bacterial burden of *Staphylococcus aureus* within tissue abscesses, with *in vitro* calprotectin killing activity against *S. aureus* significantly reduced with the supplementation of either zinc or manganese [173]. In addition to its antimicrobial activity, calprotectin can also interact with host cell surface receptors such as TLR4 to promote proinflammatory signaling [174, 175], providing amplification of the proinflammatory immune response.

While calprotectin is effective at sequestering extracellular zinc, intracellular zinc levels are primarily controlled by other mechanisms. In addition, sequestration of zinc by calprotectin is greatly enhanced in the presence of calcium, which is highly abundant in the extracellular environment but not intracellularly [172]. This means that control of intracellular pathogens is mediated by calprotectin-independent mechanisms. Nutritional immunity within host cells is mediated by the same mechanism as intracellular homeostasis: expression of zinc transporters and MT proteins. While ZIP, ZnT, and MT expression is primarily controlled by MTF-1 in response to changes in zinc concentration, expression can also be influenced by proinflammatory cytokines such as IL-6 or GM-CSF [102, 176]. In response to these signals, expression of ZIP2 and ZIP14 is upregulated, leading to influx of zinc from the extracellular environment into the cell [176]. Upregulation of ZIP2 or ZIP14 may also mediate export of zinc from the phagosome, as phagosomal zinc was decreased after infection in GM-CSF-treated macrophages. Although this assists in removing free zinc from the extracellular environment for defense against extracellular pathogens, it also increases the overall zinc concentration of the host cell. Mechanisms to either sequester free cytosolic zinc or shift it to other intracellular compartments are simultaneously upregulated to limit zinc availability. In addition to upregulating ZIP2 expression, GM-CSF also upregulates MT expression to bind excess cytosolic zinc and induces expression of zinc exporters ZnT4 and ZnT7, which localize to the Golgi membrane and facilitate compartmentalization of cytosolic zinc within the Golgi

[176]. Together, these mechanisms result in limitation of available cytosolic zinc despite import of zinc into the cell.

Intoxication of pathogens with excess zinc has emerged as an alternative host immune strategy [177]. During macrophage infection with *Mycobacterium tuberculosis* or nonpathogenic *E. coli*, the phagosomal compartment containing the bacteria becomes flooded with excess zinc. Zinc intoxication of the phagosome is mediated by intracellular stores of zinc rather than import of zinc from the extracellular environment, as an inhibitor of NADPH oxidase, which facilitates release of zinc from MTs, eliminated phagosome intoxication. [178]. Zinc intoxication as an immune strategy is also implicated in infection with *Streptococcus pneumoniae*, as accumulation of zinc is observed within the tissue and serum of infected mice [127]. Mutant strains in metal exporters were significantly more sensitive to macrophage mediated killing. It is unclear what signals determine whether the host initiates zinc sequestration or zinc toxicity in response to pathogen challenge, but it is likely that differences in bacterial PAMPs or the cytokine milieu influence this response [179].

2.5: Zinc homeostasis in bacteria is primarily mediated by zinc import and export.

Bacteria must also be able to maintain zinc homeostasis in response to varying environments as well as nutrient limitations from the host. While zinc sequestering chaperones such as MTs play a significant role in maintaining

eukaryotic zinc homeostasis, similar proteins have not been well characterized in bacteria. A family of COG0523 containing proteins has been proposed to act both as zinc chaperones in bacteria as well as insertases, allowing the transfer of zinc to zinc-dependent proteins [180]. A COG0523 containing protein in *Acinetobacter baumanii* binds to zinc and is required for maintenance of a histidine-bound zinc pool [181]. The role of potential zinc chaperones in bacteria is currently under investigated, but not much is known about the widespread necessity of these proteins for zinc homeostasis.

The most well characterized mechanisms for maintenance of bacterial zinc homeostasis are zinc import and export proteins. In Gram-negative bacteria, zinc must move across both an inner and outer membrane to be accessible, with transport across the outer membrane primarily mediated by non-selective porins [182]. Zinc export is facilitated primarily by three families of transporters: P-type ATPases, Cation diffusion facilitator (CDF) proteins, and RND family efflux pumps. P-type ATPases use ATP hydrolysis to power export of metals from the cytosol across the inner membrane [183]. These transporters are highly specific based on the coordinating residues at their substrate binding site [184]. CDF and RND family exporters have broader substrate specificity and transport is energy-independent, relying on the proton motive force [185]. While CDF proteins transport zinc across the inner membrane, RND efflux pumps span both the inner and outer membrane to facilitate zinc export out of the cell. Although not as well characterized as zinc sequestration, intoxication of bacteria with zinc is another host defense mechanism, and bacterial zinc exporters play a critical role in evasion

of this defense mechanism. Zinc intoxication is observed during *M. tuberculosis* infection, and a mutant strain in a P-type ATPase is attenuated in growth under excess zinc conditions as well as within macrophages compared to wild-type [178].

Two major zinc uptake systems are involved in facilitating transport of zinc across the inner membrane. Typically, zinc is imported at a low level into the cell by the constitutively expressed transporter ZupT. ZupT is a member of the ZIP family of zinc transporters and share the 6-8 transmembrane domains and histidine-rich loop observed in eukaryotic ZIP transporters [186]. Although ZupT has a higher binding affinity for zinc than other metals, it has a broad affinity for metals and is capable of transporting iron, cobalt, and manganese [187]. In *Salmonella enterica* serovar Typhimurium, ZupT transport is dependent on the proton motive force [188]. Analysis of *E. coli* ZupT determined that mutation of conserved serine, histidine, and glutamate residues eliminated zinc transport (Fig. 2) [189], but the exact mechanism of these residues in transport was not determined. Although ZupT contributes to zinc uptake under homeostatic conditions, a role for ZupT under zinc limitation or in pathogenesis has not been described. ZupT activity is likely masked in zinc limitation by activity of high affinity transporters such as ZnuABC. For example, deletion of *zupT* alone does not cause any growth defect under zinc limitation In *E. coli* or *Salmonella* Typhimurium; however, disruption of both *zupT* and the high affinity *znuABC* zinc transport system genes result in a more severe defect in growth than a *znuABC* deletion alone [190, 191].

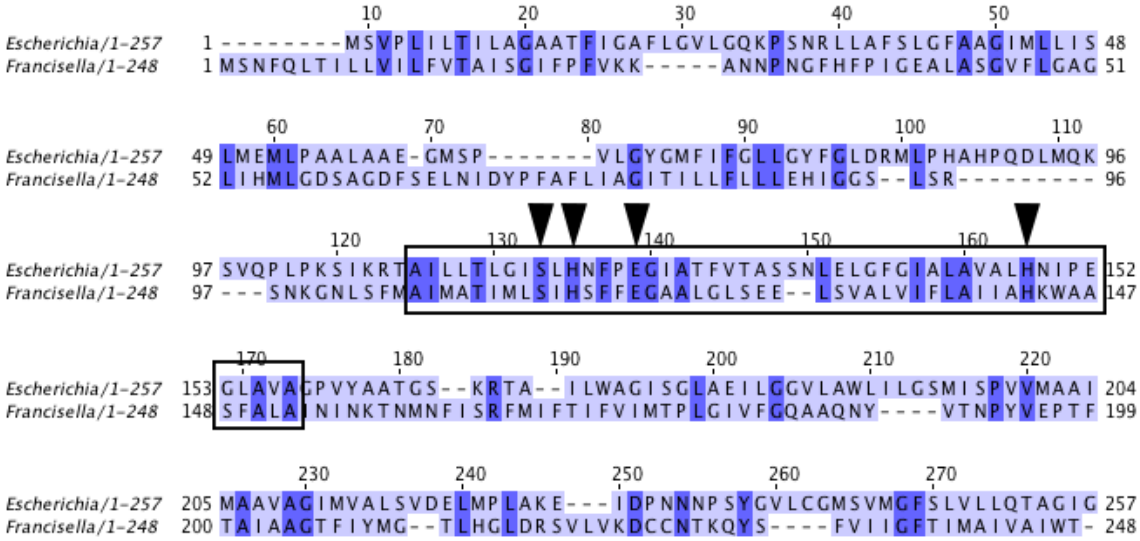
Escherichia/1-257
Francisella/1-248

Figure 2: Bacterial ZupT contains conserved amino acid residues that are required for zinc binding. Alignment of *Escherichia coli* and *Francisella novicida* ZupT protein sequences using Clustal Omega. The boxed region represents a ~50 amino acid stretch which is 35% identical between homologs. All other regions showed no significant sequence similarity. Arrowheads represent conserved amino acids that were determined to be required for *E. coli* growth under zinc limitation using strains encoding ZupT point mutants [189].

The ZnuACB complex is the most well characterized system for high affinity zinc import. It is a conserved ABC transporter composed of a periplasmic zinc-binding protein (ZnuA), a transmembrane protein (ZnuB), and an ATPase (ZnuC). In ABC transporters, hydrolysis of ATP in the ATPase domain results in a conformational change in the transmembrane domain (TMD), leading to transport of bound substrate across the membrane [192]. Substrate is ferried to the TMD by a periplasmic substrate-binding protein, which associates with the TMD and transfers substrate to the TMD binding site [193]. ZnuABC is a member of the cluster 9 family of ABC transporters, which primarily contribute to zinc and manganese transport [194]. Coordination of metals by metal-binding proteins of this family is accomplished by conserved histidine, aspartate, and glutamine residues, although these contribute to both zinc and manganese specific binding proteins [195, 196]. A structural comparison between zinc and manganese specific binding proteins determined that zinc-specific proteins utilize three conserved histidine residues and either a water molecule, an aspartate, or a gluatmate for metal coordination (Fig. 3). In contrast, manganese specific proteins utilize two histidines, a glutamate, and an aspartate [196]. Another commonly observed feature in ZnuA zinc-binding proteins is a flexible histidine-rich loop that contributes to zinc binding. Observations of a version of *Synechocytis* ZnuA lacking the histidine-rich loop determined that the histidine-rich loop has ~100 fold less affinity for zinc compared to the primary binding site [197]. The authors also observed that deletion of the loop does not significantly affect zinc binding, suggesting an alternate role for this loop. Analysis of ZnuA-zinc association constants indicates that zinc is only bound to the histidine-rich loop after the

A

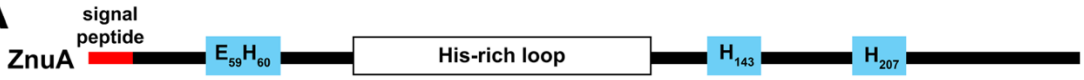
signal peptide
ZnuA
E59H60
His-rich loop
H143
H207

B

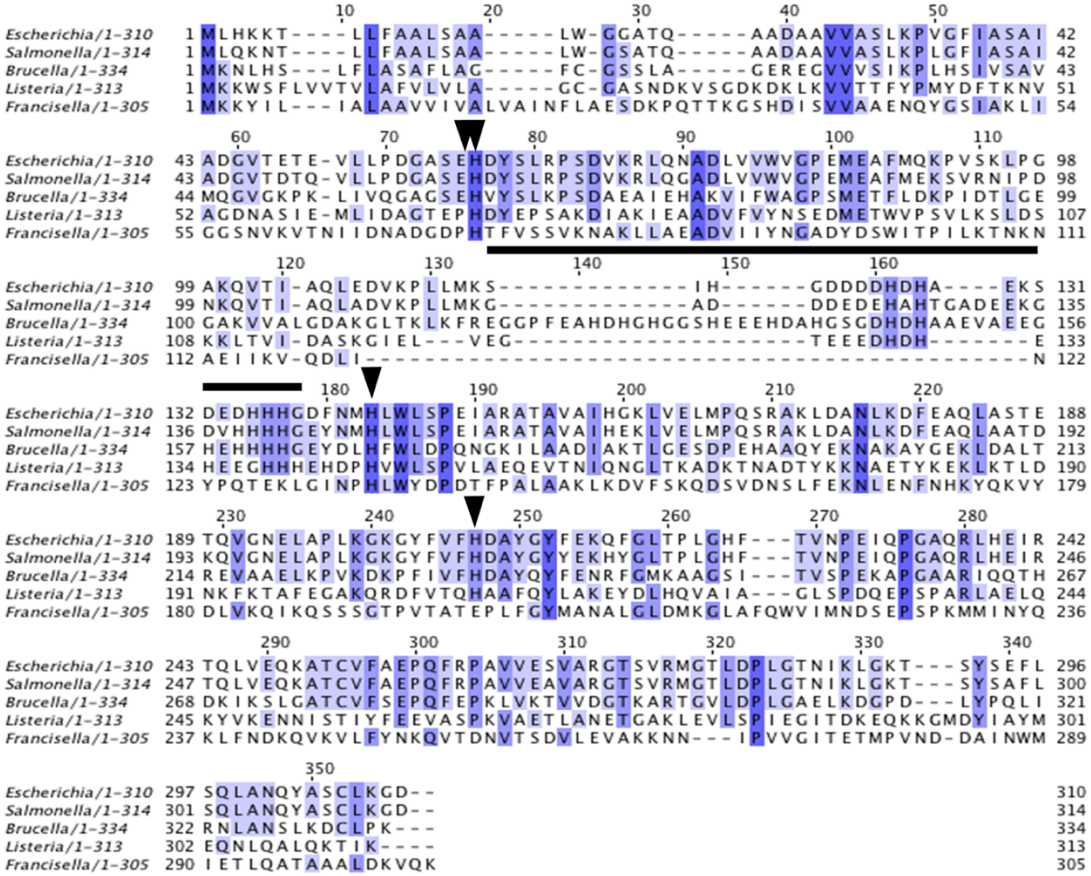
Escherichia/1-310
Salmonella/1-314
Brucella/1-334
Listeria/1-313
Francisella/1-305

Figure 3: Bacterial ZnuA has conserved zinc binding residues and a histidine-rich loop. (A) Schematic of ZnuA primary structure. Zinc binding is coordinated by conserved Glu_{59}, His_{60}, His_{143}, and His_{207} residues, while a histidine-rich loop is found from residues ~130-160. (B) Alignment of ZnuA protein sequences from *Escherichia coli*, *Salmonella* Typhimurium, *Brucella abortus*, *Listeria monocytogenes*, and *Francisella novicida* using Clustal Omega. Sequence Identities are marked by colored boxes. Conserved zinc binding residues are highlighted with arrowheads, while the histidine-rich loop is marked with a black bar.

primary binding site is exhausted and suggests that this loop may play a role in transfer of zinc to either the primary binding site or to ZnuB for transport into the cell [198]. In *Salmonella* Typhimurium, deletion of the histidine-rich loop is supplemented by expression of the small, histidine rich protein ZinT [199].

Pathogenic bacteria have developed a number of strategies for overcoming host zinc sequestration. While zinc transport across the outer membrane is mediated by non-selective porins [182], active mechanisms of zinc transport across this membrane have been described as a virulence factor in a number of pathogenic bacteria. *Neisseria meningitidis* expresses an outer membrane protein under zinc limiting conditions that is capable of binding host calprotectin and utilizing it as a zinc source, overcoming zinc sequestration [200]. A number of TonB-dependent outer membrane proteins such as ZnuD have also been identified in pathogenic *Neisseria* and *Acinetobacter* species, allowing higher affinity zinc uptake and contributing to pathogenesis [201, 202]. Secreted siderophore-like molecule that scavenge zinc at high affinity have also been observed in both bacteria [203, 204] and fungi [205]. The *Yersinia pestis* siderophore yersiniabactin is capable of binding zinc in addition to iron, and zinc-bound yersiniabactin is taken up through a different surface receptor than iron-bound yersiniabactin [203]. In the absence of ZnuABC, yersiniabactin plays a significant role in zinc acquisition under zinc limiting conditions. A similar zincophore has recently been described in *Pseudomonas aeruginosa* [204], indicating that zinc-binding metallophores may be more prevalent and important to virulence than previously appreciated. Finally, ZnuABC plays a significant role in bacterial survival within the host.

Expression of ZnuABC is critical for bacterial survival in zinc limitation as well as during infection within the host [206, 207]. In *Salmonella* Typhimurium, ZnuABC can overcome calprotectin-mediated zinc limitation, enabling the bacteria to outcompete other members of the microbiome during infection [208].

2.6: Zur is a major regulator of zinc homeostasis mechanisms

Intracellular zinc concentration in bacteria is primarily regulated by differential expression of zinc import and export proteins [185], which is controlled by transcription factors. There are a number of bacterial transcription factors that activate or repress zinc transporter gene expression, including ArsR-SmtB, ZntR, and AdcR families [209]. However, the most well characterized transcription factor for the response to zinc limitation is the Zinc uptake regulator Zur. Zur is a member of the Fur family of transcription factors which, when directly bound to metals, act as transcriptional repressors. Members of the Fur family typically contain an N-terminal winged helix domain responsible for DNA binding, as well as a C-terminal dimerization domain [108]. Zur is differentiated from other Fur family members by four conserved amino acid residues between these two domains which coordinate metal sensing and specificity [108, 210, 211]. Dimerization of Zur monomers is facilitated by zinc binding to conserved residues at the dimerization domain [211]. Mutation of zinc-binding residues at either site 1 or site 2 results in complete loss of Zur-mediated gene repression [211]. When bacteria are in a zinc-rich environment, a Zur dimer binds asymmetrically (Zur_2Zn_3) to free zinc, facilitating binding of the dimer to DNA [210]. Once bound

to DNA, the Zur dimer becomes fully saturated with zinc (Zur_2Zn_4), allowing graded gene derepression in response to changes in zinc concentrations [212]. Zur binding occurs at a conserved inverted palindromic repeats upstream of regulated genes [108]. Differences in binding affinity of Zur to different Zur binding sites also contributes to grated gene regulation [213].Under zinc limitation, zinc is no longer available for Zur binding, leading to release of Zur from the genome and derepression of Zur-regulated genes.

Many Zur-regulated genes are critical for adaptation to zinc-limiting environments. ZnuABC, which is required for zinc acquisition under zinc limitation, is typically Zur-regulated [214-217]. Zur also regulates accessory proteins that assist in zinc transport, such as *Salmonella* Typhimurium ZinT. In addition to zinc transporters, Zur regulates genes involved in maintenance of zinc homeostasis. Expression of the *A. baumanii* zinc chaperone ZigA, which is required for maintenance of the labile zinc pool is upregulated under zinc limitation by Zur [181, 215]. Zur also regulates expression of alternative ribosomal proteins under zinc limitation. When zinc is scarce, paralogs of these proteins that do not require zinc for their function are expressed [214, 218], allowing for conservation of limited zinc resources. Regulation of genes by Zur allows for control of their expression under zinc-replete conditions, preventing zinc dishomeostasis.

2.7: Research Aims of Study

Acquisition of zinc is critical for survival in the intracellular environment. However, neither the genes utilized by *Francisella* for zinc uptake and homeostasis nor the mechanisms by which expression of these genes are regulated have been characterized. Therefore, the aims of this study are to identify genes necessary for survival under zinc limitation as well as mechanisms of regulation for these genes. Once genes that contribute to zinc uptake and homeostasis have been identified, the importance of these genes to *F. tularensis* virulence will be characterized. Because many of the most vital genes for adaptation to a zinc limiting environment are regulated by Zur, characterization of the Zur regulon can identify genes that are critical for survival under zinc limitation and virulence. Therefore, a *zur* mutant strain from the *F. novicida* transposon library was used to better understand zinc-dependent regulation in *Francisella* as well as identify genes that may contribute to adaptation to the zinc limiting environment.

Chapter 3: A Limited Number of *Francisella* Genes are Regulated in a Zinc-Dependent Manner

3.1: Identification of a Zur ortholog in *Francisella*

The *F. novicida* locus FTN_0881 (Accession # ABK89769.1) encodes a 143 amino acid protein that is annotated as an Fe^{2+}/Zn^{2+} uptake regulator protein. Comparisons to the Zur protein from *E. coli* (Accession # AAC77016.2) and *Salmonella* Typhimurium (Accession # AAL56650.1) showed that the protein encoded by FTN_0881 has 36% and 35% identity, respectively, as well as 52% similarity with both proteins. The FTN_0881 protein is predicted to have an N-terminal winged helix domain for DNA binding, as well as a C-terminal dimerization domain, both of which are conserved in Fur family proteins [108]. The FTN_0881 protein also has conserved residues for coordinating zinc in each of the three zinc binding sites, including conserved D64, C80, H88, and H90 residues at site 2, which distinguish Zur orthologs from other Fur family proteins [108]. Based on these features, the designation of *zur* is proposed for this gene.

A transposon mutant strain of *zur* from a *F. novicida* U112 transposon library [23] was utilized to identify Zur-regulated genes. In the absence of Zur, expression of Zur-regulated genes should be derepressed, resulting in increased expression of these genes in a *zur* mutant strain. RNA samples from wild-type and *zur*::TN bacteria were prepared for RNA sequencing (RNA-Seq) to identify Zur-regulated genes. Principle component analysis was used to compare global

variation between wild-type and *zur*::TN mutant samples. Individual wild-type and mutant replicates clustered closely with each other, while wild-type and mutant samples separated into groups (Fig. 4). This indicates that wild-type and *zur*::TN samples are distinct from each other and that replicate samples are very similar, which provides more statistical power to conclusions drawn from the data. After analyzing samples for differences in gene expression, only five protein-encoding genes were differentially regulated (adjusted p value<0.05) in the *zur*::TN mutant compared to wild-type (Fig. 5). In other bacteria Zur typically regulates the expression of around 15-40 genes [108], although some Zur orthologs have been shown to regulate over 100 [215].

Table 1 lists the five *F. novicida* genes identified as differentially expressed in *zur*::TN compared to wild-type by RNA-Seq, and Figure 6 illustrates their genomic organization. The FTN_0880 and FTN_0879 genes appeared to be encoded in an operon and are transcribed off the opposite strand as *zur*. Co-transcription of FTN_0880 and FTN_0879 was confirmed by RT-PCR (Fig. 7). FTN_0880 encodes a protein with similarity to the COG0523 family of P-loop GTPases, which include conserved Walker A and B site residues, as well as a conserved CXCC motif for metal binding. This family is not well characterized, but has been implicated in both metallochaperone activity and insertase activity of zinc into zinc-binding proteins [180]. Recently, a COG0523 homologue in *A. baumannii* was shown to be required for full growth under zinc limitation and contribute to maintenance of the labile pool of intracellular zinc [181], highlighting the role of some COG0523 family proteins in maintenance of zinc homeostasis.

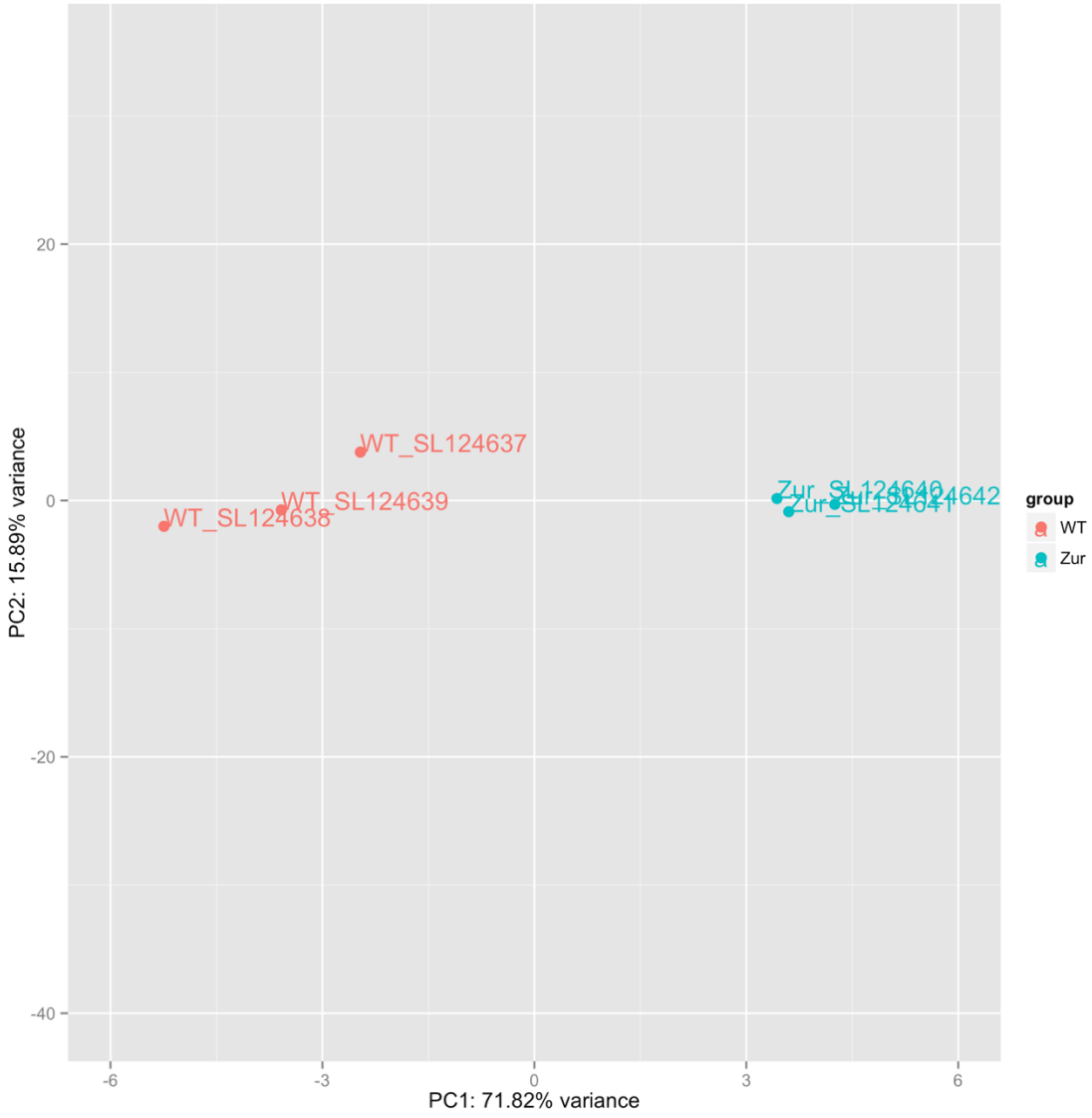
20
0
-20
-40
PC2: 15.89% variance
WT_SL124637
WT_SL124639
WT_SL124638
Zur_SL124642
Zur_SL124641
-6
-3
0
3
6
PC1: 71.82% variance
group
WT
Zur

Figure 4: Principle component analysis of *zur*::TN RNA-Seq samples. PCA analysis was performed to determine similarity between wild-type (red) and *zur*::TN samples (blue) run in RNA-Seq. Axes represent Principle Component 1 (PC1) and Principle Component 2 (PC2), with PC1 representing a majority of the variation in samples.

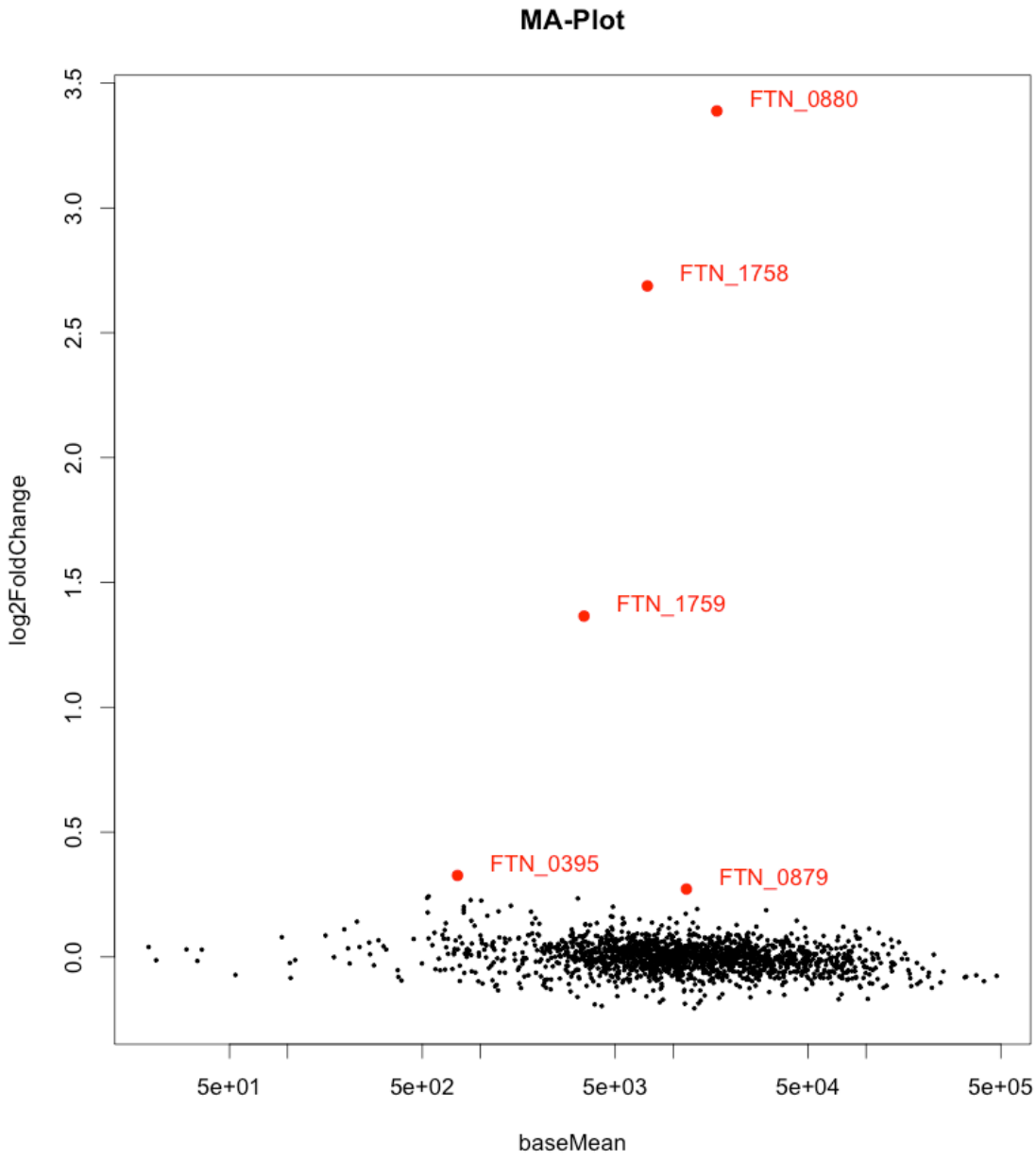
MA-Plot
log2FoldChange
baseMean
FTN_0880
FTN_1758
FTN_1759
FTN_0395
FTN_0879
3.5
3.0
2.5
2.0
1.5
1.0
0.5
0.0
5e+01
5e+02
5e+03
5e+04
5e+05

Figure 5: Five genes are differentially expressed in a *zur*::TN mutant compared to wild-type. MA plot of differences between wild-type and *zur*::TN samples. Circles represent all annotated *F. novicida* genes. The X axis represents the average expression of individual genes, while the Y axis represents the Log_2 fold change in gene expression between wild-type and *zur*::TN samples. Genes with significantly different levels of expression are highlighted in red.

Table 1: Differentially expressed genes in a *zur::*TN mutant strain compared to wild-type U112.

Gene name	Gene description[a]	Fold change	Adjusted p value
FTN_0880	Hypothetical protein	13.09	0
FTN_1758	Hypothetical protein	8.0	2.88E-244
FTN_1759	Hypothetical protein	2.71	8.46E-74
FTN_0879	Zinc (Zn^{2+})-iron (Fe^{2+}) permease (ZIP) family protein	1.26	0.000177
FTN_0395	ArsR family transcriptional regulator	1.27	0.00116

[a]Annotations as designated by NCBI

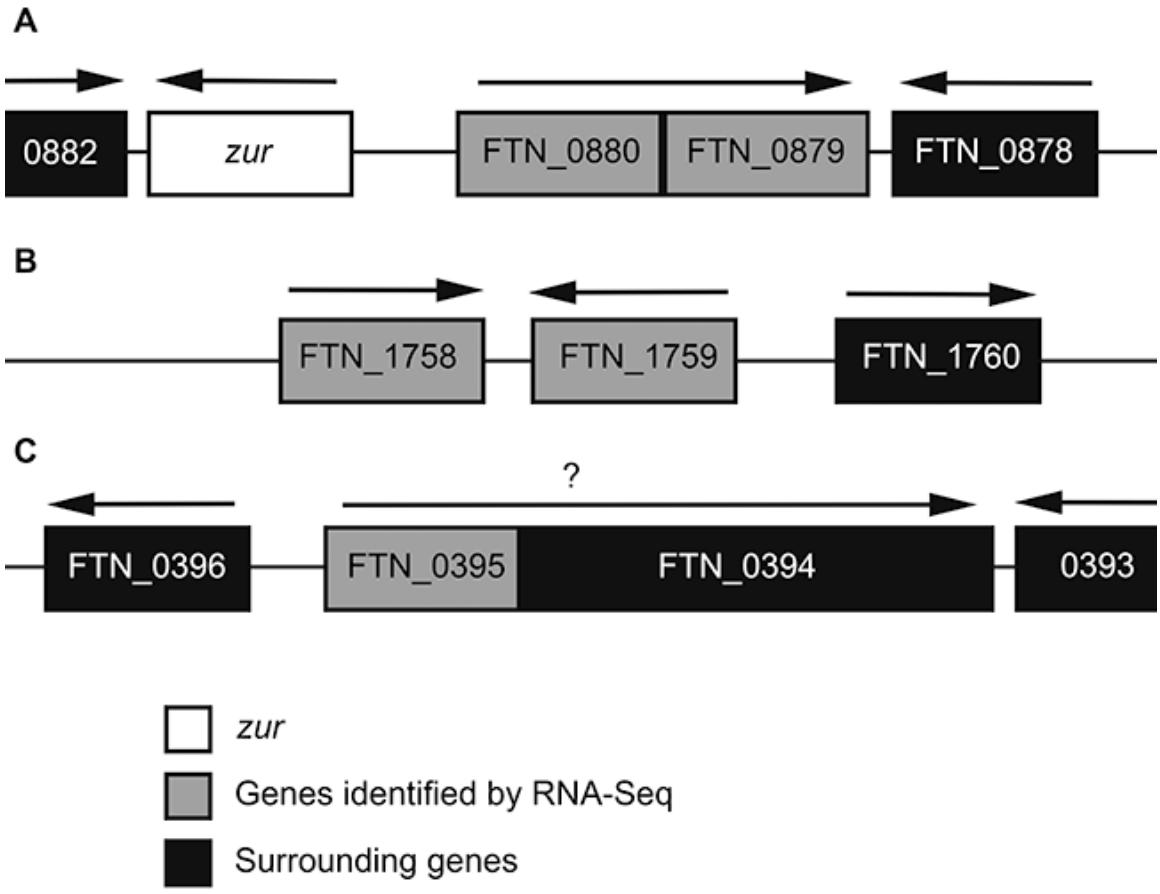
A
0882
zur
FTN_0880
FTN_0879
FTN_0878
B
FTN_1758
FTN_1759
FTN_1760
C
?
FTN_0396
FTN_0395
FTN_0394
0393
zur
Genes identified by RNA-Seq
Surrounding genes

Figure 6: Genomic organization of candidate genes. Organization of genes identified by RNA-Seq with increased expression in an *F. novicida zur::*TN mutant. Identified genes are colored in grey. (A) FTN_0880 and FTN_0879 (*zupT*) are expressed as an operon. The *zur* gene (white) is located upstream of this operon and encoded on the opposite strand. (B) FTN_1758 and FTN_1759 are located near each other on opposite strands. (C) FTN_0395 is located in a predicted operon directly upstream of FTN_0394, which is a predicted P-type heavy metal exporter.

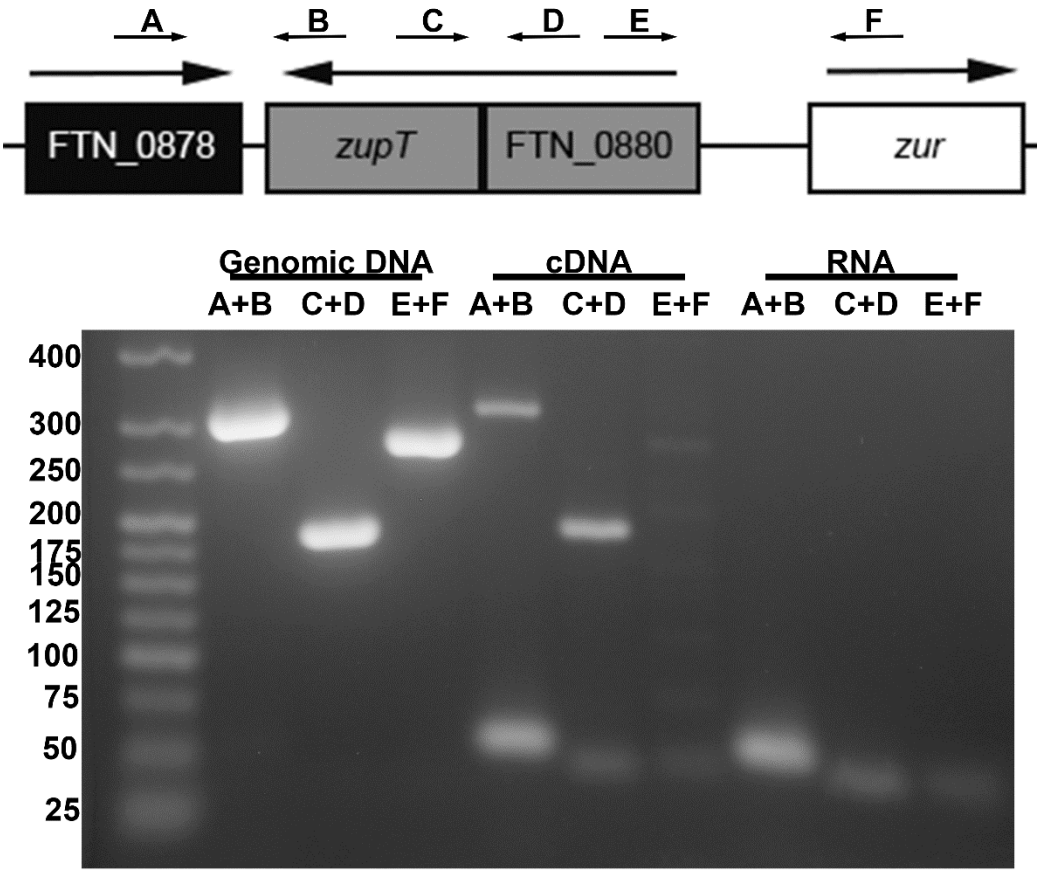
A
B
C
D
E
F
FTN_0878
zupT
FTN_0880
zur
Genomic DNA
cDNA
RNA
A+B
C+D
E+F
A+B
C+D
E+F
A+B
C+D
E+F
400
300
250
200
175
150
125
100
75
50
25

Figure 7: *zupT* and FTN_0880 are transcribed as an operon. RT-PCR was performed to amplify the intergenic regions of indicated genes in cDNA generated from isolated U112 RNA. PCR products were separated on a 2% agarose gel. PCR with genomic DNA or RNA were used as positive and negative controls, respectively.

FTN_0879 encodes a protein with a conserved Zinc/Iron Permease (ZIP) family domain, commonly found in a family of bacterial zinc permeases referred to as ZupT [195]. ZupT is reported to act as a low affinity zinc transporter with a broader metal specificity and is typically constitutively expressed regardless of intracellular zinc concentration [187]. While FTN_0879 predicted protein has low sequence similarity to the ZupT homolog from *E. coli*, (around 35% identity over a 50 amino acid residue stretch of the ~250 amino acid protein, see Figure 2), the designation of FTN_0879 as *zupT* is proposed based on the data below.

Three additional genes were also identified by RNA-Seq. FTN_1758 encodes a hypothetical protein that contains a DUF1826 domain, which is found in predicted succinylglutamate desuccinylases enzymes from other bacteria. This family of proteins may be zinc-dependent [219]; another DUF1826-containing protein in *Pseudomonas fluorescens* is downstream of a predicted Zur-binding site [180], suggesting that this gene may be Zur-regulated. FTN_1759 is a nearby gene in the opposite orientation from FTN_1758. There are no conserved domains in the predicted protein, and it is only similar to other orthologs in different *Francisella* species by pBLAST. FTN_0395 is predicted to encode an ArsR family transcriptional repressor. ArsR family members repress expression of genes required for metal export when metal concentrations are low and upregulate exporter gene expression when metal concentrations are high as a means to prevent toxicity [220]. FTN_0395 is directly upstream of a predicted heavy metal P-type exporter, suggesting that FTN_0395 encodes a regulator of metal exporter expression.

3.2: Zur regulates three genes in *F. novicida*

RNA-Seq results were validated by analyzing expression of candidate genes in both wild-type and *zur::*TN backgrounds by quantitative reverse transcription PCR (qRT-PCR). Expression of the *zupT*, FTN_0880, and FTN_1758 genes was increased at least 30-fold in the *zur::*TN mutant compared to wild-type (Fig. 8A). The FTN_0395 gene was slightly (2-fold) upregulated in the *zur::*TN mutant, while the FTN_1759 gene was not differentially expressed between wild-type and *zur::*TN strains. Complementation of the *zur* gene *in trans* partially restored expression of upregulated genes to wild-type levels, indicating that the phenotype observed is due to the loss of *zur* and not polar effects on downstream genes. Similar results were obtained when investigating gene expression from wild-type *F. novicida* grown in either complete CDM or complete CDM supplemented with 10 μM TPEN, a zinc chelator. Expression of *zupT*, FTN_0880, and FTN_1758 was highly upregulated (>30 fold) in the zinc-limiting condition compared to untreated samples (Fig. 8B). Neither FTN_0395 nor FTN_1759 were differentially expressed between conditions, indicating that these genes are not regulated by changes in zinc concentration. Expression of *zur* was also significantly increased during zinc limitation (Fig. 8C), which is consistent with the literature that most *zur* genes are autoregulated [108]. These results support the identification of FTN_0881 as *zur*, a zinc responsive transcription factor and implicates three genes as potentially involved in the Zur-mediated response to zinc limitation.

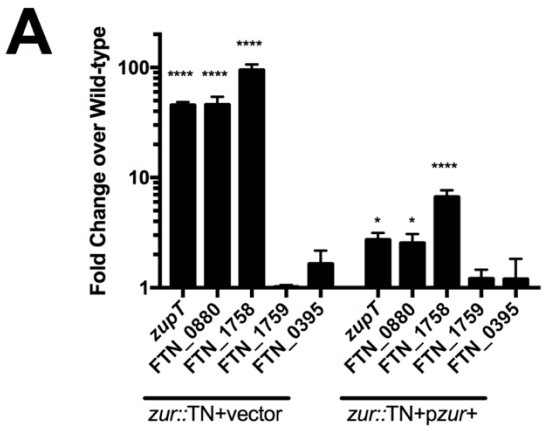

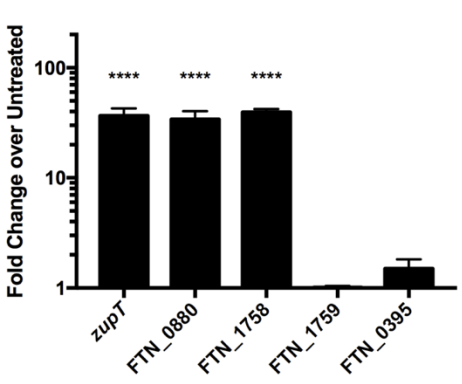

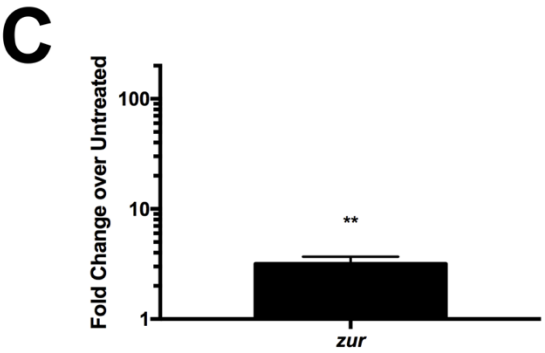

D

FTN_0880	-79	AAC**TGTTATA**T**TG**T**AACA**CTT
FTN_1758	-56	AAG**TGTTATA**A**TATAACA**TAT
FTN_0395	-130	AGC**TG**C**TATA**T**TA**G**A**TTTGCT

Figure 8: *F. novicida* Zur directly regulates three genes. Expression of genes identified by RNA-Seq in either (A) a *zur::*TN mutant carrying the empty vector (*zur::*TN+vector) and *zur::*TN complemented strain (*zur::*TN+*pzur+*) or (B) in wild-type U112 in CDM supplemented with 10 μM TPEN. Expression is shown as the fold change in expression over wild-type grown in untreated CDM from three biological replicates. (C) Expression of *zur* in wild-type U112 grown in 10 μM TPEN-treated CDM. Expression is shown as the fold change in expression over wild-type grown in untreated CDM from three biological replicates. (D) Alignment of upstream regions of FTN_0880, FTN_1758, and FTN_0395. Numbers denote the distance from the predicted translational start site. Predicted heptameric palindromic repeats are outlined while conserved nucleotides are marked in bold. Statistical analysis was performed using (A, B) a One way ANOVA with Dunnett's multiple comparison test or (C) a Student's t test compared to a reference value of 1.0. *, $p<0.05$; **, $p<0.01$; ****, $p<0.0001$.

Zur binds to a conserved inverted palindromic repeat sequence upstream of regulated genes to repress their transcription [108]. It is likely that identified Zur-regulated genes also have a consensus Zur-binding site upstream of their translational start sites. A multiple sequence alignment using Clustal Omega [221] was used to investigate the presence of a Zur consenus binding site in the upstream regions of genes with increased expression by qRT-PCR in the *zur::*TN mutant strain (FTN_0880, *zupT*, FTN_1758, and FTN_0395). As *zupT* and FTN_0880 are cotranscribed, only the upstream region of FTN_0880 was used for the multiple sequence alignment. A palindromic sequence with similarity to other Zur-binding sequences [222] was identified upstream of the predicted FTN_0880 and FTN_1758 translational start sites (Fig. 8D). As *zur* shares an upstream promoter region with FTN_0880, this binding site likely also explains *zur* auto-regulation. The promoter region of FTN_0395 had some sequence similarity with the first repeat, but this motif was found further upstream (130 base pairs) from the translational start site than in FTN_0880 (79 base pairs) and FTN_1758 (56 base pairs), which were more typical locations for Zur-binding sites. The upstream promoter region of FTN_1759 did not contain any sequences with similarity to a Zur-binding site. These data support direct Zur regulation of *zupT*, FTN_0880, and FTN_1758 as well as further support that Zur does not directly regulate FTN_0395 or FTN_1759.

3.3: Newly identified TPEN-regulated genes do not appear to be involved in zinc homeostasis

The limited number of genes directly regulated by *F. novicida* Zur suggests that other mechanisms of gene regulation may play a prominent role in *Francisella* during zinc limitation. To identify genes regulated by zinc limitation in a Zur-independent manner, RNA-Seq was performed using wild-type *F. novicida* U112 in the presence or absence of the zinc chelator TPEN. Although principle component analysis observed that untreated and TPEN-treated *F. novicida* samples were not as clearly separated as samples in the *zur*::TN RNA-Seq (Fig. 9), differences in gene expression could still be determined. Nine genes were differentially expressed in TPEN-treated bacteria compared to bacteria grown in the absence of TPEN (Fig. 10). Four of the identified genes were also identified in the *zur*::TN RNA-Seq experiment (Fig. 11). FTN_0395 was not differentially regulated in TPEN-treated U112 compared to untreated, which was consistent with *zur*::TN qRT-PCR results and the hypothesis that increased expression in *zur*::TN is due to off-target effects of the mutation on intracellular zinc concentrations rather than direct Zur regulation of the gene. As in the *zur*::TN RNA-Seq experiment, FTN_1759 was similarly upregulated as observed with the FTN_1758 gene.

All nine genes identified by RNA-Seq in TPEN-treated U112 are listed in Table 2. Five new genes were observed as differentially expressed in the presence of TPEN but not in a *zur*::TN mutant by RNA-Seq. Changes in gene expression

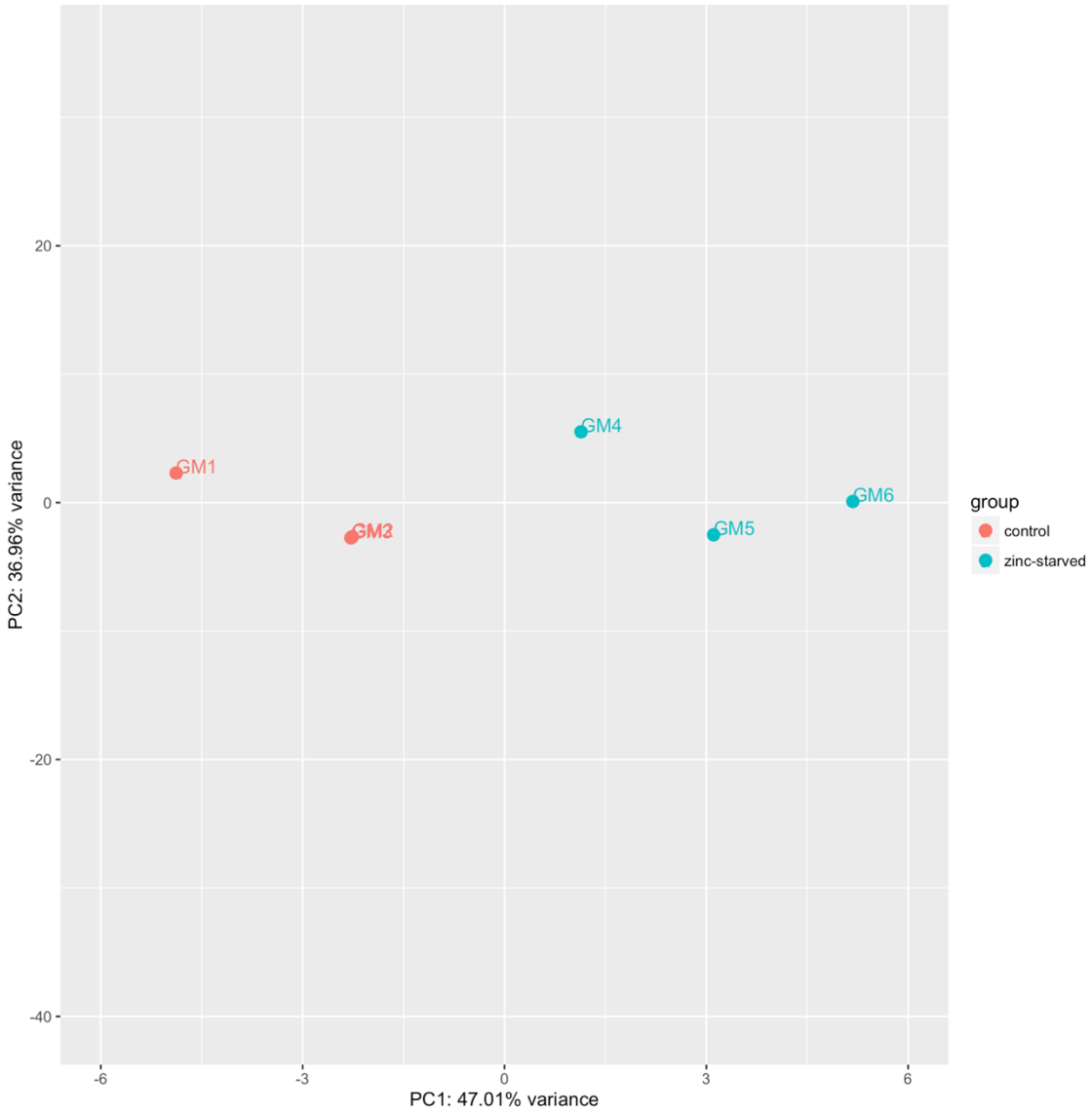
20
0
-20
-40
PC2: 36.96% variance
-6
-3
0
3
6
PC1: 47.01% variance
GM1
GM2
GM4
GM5
GM6
group
control
zinc-starved

Figure 9: Principle component analysis of TPEN-treated *F. novicida* RNA-Seq samples. PCA analysis was performed to determine similarity between untreated (red) and TPEN-treated (blue) U112 samples run in RNA-Seq. Axes represent Principle Component 1 (PC1) and Principle Component 2 (PC2), with variation divided around equally between PC1 and PC2.

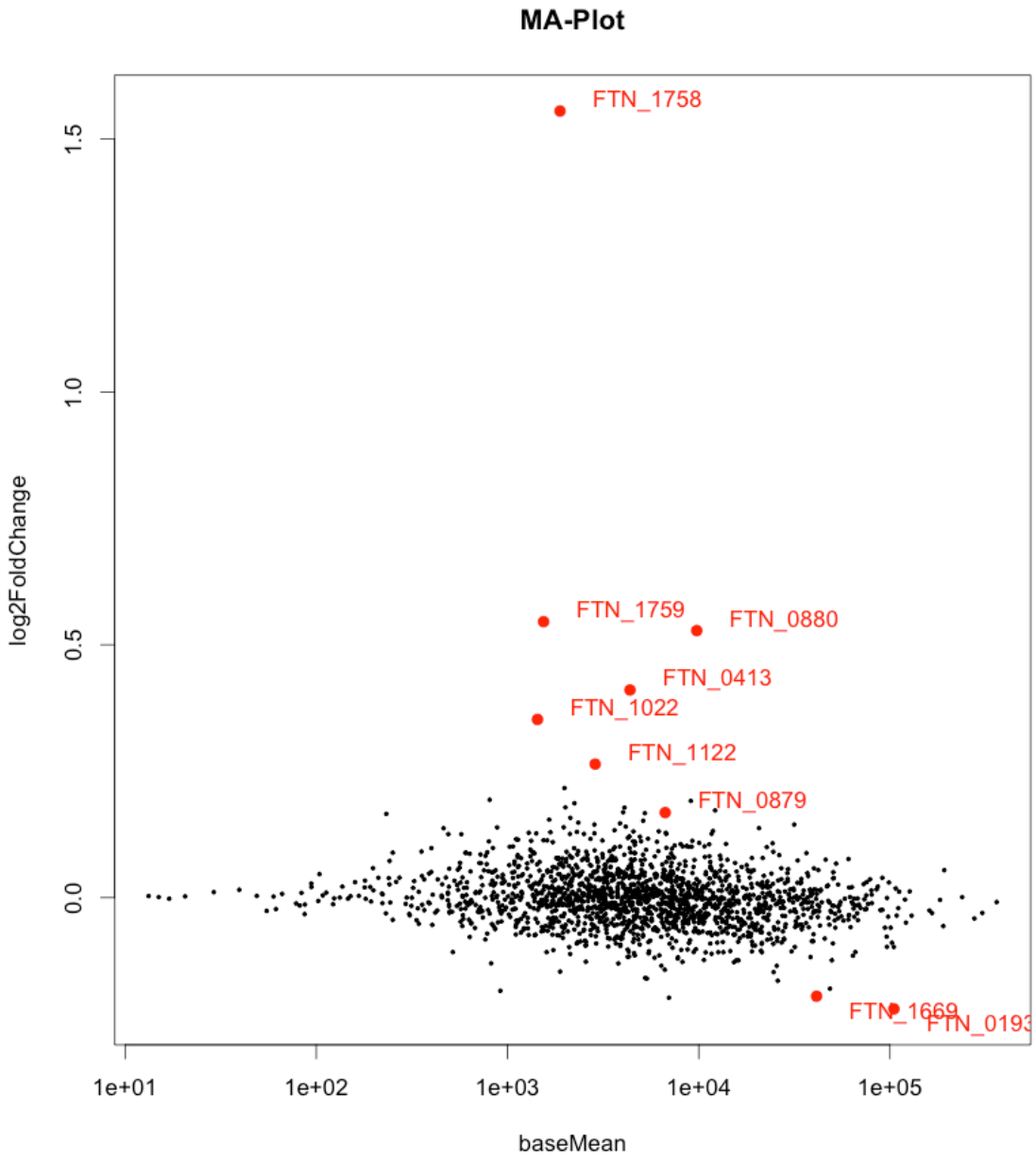
MA-Plot
FTN_1758
FTN_1759
FTN_0880
FTN_0413
FTN_1022
FTN_1122
FTN_0879
FTN_1669
FTN_0193
log2FoldChange
1.5
1.0
0.5
0.0
1e+01
1e+02
1e+03
1e+04
1e+05
baseMean

Figure 10: Nine genes are differentially expressed in TPEN-treated *F. novicida* U112 compared to untreated. MA plot of differences between untreated and TPEN-treated samples. Circles represent all annotated *F. novicida* genes. The X axis represents the average expression of individual genes, while the Y axis represents the Log_2 fold change in gene expression between untreated and TPEN-treated samples. Genes with significantly different levels of expression in TPEN-treated samples are highlighted in red.

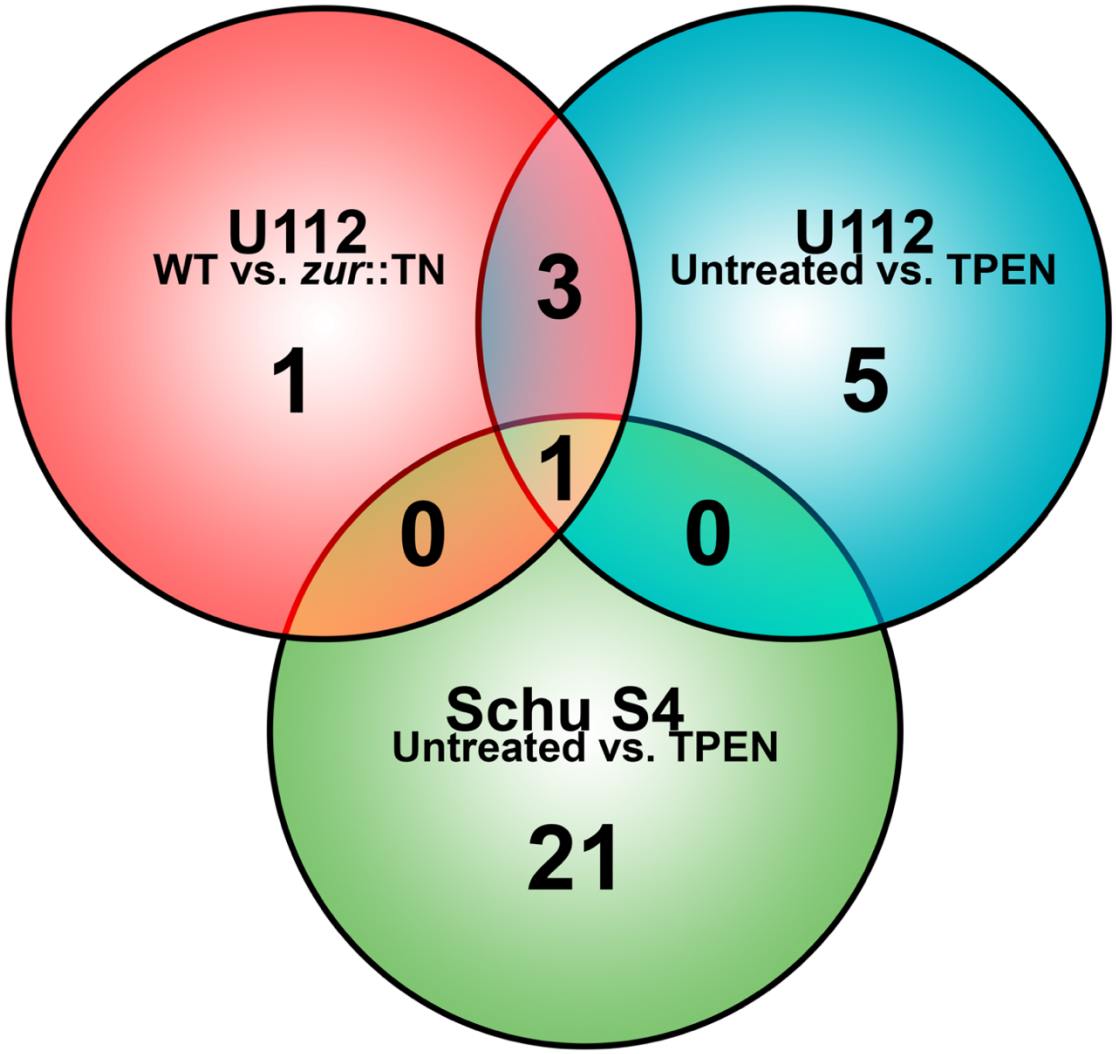
U112
WT vs. zur::TN
1
3
U112
Untreated vs. TPEN
5
1
0
0
Schu S4
Untreated vs. TPEN
21

Figure 11: Venn diagram of genes identified by RNA-Sequencing.

Visualization of the genes identified as differentially expressed in RNA-Seq experiments with wild-type vs. *zur*::TN *F. novicida* U112 (5 total identified genes), untreated vs TPEN-treated *F. novicida* U112 (9 total identified genes), and untreated vs. TPEN-treated *F. tularensis* ssp. *tularensis* Schu S4 (22 total identified genes) Expression of one gene was significantly changed in all three experiments, while expression of three additional genes were significantly changed in both U112 experiments.

Table 2: Differentially expressed genes in TPEN-treated U112 compared to untreated.

Gene name	Gene description[a]	Fold change	Adjusted p value
FTN_1758	Hypothetical protein	2.94	3.63E-131
FTN_0880	Hypothetical protein	1.44	5.46E-26
FTN_1759	Hypothetical protein	1.46	5.91E-15
FTN_0413	Type IV pili, pilus assembly protein	1.33	6.85E-09
FTN_1022	Hypothetical protein	1.28	8.68E-09
FTN_0879	Zinc (Zn^{2+})-iron (Fe^{2+}) permease (ZIP) family protein	1.26	0.000662
FTN_0193	*cydA* Cytochrome bd-I terminal oxidase subunit I	-1.16	0.00402
FTN_1122	Hypothetical Protein	1.20	0.00562
FTN_1669	*nuoL* NADH dehydrogenase I subunit L	-1.15	0.01

[a]Annotations as designated by NCBI

were mixed, with increased expression observed in three genes and decreased expression in two genes. Although five new genes were identified, only one of these genes appears to be involved in metal regulation. That gene, FTN_1022, is predicted to encode a hypothetical protein with a conserved helix-turn-helix domain found in DNA-binding proteins and has similarity to ArsR family transcriptional regulators by pBLAST. However, it is unclear whether this gene is responsive to zinc, as ArsR family regulators are typically upregulated in response to elevated metal concentrations. Of the remaining four genes, none appear to function in either zinc acquisition or homeostasis. FTN_0413 is predicted to encode *pilV*, a pilE-like subunit of the Type IV pilus adhesin. FTN_0193 has been annotated as *cydA*, which encodes the first subunit of the cytochrome bd terminal oxidase, which reduces oxygen as a component of the electron transport chain. Similar decreased expression of *cydA* was observed during copper stress in *Bacillus subtilis* [223]. FTN_1122 encodes a hypothetical protein with no conserved domains and only has homologs in other *Francisella* species. Finally, FTN_1669 is annotated as *nuoL*, which encodes the NADH:quinone oxicoreductase, which plays a major role in aerobic respiration and energy metabolism [224]. None of these genes have been identified as induced under zinc limitation or implicated in the response to zinc limitation in other organisms. suggesting that the observed changes in expression may be due to zinc-independent effects of TPEN treatment.

RNA-Seq was also performed with the virulent *F. tularensis* ssp. *tularensis* Schu S4 strain in the presence or absence of TPEN. Principle component analysis observed that untreated and TPEN-treated Schu S4 samples were distinct but

failed to cluster tightly together (Fig. 12). Additionally, one TPEN-treated replicate was further apart than other TPEN-treated replicates and closer to control samples. This variation reduces the power of the results, making it more difficult to determine whether observed differences are statistically significant. More genes were differentially regulated in Schu S4 than in previous RNA-Seq experiments, with 22 genes identified as differentially expressed in the presence of TPEN compared to untreated conditions (Fig. 13). Differentially regulated genes included both predicted operons as well as stand-alone genes (Table 3). The *F. tularensis* homolog (FTT1000) of *F. novicida* FTN_0880, which was identified in the previous two RNA-Seq experiments, was also identified in TPEN-treated Schu S4. This gene represents the only gene that was differentially expressed in all three RNA-Seq experiments, and may indicate that this gene plays a conserved or critical role in the *Francisella* response to zinc limitation. The only identified gene with predicted zinc transporter activity was FTT0208, which encodes the predicted ATP hydrolysis component (ZnuC) of the ZnuABC zinc transporter complex. While FTT0208 was identified by RNA-Seq, it barely made the cutoff for significance and expression of neither of the other two genes of the *znuACB* operon was significantly different.

The genes with the highest increase in expression observed in TPEN-treated Schu S4 were the *fslABCD* operon and *feoB*, which are both involved in *Francisella* iron acquisition [96, 99]. Zinc uptake is not mediated by these mechanisms [225], indicating that increased expression is likely not due to these genes being involved in zinc uptake. Several other operons with no apparent role in zinc uptake were

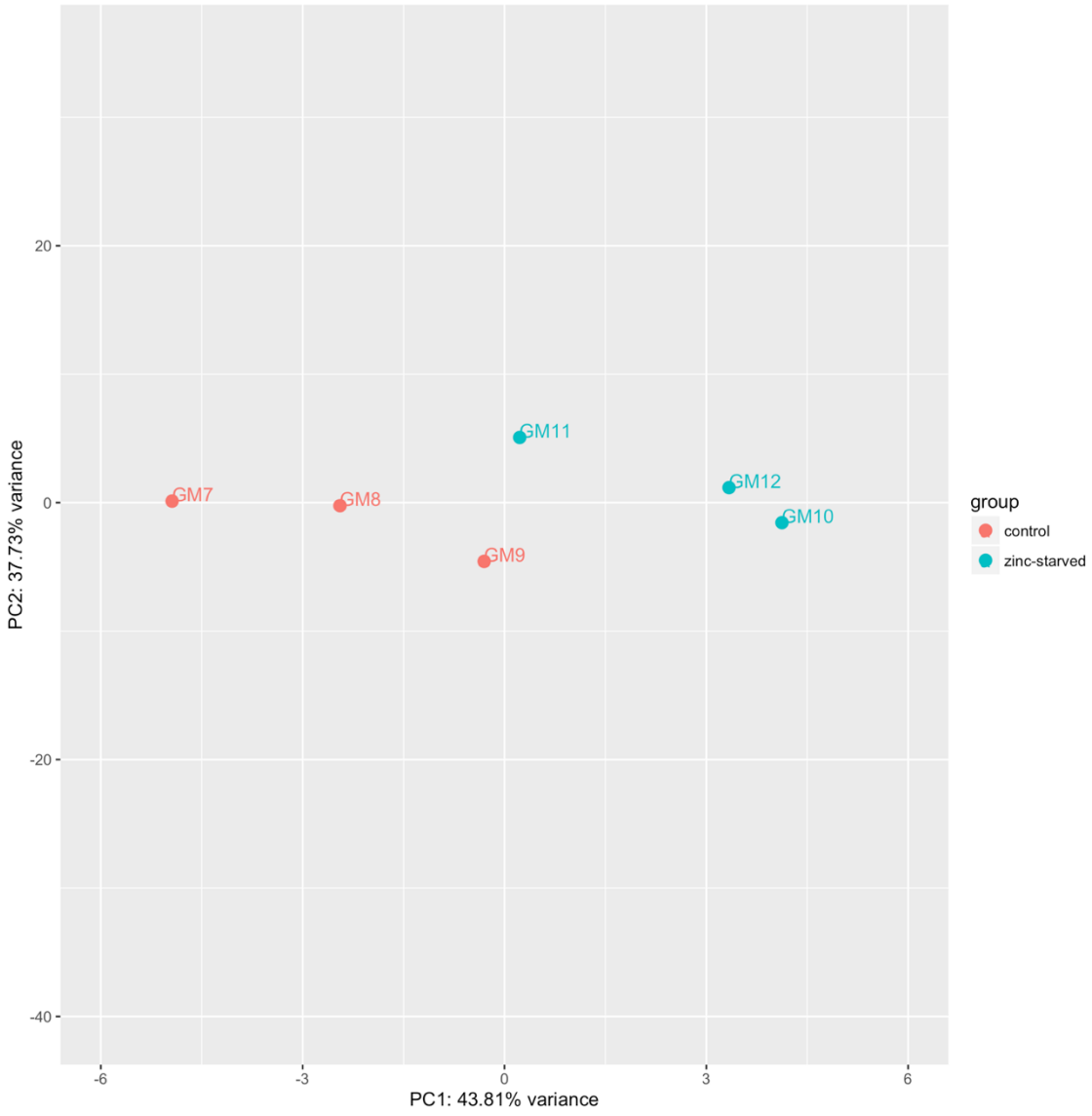
20
0
-20
-40
PC2: 37.73% variance
-6
-3
0
3
6
PC1: 43.81% variance
GM7
GM8
GM9
GM11
GM12
GM10
group
control
zinc-starved

Figure 12: Principle component analysis of TPEN-treated Schu S4 RNA-Seq samples. PCA analysis was performed to determine similarity between untreated (red) and TPEN-treated (blue) Schu S4 samples run in RNA-Seq. Axes represent Principle Component 1 (PC1) and Principle Component 2 (PC2), with variation divided around equally between PC1 and PC2.

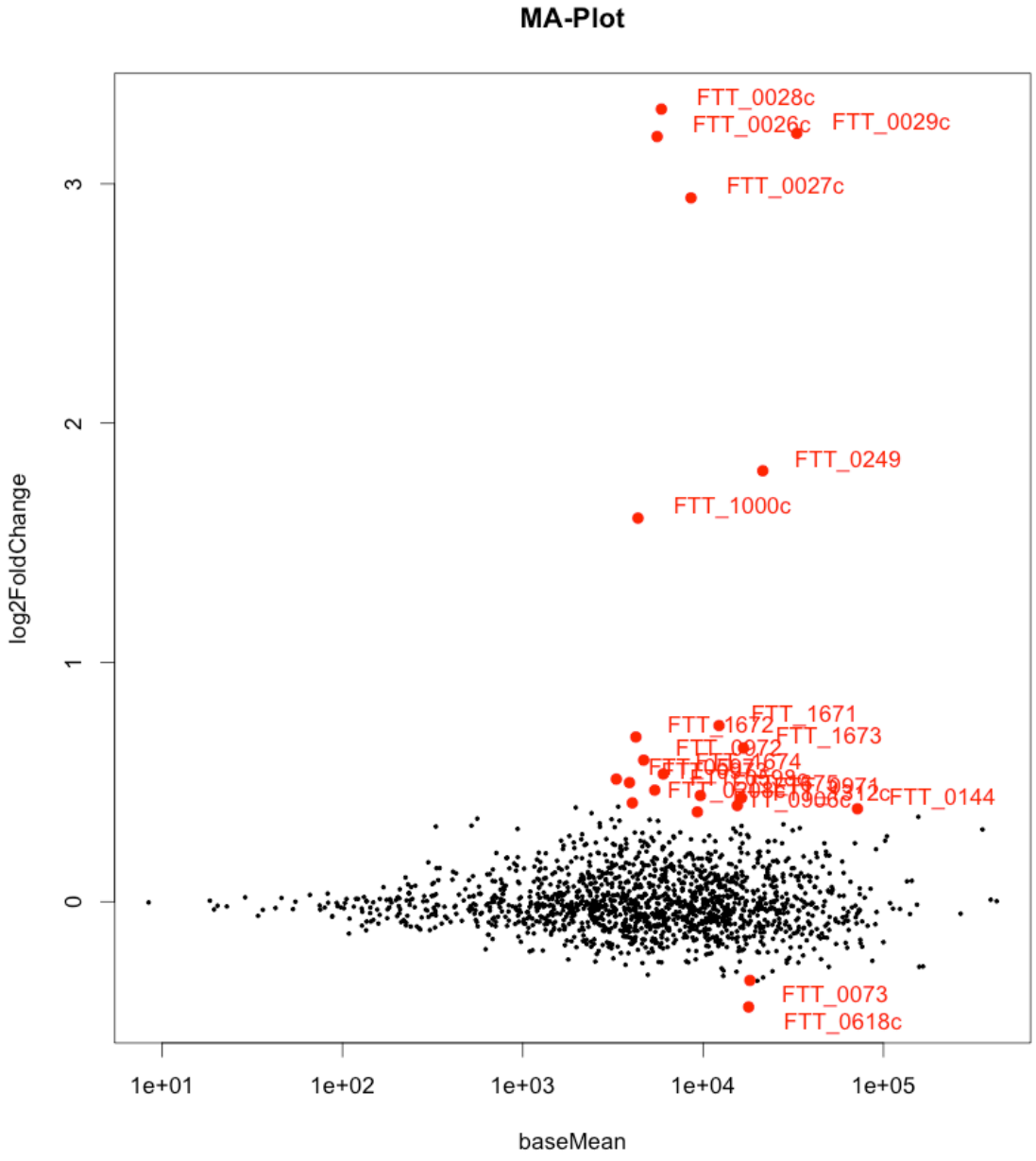
MA-Plot
FTT_0028c
FTT_0026c
FTT_0029c
FTT_0027c
FTT_0249
FTT_1000c
FTT_1671
FTT_1672
FTT_1673
FTT_0144
FTT_0073
FTT_0618c
log2FoldChange
baseMean
3
2
1
0
1e+01
1e+02
1e+03
1e+04
1e+05

Figure 13: Twenty-two genes are differentially expressed in TPEN-treated *F. tularensis* ssp. *tularensis* Schu S4 compared to untreated. MA plot of differences between untreated and TPEN-treated samples. Circles represent all annotated *F. tularensis* ssp. *tularensis* genes. The X axis represents the average expression of individual genes, while the Y axis represents the Log_2 fold change in gene expression between untreated and TPEN-treated samples. Genes with significantly different levels of expression in TPEN-treated samples are highlighted in red.

Table 3: Differentially expressed genes in TPEN-treated U112 compared to untreated.

Gene name	Gene description[α]	Fold change	Adjusted p value
FTT0028[β]	Hypothetical protein	9.92	2.04E-152
FTT0026[β]	Hypothetical protein	9.19	5.75E-143
FTT0029[β]	Hypothetical protein	9.25	9.64E-130
FTT0027[β]	lysA1 diaminopimelate decarboxylase	7.67	2.28E-111
FTT0249	*feoB* Ferrous iron transport protein	3.48	3.80E-72
FTT1000	*cobS* Cobalamin synthesis protein	3.03	2.35E-30
FTT1671[χ]	*ribD* Riboflavin biosynthesis protein	1.67	3.08E-07
FTT1672[χ]	*ribB* riboflavin synthase subunit alpha	1.61	5.81E-05
FTT0144	*rpoB* DNA-directed RNA polymerase subunit beta	1.31	0.000108
FTT0972[δ]	ABC transporter ATP-binding protein	1.51	0.000108
FTT1673[χ]	*ribA* 3,4-dihydroxy-2-butanone-4 phosphate synthase	1.56	0.000183
FTT0973[δ]	Hypothetical protein	1.41	0.000879
FTT0618	*yleA* dimethylallyladenosine tRNA methylthiotransferase	-1.35	0.00349
FTT0597	Hypothetical protein	1.43	0.0038
FTT1312	*uvrA* DNA excision repair protein subunit A	1.32	0.00494
FTT1674[χ]	*ribH* 6,7-dimethyl-8-ribityllumazine synthase	1.45	0.00519
FTT0598	Sodium-dicarboxylate symporter family protein	1.38	0.00531
FTT0906	*topA* DNA topoisomerase I	1.30	0.00708

FTT0971[δ]	Cysteine desulfurase	1.35	0.0238
FTT0073	*sdhD* Succinate dehydrogenase hydrophobic membrane anchor protein	-1.25	0.0238
FTT1675[χ]	*def2* peptide deformylase	1.36	0.0292
FTT0208	ABC transporter ATP-binding protein	1.33	0.0301

[α]Annotations as designated by NCBI

[β]Members of the *fslABCD* siderophore synthesis operon [96].

[χ]Members of the putative ribAB operon.

[δ]Members of the putative sufBCD operon

also upregulated, including the *ribAB* operon, which is involved in riboflavin production [226], and the *sufBCD* operon, which is involved in biosynthesis of iron-sulfur clusters, particularly under conditions of stress such as iron limitation [227]. Other differentially expressed genes appear to be involved in DNA repair (*rpoB*, *uvrA*, *topA*). Differential expression of genes in TPEN RNA-Seq experiments have not been confirmed by qPCR as most of the genes identified do not appear to play a role in zinc transport. These RNA-Seq experiments suggest that *Francisella* does not utilize Zur-independent mechanisms of zinc-specific gene regulation.

3.4: *F. novicida* encodes *znuACB* homologues that are not regulated by Zur

Only one Zur-regulated gene is annotated as having transporter activity. This gene, *zupT* (FTN_0879), encodes a ZIP family protein that acts as a low affinity zinc transporter in other bacteria. No high affinity transporter homologs were identified as Zur-regulated by RNA-Seq, suggesting that these genes are either absent from the *F. novicida* genome or regulated by a zinc-independent mechanism. An operon with limited similarity to the high affinity ZnuABC zinc transporter was identified in TPEN-treated *F. tularensis* ssp. *tularensis* Schu S4 by RNA-Seq, indicating that this locus may contribute to zinc uptake. PCR was performed with cDNA generated from *F. novicida* and it was confirmed that these genes are encoded in an operon (Fig. 14). Based on the data below, the designation of this operon as *znuACB* is proposed.

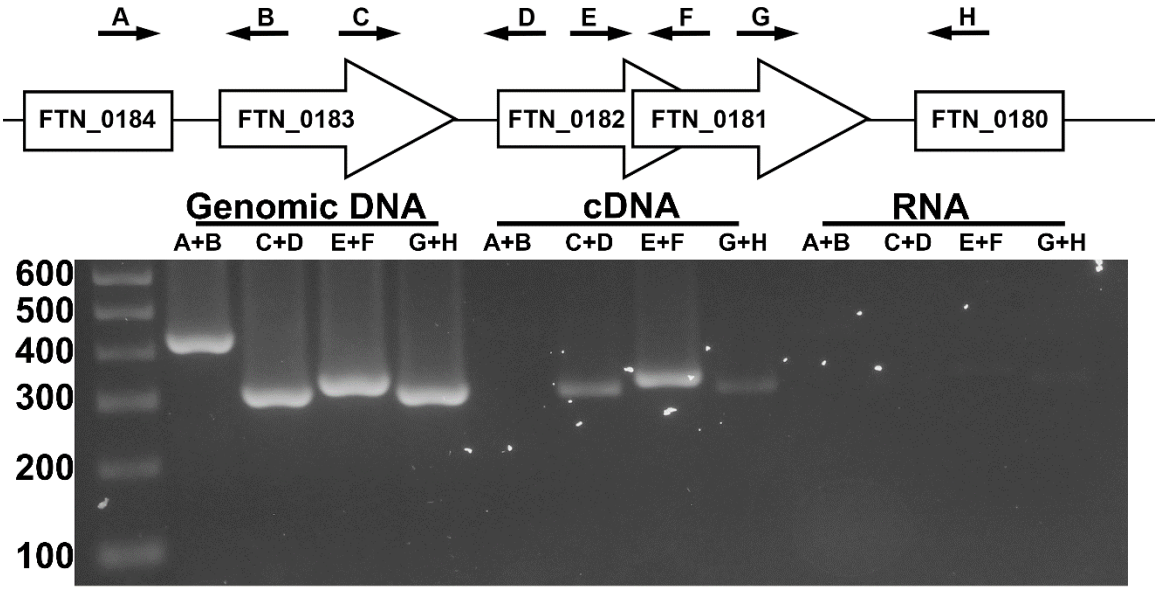
A
B
C
D
E
F
G
H
FTN_0184
FTN_0183
FTN_0182
FTN_0181
FTN_0180
Genomic DNA
cDNA
RNA
A+B
C+D
E+F
G+H
A+B
C+D
E+F
G+H
A+B
C+D
E+F
G+H
600
500
400
300
200
100

Figure 14: FTN_0183-FTN_0181 are encoded as an operon. RT-PCR was performed to amplify the intergenic regions of indicated genes in cDNA generated from isolated U112 RNA. PCR products were separated on a 2% agarose gel. PCR with genomic DNA or RNA were used as positive and negative controls, respectively.

While expression of a *znuC* homolog was slightly increased by RNA-Seq in TPEN-treated Schu S4, expression of neither *znuA* nor *znuB* was increased, and none of these genes were identified in RNA-Seq performed on TPEN-treated *F. novicida* U112, suggesting that this operon is unlikely to be regulated by zinc limitation. To better understand the regulation of this operon in response to zinc, expression of *znuA* transcript was analyzed by qRT-PCR. As previously described, expression of the *F. novicida zupT* homolog is increased >30 fold in a *zur::*TN mutant or during zinc limitation (Fig. 8A-B). In contrast, no difference in *znuA* expression was identified by qRT-PCR during either of these conditions in U112 (Fig. 15A-B) or under zinc limitation in Schu S4 (Fig. 15C), suggesting that *znuA* expression does not respond to differences in zinc concentration. Although no changes in expression were observed between untreated and TPEN-treated conditions, levels of *znuA* transcript were estimated by comparing qRT-PCR C_T values, the point at which fluorescence due to amplification surpasses a threshold level. Lower C_T values correlate with higher gene transcript. C_T values for *znuA* were similar in both conditions to *zupT* C_T values in the presence of TPEN (Fig. 15D), suggesting that while *znuA* expression does not respond to changes in zinc concentration, it is homeostatically expressed at high levels and may play a biologically important role in zinc uptake for *Francisella*.

3.5: *F. novicida zupT* facilitates growth under zinc limitation

If *zupT* and *znuACB* contribute to zinc uptake in *F. novicida*, single transposon mutant strains should have impaired zinc uptake compared to wild-type, which may affect their ability to grow under zinc limitation. To investigate

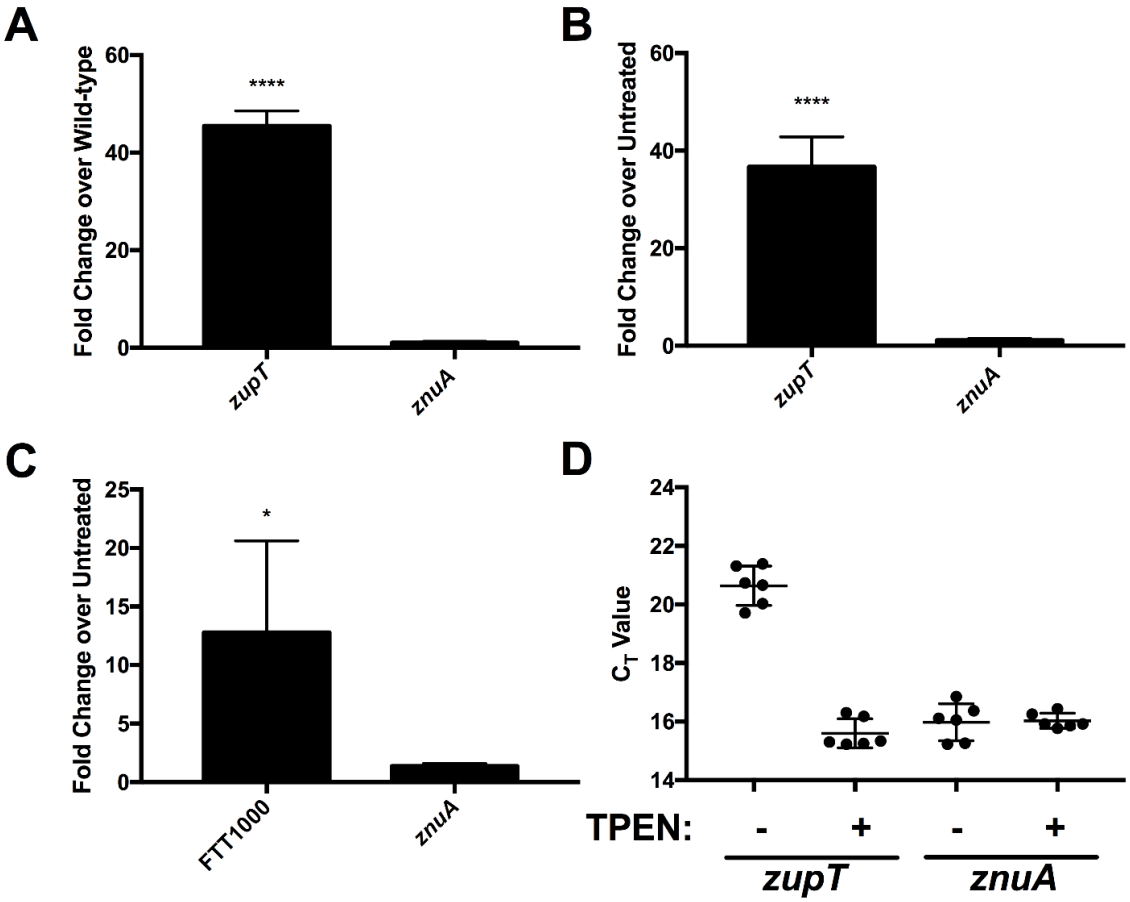
A
Fold Change over Wild-type
60
40
20
0
****
zupT
znuA
B
Fold Change over Untreated
60
40
20
0
****
zupT
znuA
C
Fold Change over Untreated
25
20
15
10
5
0
*
FTT1000
znuA
D
C_T Value
24
22
20
18
16
14
TPEN:
-
+
-
+
zupT
znuA

Figure 15: Expression of *znuA* is not regulated by Zur but is highly expressed. (A-B) Expression of *zupT* and *znuA* in either (A) a *zur::*TN mutant strain grown in complete CDM or (B) wild-type U112 grown in CDM supplemented with 10 μM TPEN. Expression is shown as fold change in expression over wild-type grown in untreated CDM from three biological replicates. (C) Expression of FTT1000 and *znuA* in wild-type Schu S4 grown in CDM supplemented with 4 μM TPEN. Expression is shown as fold change in expression over wild-type grown in untreated CDM from three biological replicates. Because *zupT* is a pseudogene in Schu S4, FTT1000 (the Schu S4 homolog of FTN_0880) was used as a control for increased gene expression. (D) C_T values for *zupT* or *znuA* from wild-type U112 grown in untreated or 10 μM TPEN-treated CDM. Statistical analysis was performed using a One way ANOVA with Dunnett's multiple comparison test to a reference value of 1.0. *, $p<0.05$; ****, $p<0.0001$.

the contribution of these transporters, growth of single *zupT* and *znuA* transposon mutants in *F. novicida* was examined under zinc-limiting conditions. No difference in growth was observed between wild-type and single transposon mutant strains grown in untreated and TPEN-treated CDM (data not shown), possibly due to utilization of intracellular zinc stores. To test this, wild-type and mutant strains were first starved overnight in TPEN-treated CDM to exhaust intracellular zinc stores, and then diluted into either complete or TPEN-treated CDM to test bacterial growth. Growth of a *zupT::*TN mutant strain was significantly delayed compared to wild-type in the presence of TPEN (Fig. 16A). Complementation of this strain *in trans* resulted in a restoration of growth to wild-type levels. Growth of *zupT::*TN was also restored with the addition of 2 μM $ZnSO_4$ to TPEN-treated cultures (Fig. 16B), while supplementation with 2 μM $MnCl_2$ failed to restore growth (Fig. 16C), suggesting that the growth defect observed was specifically due to zinc limitation. No difference in growth was observed in a *znuA::*TN mutant strain compared to wild-type in TPEN-treated media (Fig. 16A), suggesting that ZnuA may not play a major role in zinc transport in *F. novicida* or may transport metals other than zinc.

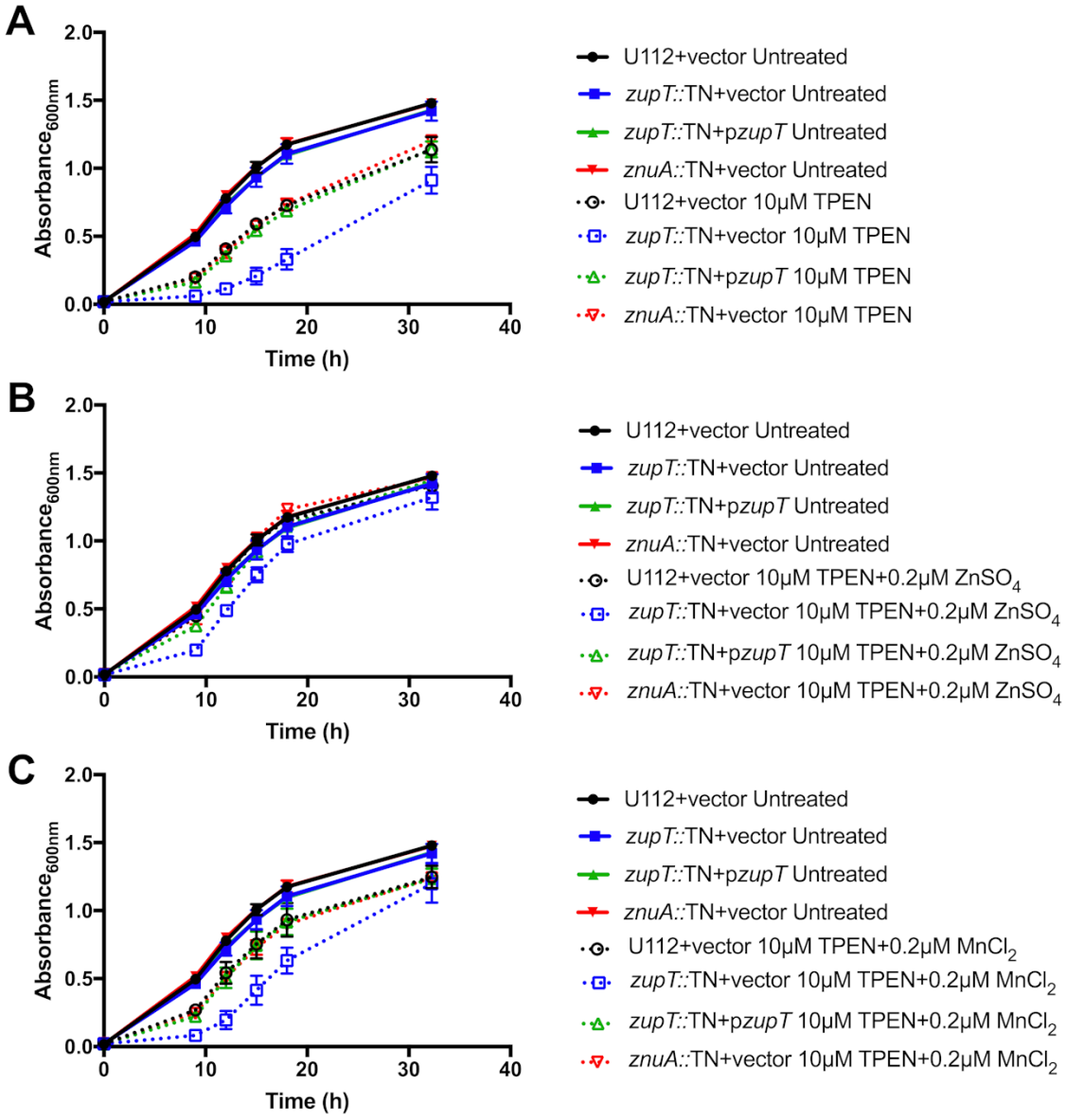
A
B
C
Absorbance600nm
Time (h)
0.0
0.5
1.0
1.5
2.0
0
10
20
30
40
U112+vector Untreated
zupT::TN+vector Untreated
zupT::TN+pzupT Untreated
znuA::TN+vector Untreated
U112+vector 10μM TPEN
zupT::TN+vector 10μM TPEN
zupT::TN+pzupT 10μM TPEN
znuA::TN+vector 10μM TPEN
U112+vector 10μM TPEN+0.2μM ZnSO4
zupT::TN+vector 10μM TPEN+0.2μM ZnSO4
zupT::TN+pzupT 10μM TPEN+0.2μM ZnSO4
znuA::TN+vector 10μM TPEN+0.2μM ZnSO4
U112+vector 10μM TPEN+0.2μM MnCl2
zupT::TN+vector 10μM TPEN+0.2μM MnCl2
zupT::TN+pzupT 10μM TPEN+0.2μM MnCl2
znuA::TN+vector 10μM TPEN+0.2μM MnCl2

Figure 16: Growth of *zupT*::TN is significantly delayed during zinc limitation. Growth of wild-type plus vector (black), *zupT::*TN plus vector (blue), *znuA::*TN plus vector (red), and *zupT::*TN plus p*zupT* (green) was measured by taking optical density readings at 600 nm (OD_{600}) of TPEN-starved cultures over time. Growth of strains in complete media (solid lines) is shown on all panels for comparison. Strains were grown (dotted lines) in either (A) CDM supplemented with 10 μM TPEN, (B) CDM supplemented with 10 μM TPEN and 2 μM $ZnSO_4$, or (C) CDM supplemented with 10 μM TPEN and 2 μM $MnCl_2$. Data presented is the average of three separate experiments.

Chapter 4: ZnuA is Required for Zinc Uptake and Optimal Intracellular Replication in Schu S4

4.1: *znuA* is essential in *F. tularensis* subsp. *tularensis* Schu S4

Although *F. novicida* is used as a model for more virulent *F. tularensis* subsp. *tularensis* strains, it has several differences that make comparisons between species difficult. Most notably, the more virulent strains are enriched in pseudogenes, many in metabolic pathways [20, 228]. This gene loss is observed in zinc-regulated genes, as well: of the three identified Zur-regulated genes in *F. novicida*, only one (FTN_0880) is thought to encode a functional protein in the *F. tularensis* subsp. *tularensis* Schu S4 strain (FTT1000). Notably, the *zupT* gene is disrupted by a premature stop codon in *F. tularensis* ssp. *tularensis* Schu S4, indicating that it is likely nonfunctional. While a *znuA::*TN mutant in *F. novicida* U112 did not exhibit a growth defect under zinc limitation, the loss of *zupT* in Schu S4 may result in a more prominent role for the ZnuABC transporter in this strain. Loss of *zupT* and other Zur-regulated genes likely impairs the ability of Schu S4 to acquire zinc and establish intracellular zinc stores, as Schu S4 exhibits increased sensitivity to zinc limitation compared to the U112 strain (Fig. 17) and is incapable of growth under zinc limitation after overnight zinc starvation (data not shown).

Because *znuACB* is likely the primary mechanism of zinc uptake in the virulent Schu S4 strain, the construction of a clean *znuA* deletion strain was attempted using an allelic replacement technique that has been previously

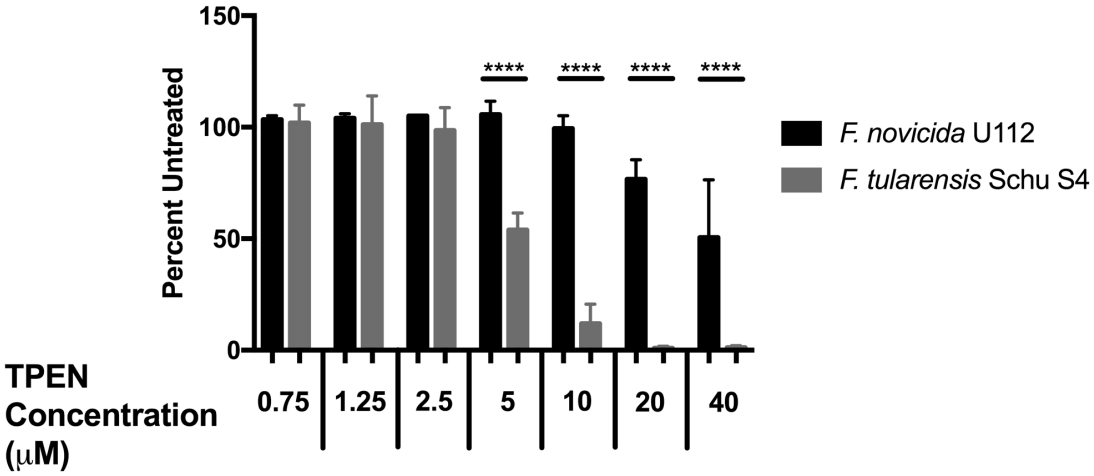
150
100
50
0
Percent Untreated
****
****
****
****
0.75
1.25
2.5
5
10
20
40
TPEN Concentration (μM)
F. novicida U112
F. tularensis Schu S4

Figure 17: *F. tularensis* ssp. *tularensis* Schu S4 is more sensitive to zinc limitation than *F. novicida* U112. Growth of either wild-type U112 (black) or Schu S4 (grey) strains in increasing concentrations of TPEN after 24 hours. Growth is presented as the percentage of untreated U112 or Schu S4, respectively. Data presented is the average of three separate experiments. Statistical analysis was performed using a One way ANOVA with Tukey's multiple comparison test. ****, $p<0.0001$.

described [98, 229]. Briefly, a suicide plasmid containing the upstream and downstream regions of *znuA* was introduced into Schu S4, leading to homologous integration into the genome. A recombination event and subsequent loss of the suicide plasmid should result in strains that randomly maintained either the genomic *znuA* copy or a clean *znuA* deletion. Despite multiple attempts, a clean deletion strain was not obtained using this method. Further investigation determined that, although the plasmid containing upstream and downstream regions of *znuA* was incorporated into the genome, recombination always favored maintaining the genomic *znuA* copy over the clean deletion of *znuA*, suggesting that there is strong selective pressure to maintain the *znuA* gene in Schu S4. To investigate the role of *znuA* in Schu S4, an inducible repression system was used (a kind gift of Dr. Tom Kawula) [230]. The *znuA* gene was first introduced into a *Francisella* plasmid so that *znuA* would be under the control of a promoter regulated by reverse TetR (RevTet) repression. Expression is turned off after the addition anhydrotetracycline (ATc), a tetracycline analogue that lacks antibiotic activity. A wild-type Schu S4 strain carrying the RevTet *znuA* plasmid was created, and then a genomic *znuA* deletion strain was generated in the presence of the RevTet *znuA* construct by the introduction of the *znuA* suicide plasmid as described above, resulting in a strain in which *znuA* expression can be repressed (Δ*znuA* p*znuA*).

Growth assays performed with the Δ*znuA* p*znuA* mutant in complete CDM produced variable results, possibly due to small variations in zinc within the

media. To control for media zinc concentrations, CDM was first Chelex®-treated to chelate metals before adding metals back at defined concentrations. Chelex®-treated CDM (Che-CDM) was then stored in acid-washed glassware to prevent leeching of zinc into the media. Wild-type Schu S4 containing p*znuA* and the Δ*znuA* p*znuA* mutant were first grown in Che-CDM supplemented with ATc to allow for ZnuA protein turnover. After 24 hours of growth in ATc, bacteria were diluted into Che-CDM with ATc, and qRT-PCR was used to confirm *znuA* repression relative to expression in untreated Che-CDM. Expression of *znuA* was significantly reduced in the Δ*znuA* p*znuA* mutant with addition of ATc compared to untreated conditions (Fig. 18A), indicating that ATc treatment successfully represses plasmid *znuA* expression. A Schu S4 strain expressing a RevTet construct encoding a hemagglutinin (HA)-tagged version of *znuA* was generated, and analysis of *znuA* protein levels by Western blot also showed decreased protein expression after ATc treatment (Fig. 18B). However, deletion of the genomic *znuA* gene in this strain was unsuccessful, possibly due to inefficient function of the tagged protein.

4.2: *znuA* is required for Schu S4 growth under zinc-limitation

If the ZnuABC transporter is a primary mechanism of zinc acquisition in Schu S4, the Δ*znuA* p*znuA* strain should also be impaired in its ability to acquire zinc. To estimate intracellular zinc levels, expression of the Zur-regulated gene FTT1000 (FTN_0880) was compared in the presence or absence of ATc by qRT-

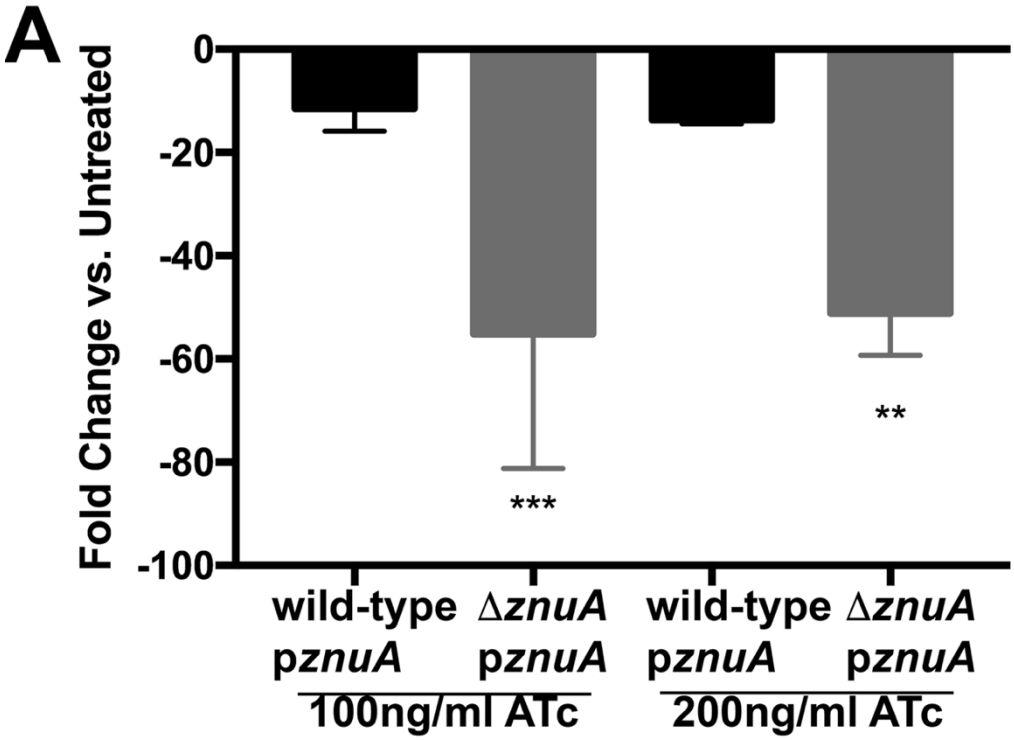
A
Fold Change vs. Untreated
0
-20
-40
-60
-80
-100
***
**
wild-type pznuA
ΔznuA pznuA
wild-type pznuA
ΔznuA pznuA
100ng/ml ATc
200ng/ml ATc

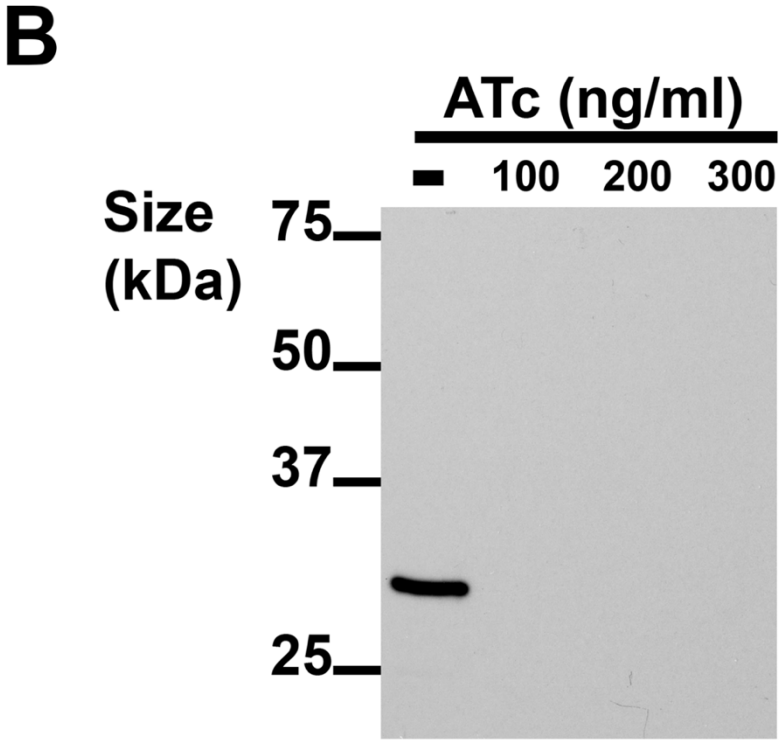
B
ATc (ng/ml)
-
100
200
300
Size (kDa)
75
50
37
25

Figure 18: Addition of ATc represses *znuA* expression. (A) Expression of *znuA* in either wild-type p*znuA* or the Δ*znuA* p*znuA* mutant grown in Che-CDM supplemented with either 100 ng/ml or 200 ng/ml ATc. Expression is shown as the fold change in expression over wild-type p*znuA* or Δ*znuA* p*znuA* strains grown in untreated Che-CDM from three biological replicates. Statistical analysis was performed using a One way ANOVA with Dunnett's multiple comparison test. **, $p<0.01$; ***, $p<0.001$. (B) Blot of whole cell lysates obtained from wildtype p*znuA*-HA after 24 hours of growth in either untreated CDM or CDM supplemented with 100 ng/ml, 200 ng/ml, or 300 ng/ml ATc. Whole cell lysates were loaded onto a polyacrylamide gel and transferred to a PVDF membrane. Nonspecific binding was blocked by incubating the blot overnight at 4°C in PBS-T with 5% milk. Blot was incubated with 1:10000 mouse anti-HA followed by 1:5000 goat anti-mouse. Expected band size for ZnuA-HA is 33.7 kDa.

PCR. If intracellular zinc is low, Zur-regulated genes should be derepressed, and FTT1000 gene expression should increase. Expression of FTT1000 was increased at least 10-fold in the Δz*nuA* pz*nuA* mutant treated with ATc compared to wild-type pz*nuA* treated with ATc (Fig. 19A), suggesting that repression of *znuA* expression results in decreased intracellular zinc.

The effect of *znuA* expression on *F. tularensis* ssp. *tularensis* growth was characterized by comparing growth of wild-type pz*nuA* and Δz*nuA* pz*nuA* strains in the presence and absence of ATc as described above. No difference in growth was observed between wild-type pz*nuA* and Δz*nuA* pz*nuA* strains in either untreated Che-CDM or Che-CDM supplemented with ATc (Fig. 19B). If *znuA* is acting as a zinc transporter, the Δz*nuA* pz*nuA* mutant should be unable to grow under zinc limitation when *znuA* expression is repressed. To test this, growth of the *Δz*nuA* pz*nuA* mutant strain was compared in the presence and absence of the zinc chelator TPEN. In bacteria that were not treated with ATc, no difference in growth of wild-type pz*nuA* and Δz*nuA* pz*nuA* strains was observed. However, when bacteria were first pretreated with ATc and then grown in Che-CDM supplemented with both ATc and TPEN, wild-type pz*nuA* grew normally while the Δz*nuA* pz*nuA* mutant failed to grow (Fig. 19B). These data demonstrate that, while treatment of the Δz*nuA* pz*nuA* mutant with ATc to repress *znuA* expression or TPEN to limit zinc concentrations do not affect bacterial growth, combination

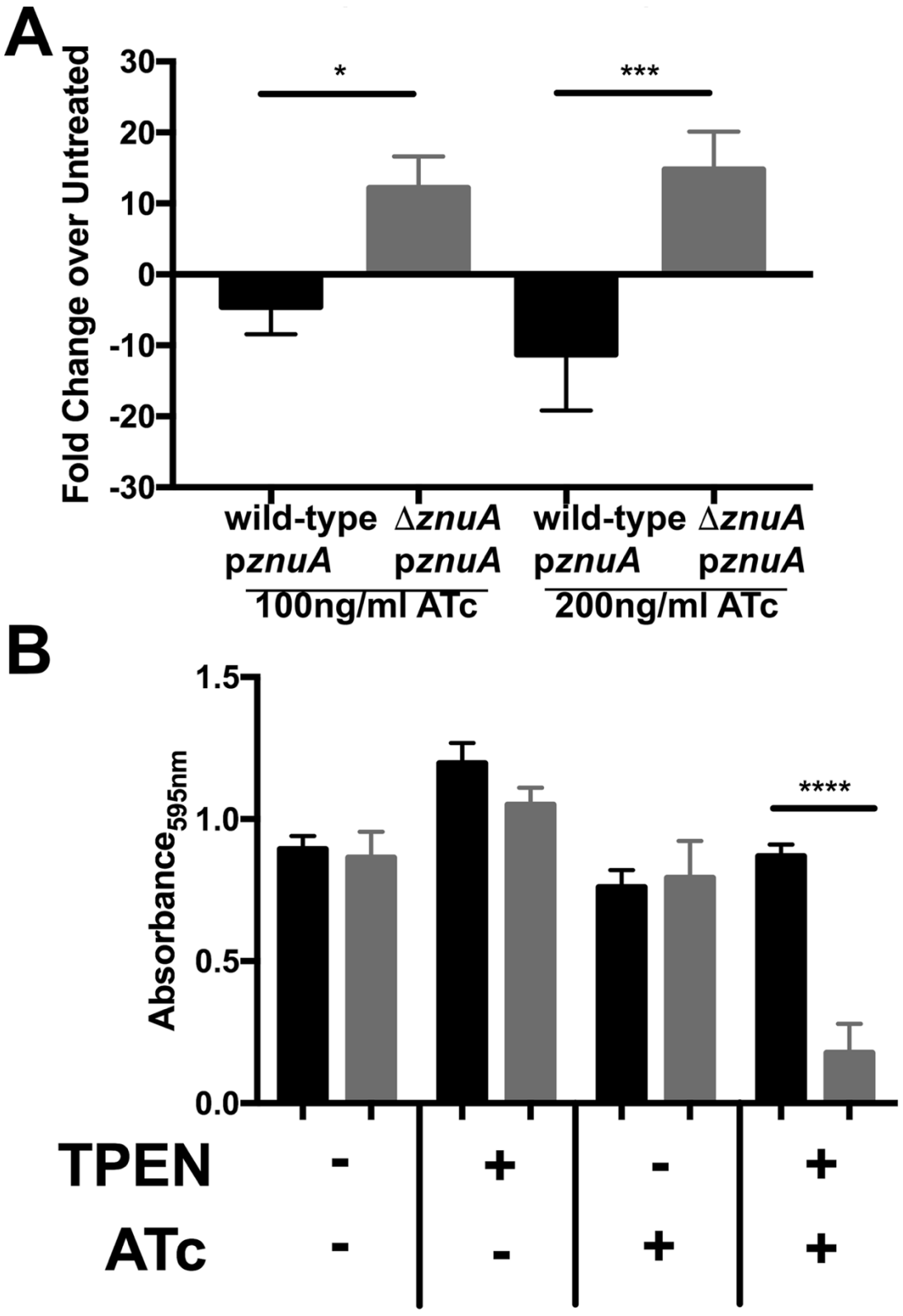
A
Fold Change over Untreated
30
20
10
0
-10
-20
-30
*
***
wild-type pznuA
ΔznuA pznuA
wild-type pznuA
ΔznuA pznuA
100ng/ml ATc
200ng/ml ATc
B
Absorbance595nm
1.5
1.0
0.5
0.0
****
TPEN
ATc
-
+
-
+
-
-
+
+

Figure 19: Growth of the Δ*znuA* p*znuA* mutant is impaired in the presence of both ATc and TPEN. (A) Expression of FTT1000 in either wild-type p*znuA* or the Δ*znuA* p*znuA* mutant grown in Che-CDM supplemented with either 100 ng/ml or 200 ng/ml ATc. Expression is shown as fold change in expression over wild-type p*znuA* or Δ*znuA* p*znuA* strains grown in untreated Che-CDM from three biological replicates. (B) Growth of either wild-type p*znuA* (black) or Δ*znuA* p*znuA* (grey) strains in either untreated Che-CDM or Che-CDM supplemented with 1.25 μM TPEN, 100 ng/ml ATc, or both TPEN and ATc after 24 hours. Strains grown in ATc were grown for 24 hours in Che-CDM supplemented with 100 ng/ml ATc prior to growth assay. Data presented is the average of three separate experiments. Statistical analysis was performed using a One way ANOVA with Dunnett's multiple comparison test. *, $p<0.05$; **, $p<0.01$; ***, $p<0.001$; ****, $p<0.0001$.

treatment greatly impairs bacterial growth. The decreased intracellular zinc as predicted by the increase in FTT1000 expression and the inability of the Δ*znuA* p*znuA* strain to grow in the presence of ATc and zinc limitation support that ZnuABC may be the sole mechanism of zinc uptake in Schu S4.

4.3: Growth of the *ΔznuA* p*znuA* mutant is impaired within J774A.1 macrophage-like cells

The role of zinc uptake has not been characterized for *Francisella* during intracellular growth. As *Francisella* quickly escapes from the phagosomal compartment to reside and grow within the host cell cytosol, limitation of zinc in this environment would likely have the greatest impact on bacterial growth.

To better understand the effect of the host cell cytosol on *Francisella* intracellular zinc levels, expression of the Zur-regulated gene FTT1000 was observed as a marker of zinc limitation during wild-type *F. tularensis* ssp. *tularensis* Schu S4 growth in J774A.1 macrophage-like cells. FTT1000 was significantly upregulated by qRT-PCR at eight hours post-infection (Fig. 20A), a timepoint when bacterial replication has likely begun, suggesting that the host cell cytosol is a zinc limiting environment. Similar upregulation of FTT1000 was observed in primary bone marrow-derived macrophages (data not shown). To characterize the significance of ZnuABC for intracellular replication, J774A.1 cells were infected with either wild-type p*znuA* or *ΔznuA* p*znuA* bacteria that were either untreated or pretreated with 100 ng/μl ATc. Growth of ATc-treated *ΔznuA* p*znuA* bacteria was significantly reduced compared to ATc-treated wild-type p*znuA* at both 24 and 48

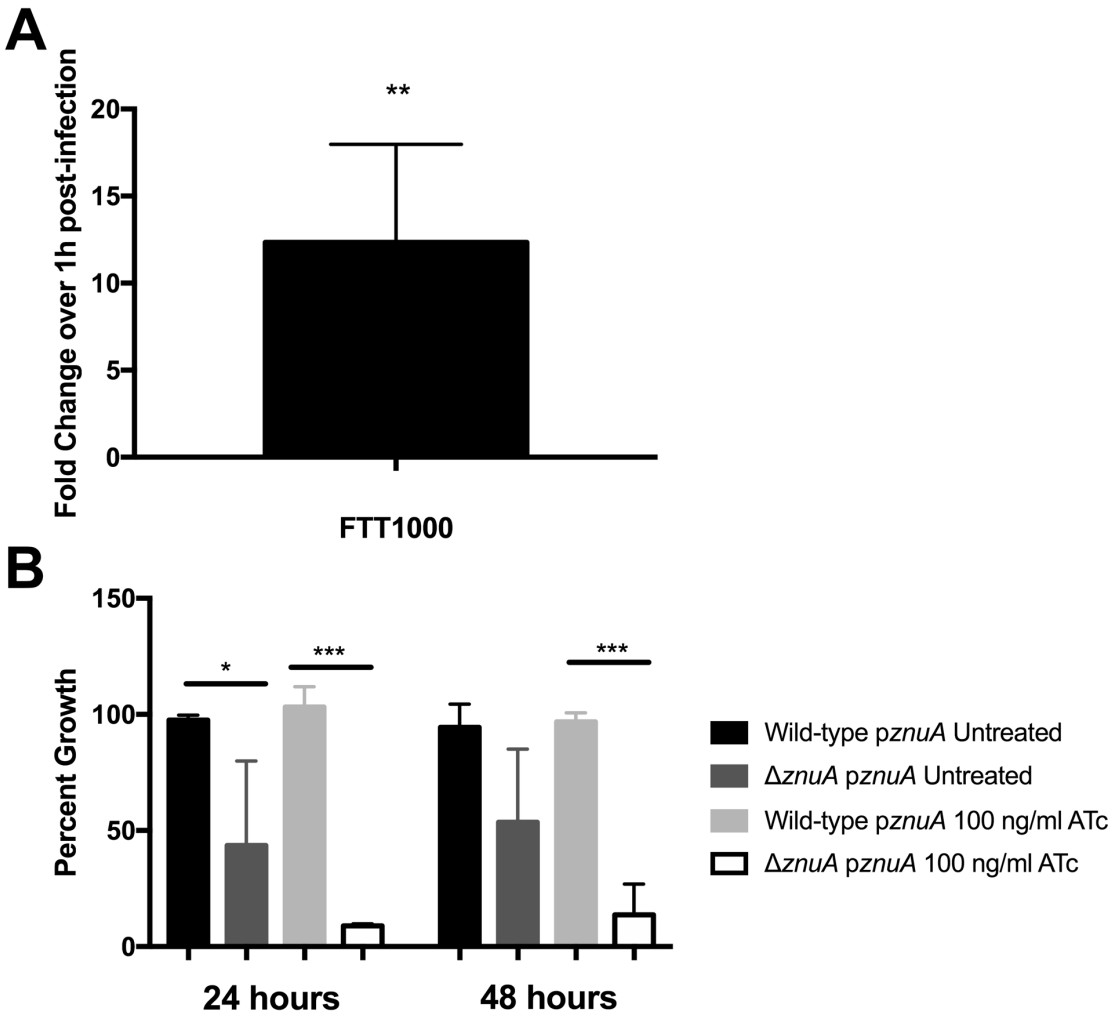
A
Fold Change over 1h post-infection
20
15
10
5
0
**
FTT1000
B
Percent Growth
150
100
50
0
*
***
***
24 hours
48 hours
Wild-type pznuA Untreated
ΔznuA pznuA Untreated
Wild-type pznuA 100 ng/ml ATc
ΔznuA pznuA 100 ng/ml ATc

Figure 20: The Δ*znuA* p*znuA* mutant is attenuated in intracellular growth within J774A.1 cells. (A) Expression of FTT1000 in wild-type Schu S4 grown within J774A.1 cells at eight hours post-infection. Expression is shown as the fold change in expression over wild-type at one hour post-infection. (B) Percent growth of untreated wild-type p*znuA* (black bars), untreated Δ*znuA* p*znuA* (dark grey bars), 100 ng/ml ATc-pretreated wild-type p*znuA* (light grey bars) or 100 ng/ml ATc-pretreated Δ*znuA* p*znuA* (white bars) strains in J774A.1 cells. Data represents the percent growth of each strain compared to either untreated or 100 ng/ml ATc-treated wild-type from three biological replicates. Statistical analysis was performed using (A) a Student's t test against a reference value of 1.0 (B) a One way ANOVA with Tukey's multiple comparison test. *, $p<0.05$; **, $p<0.01$; ***, $p<0.0001$.

hours post-infection (Fig. 20B). Growth of untreated *ΔznuA* p*znuA* bacteria varied across experiments but trended lower than untreated wild-type p*znuA*. These data suggest that *znuA* plays an important role in overcoming the zinc-limiting environment of the host cell cytosol to facilitate bacterial growth.

4.4: Expression of eukaryotic zinc homeostasis mechanisms is largely unchanged in response to *F. tularensis* infection.

Zur-regulated genes are upregulated during *F. tularensis* ssp. *tularensis* Schu S4 growth in the host cytoplasm and the Δ*znuA* p*znuA* mutant strain (Fig. 20B), which is unable to grow under zinc limitation, is attenuated at intracellular growth within J774A.1 macrophage-like cells. These data indicate that some level of zinc limitation occurs during Schu S4 intracellular growth, but it is unclear whether the host actively sequesters zinc in response to *F. tularensis* infection. The host is capable of controlling free zinc levels as a mechanism of control against bacterial pathogens through expression of ZIP and ZnT family transporters as well as MT proteins which can sequester free zinc. However, production of proinflammatory cytokines is inhibited in *F. tularensis*-infected cells [252], so it is possible that induction of ZIP and MT proteins is also inhibited by the bacteria. Preliminary RNA-Seq data from collaborators at the University of Maryland identified three ZIP genes (ZIP1, ZIP8, AND ZIP14) as potentially differentially expressed during infection of primary murine peritoneal macrophages with Schu S4. ZIP1 is ubiquitously expressed in all cell types [138], and ZIP8 and ZIP14 contribute to zinc limitation during infection [102, 125, 231], making them attractive candidates

for further investigation. To determine whether these transporters are stimulated during *F. tularensis* infection, J774A.1 macrophage-like cells were infected with Schu S4 and gene expression was analyzed at four and eight hours post-infection. None of the ZIP genes tested showed differential expression in Schu S4-infected J774A.1 cells at four hours post-infection compared to uninfected cells (Fig. 21). At eight hours post-infection, expression of ZIP1 and ZIP8 were similarly unchanged, while ZIP14 trended towards increased expression. Significance could not be determined with this sample due to variability between replicates, with a replicate showing no change in expression at this timepoint.

Although expression of these ZIPs was unchanged, it is possible that free zinc is instead sequestered through upregulation of MT proteins during Schu S4 infection. To more thoroughly investigate the role of host zinc homeostasis mechanisms during *F. tularensis* infection, expression of the major MT isoforms MT-1 and MT-2 was analyzed in Schu S4-infected J774A.1 cells at multiple timepoints. Overall, no differences in expression of MT-1 and MT-2 were observed at most timepoints examined (Fig. 22). Although MT-2 was differentially expressed at two hours post-infection and MT-1 at eight hours post-infection, expression of these genes was decreased, suggesting less sequestration of zinc from the host cytosol at these time points. Preliminary data looking at ZIP and MT expression in *F. tularensis*-infected BMDMs also observed no difference in gene expression compared to uninfected controls (data not shown), indicating that these results are not specific to J774A.1 cells. Taken together with the expression data

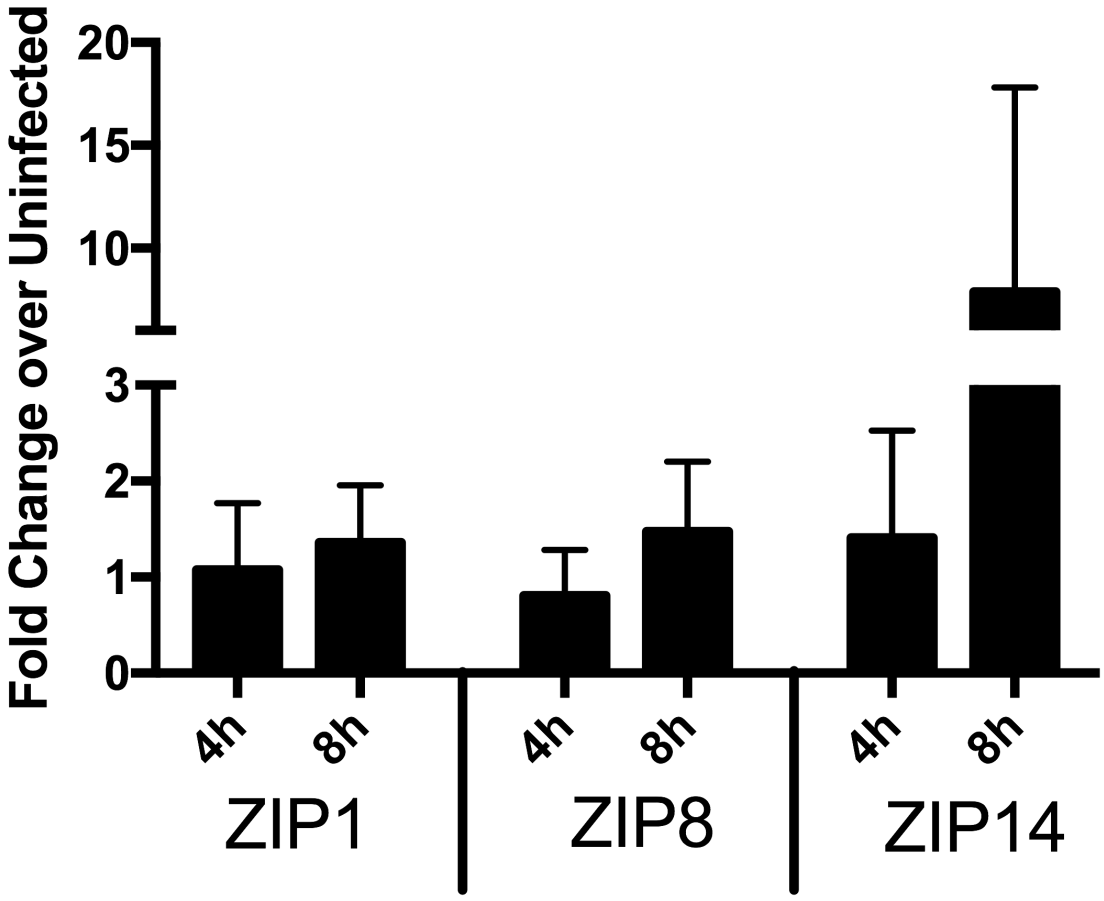
Fold Change over Uninfected
20
15
10
3
2
1
0
4h
8h
4h
8h
4h
8h
ZIP1
ZIP8
ZIP14

Figure 21: Expression of selected ZIP transporters is not significantly increased during Schu S4 infection. Expression of ZIP1, ZIP8, and ZIP14 in Schu S4-infected J774A.1 cells at four and eight hours post-infection. Expression is shown as the fold change in expression over uninfected J774A.1 cells at indicated timepoints. No statistical difference was observed using a One way ANOVA with Dunnett's multiple comparison test to a reference value of 1.0.

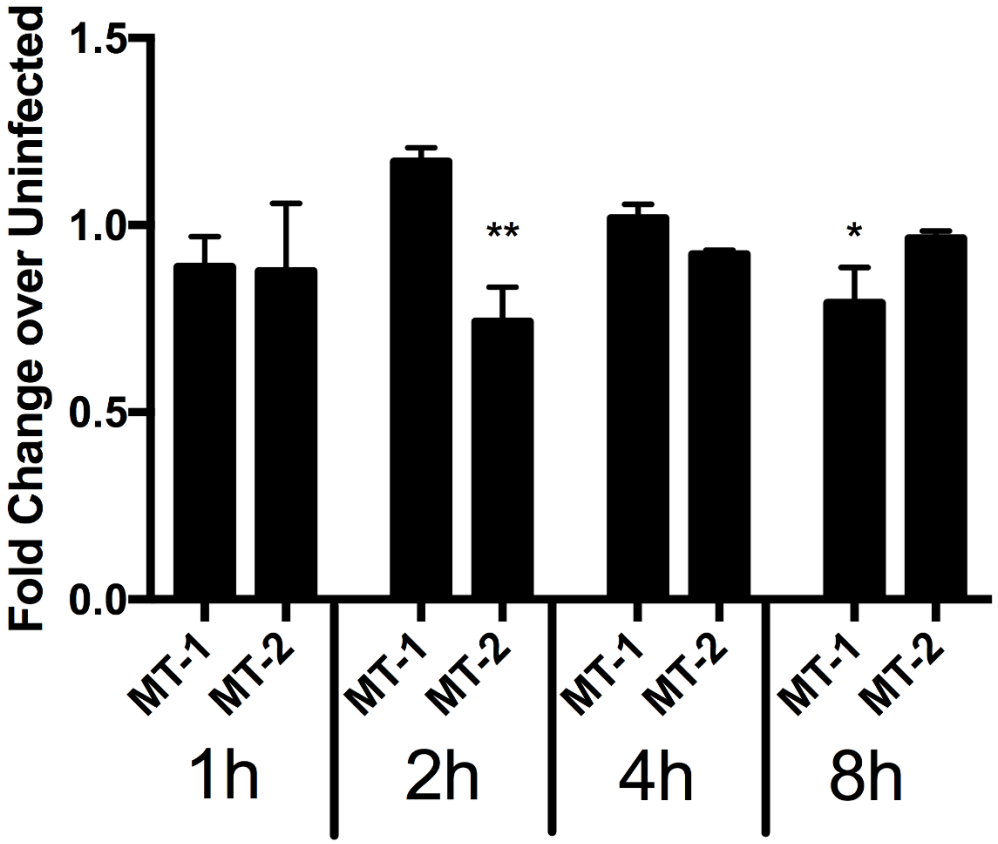
Fold Change over Uninfected
1.5
1.0
0.5
0.0
**
*
MT-1
MT-2
MT-1
MT-2
MT-1
MT-2
MT-1
MT-2
1h
2h
4h
8h

Figure 22: Expression of MT-1 and MT-2 is not significantly increased during Schu S4 infection. Expression of MT-1 and MT-2 in Schu S4-infected J774A.1 cells at one, two, four, and eight hours post-infection. Expression is shown as the fold change in expression over uninfected J774A.1 cells at indicated timepoints. Statistical analysis was performed using a One way ANOVA with Dunnett's multiple comparison test to a reference value of 1.0. *, $p<0.05$; **, $p<0.01$;

from selected ZIP genes, these data suggest that infection with Schu S4 does not elicit a zinc-sequestration response in the host.

4.5: Chelation and supplementation of zinc during infection does not impair Schu S4 intracellular growth.

Expression results with ZIP transporters and MT proteins suggest that mechanisms that sequester zinc are not stimulated during infection with *F. tularensis* ssp. *tularensis* Schu S4. The attenuation of the Δ*znuA* p*znuA* mutant strain (Fig. 20B) suggests that further zinc limitation during Schu S4 infection may be an effective strategy for suppressing bacterial growth. To test if manipulating intracellular zinc conditions can affect bacterial growth, J774A.1 cells were infected with wild-type Schu S4 in either untreated media, media supplemented with 1 μM TPEN, or media supplemented with 50 μM $ZnSO_4$. Bacterial burden was enumerated by colony counts at twenty-four hours post-infection. While bacterial levels were consistently elevated in both treatment conditions compared to growth of bacteria in untreated macrophages (Fig. 23), the levels of recovered bacteria varied from experiment to experiment and no statistically significant differences could be determined. Increased bacterial burden in zinc-supplemented cells may be due to increased macrophage numbers, as greater macrophages were attached in zinc-supplemented replicates compared to untreated or TPEN-treated macrophages by non-quantitative microscopic examination (data not shown). Overall, these data indicate that manipulation of zinc concentration during infection through either sequestration or supplementation does not limit bacterial

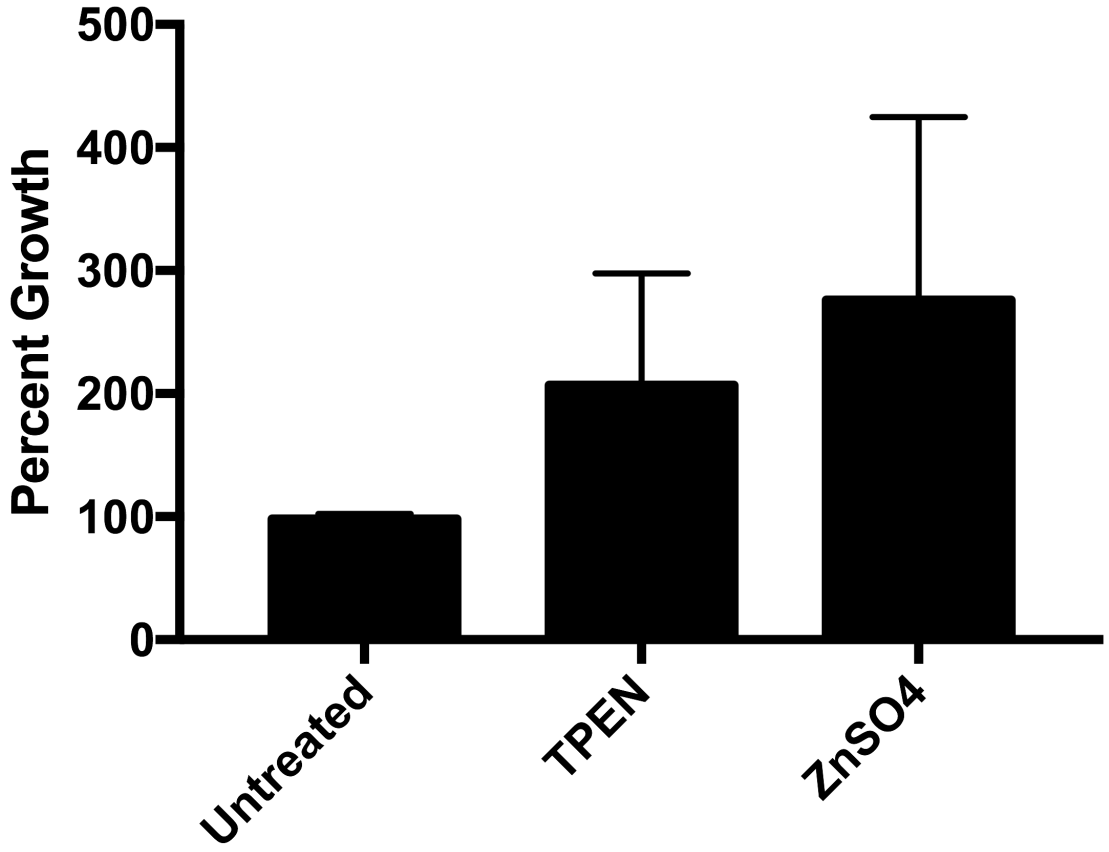
Percent Growth
500
400
300
200
100
0
Untreated
TPEN
ZnSO4

Figure 23: Limitation or supplementation of zinc during Schu S4 infection does not inhibit intracellular growth. Percent growth of wild-type Schu S4 in J774A.1 cells grown in either untreated DMEM, DMEM supplemented with 1 μM TPEN, or DMEM supplemented with 50 μM $ZnSO_4$ after 24 hours. Data represents the percent growth of each strain compared to wild-type growth in untreated J774A.1 cells in three separate experiments. No statistically significant difference was observed using a One way ANOVA with Tukey's multiple comparison test.

growth during infection, and suggest that Schu S4 is capable of adapting to zinc dishomeostasis within host cells.

Chapter 5: Discussion and Future Directions

Acquisition of zinc is critical for survival in the intracellular environment. Better understanding of regulatory mechanisms can potentially identify genes that are necessary for pathogen survival. This work characterizes the Zur regulon in *F. novicida* U112 and confirms three genes as Zur-regulated. Analysis of genes which were differentially expressed under zinc limitation identified a number of additional genes, but none of these genes appear to contribute to either zinc acquisition or homeostasis. In addition to the limited number of genes responsive to zinc limitation, only two zinc transporters were identified: ZnuABC and ZupT. The data presented suggests a model in which the importance of these transporters is dependent on the bacterial strain (Fig. 24). In the environmental isolate *F. novicida*, single *znuA* or *zupT* mutant strains either grow similarly to wild-type or show delayed growth but eventually reach wild-type levels. However, in the pathogenic *F. tularensis* subsp. *tularensis* Schu S4 strain, numerous Zur-regulated genes, including *zupT*, have been lost. As a consequence, ZnuABC appears to be the only remaining zinc transporter and *znuA* is essential. These data highlight differences in the necessity of genes between environmental and pathogenic *Francisella* strains and suggest differences in the nutritional requirements for the different environments in which these strains reside. Although acquisition of zinc is important for *F. tularensis* growth within macrophages, host zinc sequestration is not induced during Schu S4 infection. This is consistent with impaired detection of the bacteria by the host, a hallmark of *F. tularensis* infection that is also seen with

delayed neutrophil recruitment and impaired proinflammatory cytokine production.

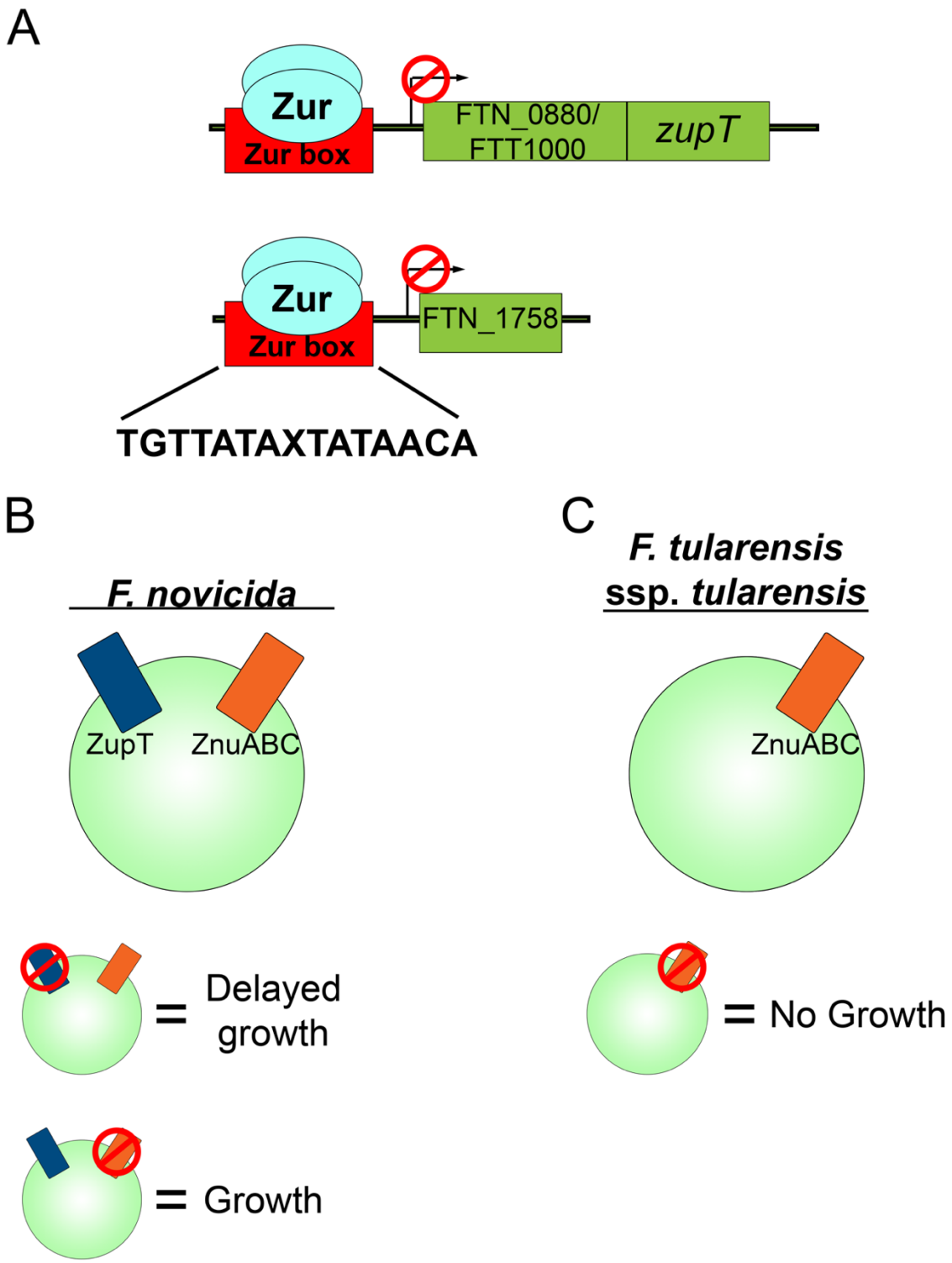
A
Zur
Zur box
FTN_0880/
FTT1000
zupT
Zur
Zur box
FTN_1758
TGTTATAXTATAACA
B
F. novicida
ZupT
ZnuABC
= Delayed growth
= Growth
C
F. tularensis
ssp. tularensis
ZnuABC
= No Growth

Figure 24: Model of Zur-mediated regulation and phenotypes of zinc transporter mutants. (A) Only three genes (FTN_0880, *zupT*, and FTN_1758) were confirmed to be regulated by Zur in *F. novicida*. Regulation of these genes is likely due to binding of Zur to an inverted repeat sequence upstream of regulated genes. While additional genes were identified by RNA-Seq in response to zinc limitation, these genes do not appear to contribute to zinc uptake or homeostasis, and may instead represent an iron limitation response. Overall, these data suggest that the three Zur regulated genes are the only zinc responsive genes that contribute to the response to zinc limitation. (B) ZupT and ZnuABC were the only zinc transporters identified by this work. In the environmental strain *F. novicida*, both genes are intact. Single deletion mutants in either *zupT* or *znuA* result in either delayed growth that eventually reaches wild-type levels, or no difference in growth compared to wild-type, respectively. These data suggest that neither transporter is essential on its own in this background. (C) In the pathogenic strain *F. tularensis* ssp. *tularensis,* the *zupT* gene is disrupted, leaving ZnuABC as the only functional zinc transporter. In this background *znuA* is essential, and repression of *znuA* expression in a knockdown eliminates bacterial growth. These data suggest that ZnuABC compensates for the loss of a functional ZupT transporter which leads to the essentiality of this gene.

5.1: Zinc uptake and homeostasis is controlled by a limited set of genes

RNA-Seq was performed to identify Zur-regulated genes in *F. novicida* U112. Five genes had significantly increased expression in a *zur::*TN mutant compared to wild-type (Table 1), three of which were confirmed by qRT-PCR as upregulated both in *zur::*TN and during zinc limitation (Fig. 8). While expression of FTN_0395 was slightly increased in a *zur::*TN mutant, it did not show differences in expression in response to zinc concentration and did not contain a consensus Zur-binding site, suggesting that it is not directly regulated by Zur. The slight increase in FTN_0395 expression in the *zur::*TN strain could be due to disruption of zinc homeostasis in the absence of Zur. Expression of an ArsR family transcriptional regulator was similarly increased in an *A. baumanii zur::*TN mutant [215]. FTN_1759 was also identified by RNA-Seq, but showed no difference in expression in either *zur::*TN or under zinc limitation. Detection of this gene may be due to expression of FTN_1758, which is highly upregulated and within close proximity to the gene.

Identifying only three Zur-regulated genes was unexpected, as analyses of Zur-regulated genes in other bacteria have identified regulons ranging from 15 to 100 genes [108, 215]. Genes with increased expression in *F. novicida zur::*TN also had increased expression under zinc limitation, and the upstream region of these genes contained predicted Zur-binding sequences (Fig. 8), indicating that while regulation by Zur in *Francisella* functions similarly to other bacteria, the *Francisella* Zur regulon is reduced. One possible explanation is that the *Francisella* genome

has pared the Zur regulon down to only those genes that are essential for growth under zinc limitation. However, the fact that *znuACB*, which is important for growth under zinc limitation, is present in *Francisella* but unregulated by Zur (Fig. 15) indicates that *Francisella* Zur-regulated genes are not the only genes required for growth under zinc limitation.

The limited number of Zur-regulated genes led to a hypothesis that *Francisella* encodes Zur-independent but zinc-dependent mechanisms of regulation for genes required for zinc uptake. However, RNA-Seq experiments investigating differences in gene expression under zinc limtiation in either *F. novicida* U112 or *F. tularensis* ssp. *tularensis* Schu S4 did not identify a large number of novel genes. Only 9 genes were identified as differentially expressed in U112 (Table 2) and 22 genes in Schu S4 (Table 3) in the presence of TPEN. Four of five genes identified by RNA-Seq in *zur*::TN were also identified by RNA-Seq in TPEN-treated U112 (Fig. 11). The only gene that was not differentially expressed in TPEN was FTN_0395, which was not significantly increased under these conditions by qRT-PCR. Although there was a high degree of similarity in identified genes in U112 RNA-Seq experiments, expression of only one gene was increased in both the Schu S4 RNA-Seq experiment and either U112 experiment (Fig. 11). The limited overlap in genes between these two subspecies is likely due to the reduced genome of Schu S4 compared to U112: only four of the nine genes identified by RNA-Seq in U112 are intact in the virulent Schu S4 strain. Of these genes, FTN_0880 was similarly upregulated in Schu S4 as observed in U112, while FTN_1022, FTN_0193, and FTN_1669 were not differentially expressed. The limited number of novel

genes identified in the presence of TPEN suggests that Zur-independent regulation of genes necessary for zinc uptake or zinc homeostasis is not likely.

The improbability of Zur-independent regulation is further supported by the predicted functions of the novel genes identified in TPEN-treated bacteria. Of the five new genes identified in *F. novicida*, only one appears to play a role in zinc uptake or homeostasis. Although one gene appears to encode an ArsR family regulator (FTN_1022), it is unclear whether this is due to zinc limitation or zinc dishomeostasis as suggested for FTN_0395. Other identified genes are not predicted to participate in zinc uptake or homeostasis: two genes encode proteins involved in aerobic respiration, one encodes a component of the Type IV pilus, and one encodes a hypothetical protein of unknown function. In *F. tularensis*, two TPEN-identified genes are implicated in zinc uptake or homeostasis: FTT1000 (FTN_0880), which was also upregulated in *zur*::TN, and *znuC*, which is part of an operon whose expression was confirmed to be independent of zinc concentration by qRT-PCR. No other genes identified in RNA-Seq experiments with TPEN-treated bacteria are predicted to contribute to either zinc uptake or homeostasis. Further investigation of the predicted functions of these genes indicate that expression of most identified genes is increased as part of an iron limitation or oxidative stress response rather than a response to zinc limitation. The most highly upregulated genes in *F. tularensis* are involved in iron acquisition, while other genes encode operons thought to function in riboflavin biosynthesis or generation of Fe-S clusters, both of which contribute to adaptation to iron limitation and the resulting oxidative stress [227, 232]. The functions of individual genes with

increased expression, such as genes encoding the DNA repair protein UvaR, DNA Topoisomerase I, and the DNA directed RNA polymerase RpoB, also suggest that TPEN-treated bacteria are responding to stress or DNA damage. Expression of genes involved in energy production was decreased in both *F. novicida* and *F. tularensis*, consistent with a bacterial response to growth under nutrient limitation or stress. This stress response may be due to off target chelation of iron by TPEN. An RNA-Seq experiment looking at genes differentially expressed in *E. coli* in the presence of TPEN also found upregulation of iron uptake and redox genes [233]. TPEN is considered a zinc specific metal chelator, but it also has some affinity for iron [234]. Alternatively, upregulation of these genes may be due to disruption of Fur, which regulates genes required for iron acquisition. Fur is a zinc-binding protein [115], so it is possible that zinc sequestration may interfere with Fur-meditated gene regulation. A much larger number of stress response genes were upregulated in *F. tularensis* compared to *F. novicida*, indicating that these bacteria are experiencing greater stress and consistent with increased sensitivity to TPEN treatment observed in *F. tularensis* Schu S4 (Fig. 17).

While it is unlikely that genes identified by TPEN RNA-Seq contribute to zinc acquisition, these genes need to be investigated further for confirmation. The iron acquisition genes identified have been previously shown not to contribute to zinc uptake in *Francisella* [225], but the role of other identified genes has not been investigated. Quantitative RT-PCR can be performed on remaining RNA-Seq genes to confirm that they are truly regulated by zinc limitation. To investigate whether upregulation of these genes is zinc-specific, TPEN-treated bacteria can be

supplemented with zinc to check for restoration of gene expression to homeostatic levels. Alternatively, bacteria can be treated with different metal chelators such as EDTA to prevent a TPEN-induced stress response. If upregulation of other identified genes is confirmed to be due to an oxidative stress response, it would indicate that the three Zur-regulated genes are the only *Francisella* genes regulated in a zinc-dependent manner. The absence of Zur-independent regulation mechanisms is consistent with previous investigation that found Zur to be the primary mechanism of zinc-dependent regulation among γ-proteobacteria [235]. The reduced number of zinc-regulated genes, along with the constitutive expression of *znuA* (Fig. 15) suggest that regulation of zinc import and homeostasis genes may be minimized due to bacterial adaptation to a zinc limiting environment. However, this hypothesis is not supported by the conservation of Zur among all *Francisella* strains analyzed or the essentiality of the Zur-regulated gene FTN_0880/FTT1000. Rather, these data suggest that Zur regulation is still important, but the genes involved in zinc uptake and homeostasis may be streamlined due to the small genome size of the bacteria.

Of note, only one Zur-regulated gene, FTN_0880/FTT1000, was maintained in *F. tularensis* ssp. *tularensis* Schu S4. This gene was also the only gene that was differentially expressed in all three RNA-Seq experiments. Attempts to delete FTT1000 in Schu S4 were unsuccessful, even in the presence of an *in trans* copy, suggesting that this gene is essential. The protein encoded by FTT1000 is a member of the COG0523 family of P-loop GTPases, which are hypothesized to have zinc chaperone and insertase activity. There is some evidence that these proteins

contribute to virulence. Mutation of a COG0523 family protein leads to an attenuation in intracellular growth within macrophages in *Brucella suis* [236] and dissemination in *A. baumannii* [181], suggesting that this family of proteins may contribute to virulence in other bacteria. In *F. novicida*, FTN_0880 is also regulated by PmrA, a transcription factor that also regulates the *Francisella* pathogenicity island [237]. Additionally, FTT1000 is expressed *in vivo* during murine infection with a virulent *F. tularensis* strain [238]. As this family of proteins is not well characterized, further investigation into the function and role in virulence of FTT1000 is necessary. However, because deletion of FTT1000 in Schu S4 has been unsuccessful, investigation of its function will likely require more biochemical approaches.

5.2: Differences in structure from traditional ZupT and ZnuA proteins may explain differences in gene regulation.

The *F. novicida zupT* gene was the only identified Zur-regulated gene annotated as a metal transporter. Regulation of *zupT* by Zur was unexpected, as characterized *zupT* homologs are not Zur-regulated and typically constitutively expressed. The only identified Zur-regulated *zupT* homolog is from *Cupriavidus metallidurans* [239], a bacterium that is adapted to growth in a high metal environment and lacks a ZnuABC-type zinc transporter, making ZupT the primary zinc uptake mechanism. The delayed growth of *F. novicida zupT*::TN under zinc limiting conditions (Fig. 16) highlights the elevated role of the protein in *Francisella* zinc uptake, as *zupT* mutant strains in other bacteria often have no

phenotype unless accompanied by mutations in other zinc transporters [190, 191]. Increased ZupT activity may be due to differences in *F. novicida zupT* promoter strength or ZupT zinc binding affinity. Regulation of *zupT* by Zur may be indicative of a stronger promoter in *F. novicida* compared to other *zupT* homologs and that repression of gene transcription is required under zinc-replete conditions, as overexpression of *zupT* in *E. coli* K12 renders bacteria hypersensitive to zinc [240]. Another possible explanation for the increased role of ZupT in *Francisella* zinc uptake is differences in amino acid sequence that enhance zinc binding affinity. The *F. novicida* ZupT protein has only around 35% identity over a 50 amino acid stretch of the ~250 amino acid protein with the *E. coli* ZupT homolog (Fig. 2), supporting the possibility that there could be structural differences that would enhance zinc binding affinity. Although ZupT has conserved serine, histidine, and glutamate residues (S114, H116, E120, and H143) that are required for zinc import [189], it is predicted to fold into a different structure with additional transmembrane domains and is missing a variable histidine-rich loop found in other ZIP and *zupT* homologs. Differences in these structural features of ZupT may be sufficient to alter its zinc binding affinity and enhance zinc transport.

It was also unusual that *znuACB* expression was not regulated by Zur in either *Francisella* species tested (Fig. 15). The *znuACB* operon is often regulated by Zur in other bacteria [202, 216, 241], presumably to regulate its expression and prevent zinc toxicity in a zinc replete environment. The *Francisella* Zur regulon is reduced compared to other bacteria, so this may just be a reflection of the minimized role of Zur in zinc-dependent regulation or of regulation of zinc-

dependent genes in general. However, Zur is intact in all *Francisella* isolates, and a number of Zur-regulated genes contribute to zinc uptake and homeostasis, indicating that Zur regulation may still be necessary in *Francisella*. Instead of indicating a minimized role for Zur regulation, constitutive expression of *znuACB* may reflect a restriction of *Francisella* to zinc poor environments that make it unnecessary to regulate expression of a high affinity zinc importer. The absence of a growth phenotype in a *F. novicida znuA*::TN mutant (Fig. 16) was unusual, as single *znuA* mutants are typically unable to grow in zinc limiting conditions [206, 207]. It is likely that functional ZupT compensates for the loss of *znuA* in *F. novicida*, as a knockdown of *znuA* in the *F. tularensis* ssp. *tularensis* background, which lacks *zupT*, is severely attenuating (Fig. 19). Testing of a double *znuA*/*zupT* mutant in *F. novicida* can confirm that growth of a *znuA*::TN strain under zinc limitation is due to compensation by *zupT* and not by compensation of a different gene that is also lost in *F. tularensis*. Differences in the function of *Francisella* ZnuA may also be due to differences in ZnuA structure: *F. novicida* ZnuA is missing two of the four conserved residues utilized for zinc binding (Fig. 3B). This protein also lacks a histidine-rich loop found in other ZnuA homologs. While this loop is not thought to function primarily in zinc-binding, it may aid in transfer of zinc to the transmembrane domain of ZnuABC. In *Salmonella* Typhimurium, deletion of the histidine-rich loop as well as a histidine-rich accessory protein ZinT greatly impairs bacterial growth under zinc limitation [199]. A gene encoding a small, histidine-rich protein is present in *F. novicida* (FTN_0764) and *F. tularensis* ssp. *tularensis* (FTT1110). This protein may function in a similar capacity to *Salmonella* Typhimurium ZinT, but it does not share sequence similarity or contain conserved

domains with ZinT. The absence of this loop in ZnuA may therefore contribute to differences in zinc affinity between *Francisella* ZnuA and other homologs.

Biochemical investigations of ZupT and ZnuA are necessary to better understand their zinc binding affinities and the role these proteins play in zinc uptake. Both proteins are predicted to function in zinc transport and mutants in each are attenuated in growth under zinc limitation, but transporter activity in *Francisella* has not been confirmed. Transporter activity can be estimated by measuring intracellular zinc concentrations in wild-type or single *zupT* or *znuA* mutant strains by Inductively Coupled Plasma Mass Spectrometry (ICP-MS). This technique can also characterize the specificity of ZupT and ZnuABC for zinc by measuring concentrations of other metals from bacterial samples. ZupT is reported to have broad specificity for metals such as iron, cobalt, and manganese [187], while ZnuA is more specific for zinc. Examination of mutant strains through ICP-MS can better define the specificity of these proteins for different metals. Although transport activity can be inferred from ICP-MS results, it does not specifically measure import of metal into the cell. In addition, intracellular zinc stores may mask differences in transporter activity until they are exhausted, at which point bacteria cannot be grown to levels necessary for ICP-MS analysis. This technical challenge may make assays specifically measuring the uptake of radiolabeled zinc into wild-type or mutant bacteria a more attractive option. Specificity of these transporters can be investigated by competing radiolabeled zinc with metals of interest and measuring differences in uptake. Isothermal titration calorimetry (ITC) can also be performed *in vitro* with ZupT and ZnuA to quantify binding

affinity for zinc or other metals. [242]. Differences in protein structure may explain differences in contribution of *Francisella* ZupT from homologs in other bacteria, but it may also be due to increased gene expression due to differences in promoter strength. The *F. novicida zupT* promoter can be compared to *zupT* promoters from other bacteria using a β-galactosidase assay, where a *lacZ* reporter gene is encoded downstream of promoter regions of interest. Differences in *lacZ* expression indicate differences in promoter strength. Better understanding of the gene expression as well as protein affinity and specificity for zinc will shed light on the specific roles of ZupT and ZnuABC in *Francisella* growth.

Inhibition of *znuA* expression in the Δ*znuA* p*znuA* mutant results in severely impaired growth under zinc limitation and attenuated in intracellular growth within macrophages. Based on these observations, ZnuA may represent an attractive target for vaccine or antimicrobial development. Innoculation of mice with a *Brucella abortus* or *Salmonella* Typhimurium Δ*znuA* mutant provides protection from challenge with wild-type bacteria [207, 243]. Neither *in vivo* virulence of the Δ*znuA* p*znuA* mutant compared to wild-type nor protection of Δ*znuA* p*znuA*-infected mice against wild-type challenge have been investigated. However, because the *znuA* gene appears to be essential in the virulent Schu S4 strain, generation of a Δ*znuA* live vaccine strain may not be possible in the virulent *F. tularensis* ssp. *tularensis* subspecies. A *znuA*::TN mutant has been generated in U112, but this strain is not attenuated in intracellular growth (data not shown) and vaccination with U112 does not provide protection against challenge with virulent

F. tularensis strains in the mouse model [244]. Therefore, production of antimicrobials targeting *znuA* may be a more feasible option. Antimicrobials targeting *Francisella znuA* may also represent a broad-spectrum antimicrobial due to the attenuation observed in other Δ*znuA* mutant strains. A ZnuA-binding compound has been demonstrated to inhibit *Salmonella* Typhimurium growth, providing proof-of-concept for a ZnuA-targeted antimicrobial [245]. To act as a broad-spectrum antimicrobial, identified compounds would need to target highly conserved domains on ZnuA, such as histidine, glutamate, or aspartate residues that coordinate zinc binding at the primary binding site.

It is unlikely that mechanisms besides ZupT and ZnuABC contribute to zinc uptake in *Francisella*, as none were identified bioinformatically or in RNA-Seq screens. Other pathogenic bacteria utilize ZupT and ZnuABC for zinc transport, but they can also encode a variety of additional zinc uptake mechanisms. While outer membrane proteins such as ZnuD have been observed in other virulent bacteria [201], no *znuD* homolog was identified bioinformatically in any *Francisella* genome. In addition, transport of zinc across the outer membrane by ZnuD is powered by the proton motive force in a TonB-dependent manner and *Francisella* lacks a functional *tonB* homolog [246], further indicating that porins are the primary mechanism of zinc passage across the outer membrane. Secreted zinc scavenging metallophores, such as those encoded by *Y. pestis* [203] and *P. aeruginosa* [204], represent another mechanism of zinc uptake. However, no homologs to metallophore biosynthesis genes were identified in *Francisella*. While *Francisella* encodes a siderophore for iron acquisition, this molecule does not bind

to zinc. Recently, the Type VI Secretion System has been implicated in acquisition of zinc [247]. However, no difference in bacterial growth was observed under zinc limitation between wild-type *F. tularensis* ssp. *tularensis* and an Δ*iglC* mutant (data not shown), which is unable to construct a functional T6SS. Although this does not eliminate the possibility that the T6SS contributes to zinc uptake in *Francisella*, it suggests that it is not the major mechanism of zinc uptake. Transporter assays with an Δ*iglC* mutant could determine with greater sensitivity whether or not the T6SS contributes to zinc uptake. Although it is possible that novel zinc transporters have not yet been identified, likely candidates have not been shown to contribute in *Francisella*.

5.3: Differences in zinc genes in *F. tularensis* highlight niche adaptation in virulent and environmental *Francisella* species

These data show significant differences between zinc homeostasis in *F. novicida* and *F. tularensis* ssp. *tularensis*. Wild-type *F. tularensis* Schu S4 is more sensitive to zinc limitation than *F. novicida* U112 (Fig. 17), which may be due to loss of additional mechanisms for acquiring zinc or adapting to zinc limitation in the virulent strain. Although *F. novicida* and *F. tularensis* ssp. *tularensis* share 98% genetic identity, virulent *Francisella* species are enriched in pseudogenes. Multiple Zur-regulated genes are absent or nonfunctional in Schu S4 compared to U112, potentially leading to compensation of these roles by remaining proteins. In U112, a *znuA::*TN mutant grows similarly to wild-type under zinc limitation and although growth in a *zupT::*TN mutant is delayed, it eventually reaches wild-type

levels (Fig. 16). In Schu S4, where *zupT* is a pseudogene, a Δ*znuA* p*znuA* mutant fails to grow after 24 hours under zinc limitation (Fig. 19), indicating that ZnuABC is the sole zinc transporter in this strain.

The gene loss observed in virulent *F. tularensis* subspecies represents an adaptation of these bacteria for the host environment. *F. tularensis* and *F. novicida* occupy distinct ecological niches: *F. tularensis* is a zoonotic pathogen propagated by an arthropod vector while there is no evidence of zoonotic *F. novicida* infection in nature [20]. Since diverging from an *F. novicida*-like precursor, *F. tularensis* species have lost genes in a number of metabolic pathways, such as amino acid biosynthesis and purine metabolism [20, 29, 228]. These pathways are no longer necessary for growth within the intracellular environment, as the bacteria have developed strategies to acquire these nutrients from the host [89]. Virulent *F. tularensis* subspecies have also lost genes encoding restriction systems for the destruction of foreign genetic material and quorum sensing biosynthesis genes that facilitate biofilm formation [20], consistent with adaptation to a solitary life cycle and to growth within the intracellular environment, respectively. Similarly, the absence of *zupT* and other Zur-regulated genes in Schu S4 suggests that these genes are unnecessary for growth within the host. This hypothesis is supported by analysis of the genomes of 19 environmental and virulent *Francisella* isolates. FTN_1758 and FTN_1759, genes identified by RNA-Seq in U112 *zur*::TN but absent in Schu S4, were present in all environmental isolates but absent in all virulent strains. The loss of these genes in only host-adapted strains suggests that these

genes are useful in an environmental niche but unnecessary for growth within the host.

Despite the disruption or deletion of many Zur-regulated genes in Schu S4, *znuACB* is specifically maintained, indicating that it plays a prominent role in zinc acquisition by more virulent *F. tularensis* subspecies. Growth of the Δ*znuA* p*znuA* strain is more severely affected by zinc limitation than in U112 *znuA::*TN or *zupT::*TN mutants, indicating that the ZnuABC transporter may compensate for the loss of ZupT function in Schu S4. Maintenance of the *znuACB* operon within virulent *F. tularensis* species is under strong selection, as attempts to delete the Schu S4 *znuA* gene were unsuccessful in the absence of an *in trans znuA* copy. Attempts to delete FTT1000 in Schu S4 were also unsuccessful, suggesting that there may also be pressure to maintain FTT1000 in Schu S4. Although many genes are inactivated or deleted in virulent *Francisella* species compared to environmental isolates, a core set of genes required for growth within the host appears to be maintained [248]. These genes include transporters for nutrient acquisition, such as the *fslABCD* operon, or transcriptional regulators such as *mglA*, which regulates expression of the *Francisella* pathogenicity island. Analysis of *Francisella* genomes supports the hypothesis that conserved zinc-dependent genes are critical for survival within the host. Functional copies of the *zur*, *znuACB,* and FTN_0880/FTT1000 genes are maintained in 100%, 95%, and 89%, respectively, of all isolates examined. These genes were also intact in all virulent

strains, suggesting that they are required for growth in the intracellular environment.

While disruption events have occurred in many genes in virulent *F. tularensis* strains, the majority of these gene disruptions occurred independently in different subspecies through convergent evolution [248]. For example, two genes in the isoleucine biosynthesis pathway are distinctly disrupted in *F. tularensis* ssp. *tularensis* and *F. tularensis* ssp. *holarctica* (through 100 and 300bp deletions in *tularensis* and a nonsense mutation and single nucleotide deletion in *holarctica*) [29]. This finding is consistent with the hypothesis that a core set of genes are required for growth within the host, and that all other genes are dispensable. It is unclear whether loss of dispensable genes is due to selective pressure for their removal or neutral genetic drift, in which loss of a gene does not positively or negatively affect bacterial fitness. Convergent loss of the same sets of genes in *F. tularensis* ssp. *tularensis* and *F. tularensis* ssp. *holarctica* may indicate that there is selective pressure to lose these genes, presumably as a mechanism to reduce bacterial metabolic burden. However, it is also possible that independent loss of the same genes merely indicates that these genes are no longer selected for in this environment, and inactivation is due to neutral genetic drift. Levels of synonymous mutations (silent substitutions that do not affect amino acid sequence) can be compared to non-synonymous mutations (which change amino acid sequence) to estimate the strength and mechanism of selective pressure on a gene [249]. Analysis of the genomes of environmental and virulent *Francisella* isolates found that host-adapted strains were subject to lower levels of selective

pressure than environmental isolates, consistent with low population sizes and limited recombination events in a favorable intracellular environment [248]. As few as ten bacteria can establish a *F. tularensis* infection in which the bacteria replicate to very large numbers, and this low infectious dose can lead to an evolutionary bottleneck where neutral gene inactivations are passed down to progeny and because the dominant genotype within a population. One such example may be the *zupT* gene, which is disrupted in all *F. tularensis* ssp. *tularensis* strains but no *F. tularensis* ssp. *holarctica* strains. It is possible that loss of *zupT* was selected for in *F. tularensis* ssp. *tularensis* by environmental selective pressures that are not present in the environment of *F. tularensis* ssp. *holarctica*, but this is unlikely due to the common host environment these strains inhabit. It may be more likely that loss of *zupT* in *F. tularensis* ssp. *tularensis* strains represents an early disruption event that was neutral due to compensation by ZnuABC. Evolutionary bottlenecking resulted in the Δ*zupT* genotype being passed to all *F. tularensis* ssp. *tularensis* strains, while this event has not yet occurred in *F. tularensis* ssp. *holarctica*. Under this hypothesis, *znuA* should not be essential in *F. tularensis* ssp. *holarctica*, and restoration of an intact *zupT* gene to *F. tularensis* ssp. *tularensis* should not result in decreased fitness compared to the wild-type strain.

This work highlights the need for caution when applying results from environmental *F. novicida* isolates to virulent strains. *F. novicida* U112 is commonly used as a surrogate for investigating the roles of genes in more virulent *F. tularensis* strains because it can be manipulated under BSL2 conditions and a transposon

library with insertions in all non-essential genes is available [23]. However, there is growing evidence that results obtained with *F. novicida* mutants do not always translate to more virulent strains. This is most often observed in mutations that attenuate intracellular growth or virulence in *F. novicida* but show no attenuation when replicated in *F. tularensis* [250, 251]. This work shows an alternate effect, where a gene is dispensable in *F. novicida* but essential in *F. tularensis* due to the reduced genome in this species. This indicates that some genes that are critical for *F. tularensis* virulence may not be detectible with high throughput screens in *F. novicida*. Although the *F. novicida* transposon library is a useful tool, it may not be able to exhaustively identify virulence factors in *F. tularensis*.

5.4: Host failure to sequester zinc during *F. tularensis* infection contributes to efficient bacterial growth.

None of the ZIPs or MTs tested showed a pattern of differential expression in *F. tularensis*-infected cells compared to uninfected cells. However, there are several limitations which minimize the conclusions that can be drawn from these data. First, the absence of ZIP induction does not necessarily mean that there are no changes in ZIP activity, as extracellular signals can result in post-translational changes to ZIP protein levels [148]. In addition, while no change in expression of the selected ZIPs was observed (Fig. 21), expression of ZIP genes was not exhaustively examined. There are 11 additional ZIP proteins and 10 ZnT proteins that may show differences in gene expression if examined. As ZIPs and ZnTs are expressed differently in different cell types and intracellular localizations,

differences in specific ZIP or ZnT expression may be cell specific. Investigating expression of other ZIP and ZnT genes would more comprehensively determine if a zinc-dependent immune response is elicited during Schu S4 infection. However, no difference in MT expression was observed during Schu S4 infection (Fig. 22), supporting the hypothesis that a zinc-dependent immune response is not elicited by *F. tularensis*. Furthermore, differential expression of MT-1 or MT-2 was also not observed in Schu S4-infected BMDMs (data not shown), suggesting that this phenotype is not due to cell type specific factors. Although there are additional MT isoforms that were not examined, MT-1 and MT-2 are the most ubiquitously expressed and are activated by proinflammatory signaling [134], indicating that these are the most likely isoforms to be induced during infection.

Overall, investigation of ZIP and ZnT expression needs to be more thoroughly investigated but initial results indicate that a zinc-dependent immune response is not elicited during Schu S4 infection. The pattern of ZIP and MT gene expression in Schu S4-infected cells is consistent with a suppressed immune response. Infection with *F. tularensis* is typically associated with insufficient immune activation and delayed proinflammatory cytokine production [26, 79]. The exact mechanism of impaired immune activation is not known, but *F. tularensis*-infected macrophages are no longer responsive to stimulation with *E. coli* LPS [252], implicating active suppression of the immune response. Expression of ZIP and MT genes is regulated by proinflammatory signaling [102, 176], so unchanged expression of these genes is consistent with the overall repression of the immune response in infected cells. Of note, the three ZIP genes analyzed in

this work were selected due to preliminary RNA-Seq data from murine peritoneal macrophages infected with Schu S4. However, these cells were elicited with thioglycolate before isolation, which may alter gene expression in these cells compared to naïve macrophages and may explain why ZIPs were upregulated in these cells but not in the J774s tested here.

In the absence of increased ZIP or MT expression, zinc was sequestered during infection to mimic a zinc-limiting immune response. While sequestration or supplementation of zinc during Schu S4 infection did not reduce bacterial growth after 24 hours (Fig. 23), this does not necessarily indicate that limiting intracellular zinc concentration does not affect Schu S4 intracellular growth. Expression of ZIP and ZnT genes was not examined during this experiment, so it is possible that upregulation of ZIPs or ZnTs in response to changing zinc concentration compensated for TPEN or $ZnSO_4$ treatment, leading to no change in zinc levels within the cell. In addition, increased intracellular zinc does not necessarily mean that free cytosolic zinc levels are altered, as MT-mediated sequestration or transport of zinc into intracellular compartments may maintain cytosolic zinc at homeostatic levels. The concentration of TPEN added to host cells does not impair Schu S4 growth i*n vitro* (Fig. 17) and higher levels of TPEN resulted in elevated host cell death (data not shown). These data indicate that zinc sequestration has a larger effect on host cells than on the bacteria, making the effects of zinc limitation on Schu S4 intracellular growth difficult to measure.

Additional experiments are necessary to further define the role zinc limitation plays during *Francisella* infection. Cells could be pretreated with cytokines that increase MT and ZIP expression before Schu S4 infection, but any attenuation in growth may be due to off-target effects on other immune mechanisms. Constitutive expression of plasmid-encoded ZIP or MT genes may be a mechanism to restrict free cytosolic zinc within the host [102], and overexpression of these genes may be able to overcome the suppression of immune activation observed during Schu S4 infection. Differences in free cytosolic zinc could be measured using fluorescent reporter dyes, such as Zinquin or FluoZin-3 [253] to ensure changes in zinc concentration. While differences may not be observed with wild-type Schu S4, the Δ*znuA* p*znuA* mutant should be more sensitive to changes in zinc concentration and be a useful tool for identifying more subtle differences.

Appendix A: *Francisella* FopA is an Outer Membrane Protein Necessary for Maintenance of Bacterial Membrane Integrity

A.1: Abstract

Francisella tularensis is a facultative intracellular pathogen and the cause of the potentially life-threatening disease tularemia. Infection with highly virulent strains of *Francisella* is characterized by a delayed immune response until 48-72 hours post-infection despite rapid replication within the host. Suppression of the host immune response contributes to this delay, as macrophages and dendritic cells infected with *Francisella* are no longer responsive to *in vitro* stimulation with *E. coli* LPS. However, the mechanism by which *Francisella* is capable of suppressing immune responsiveness is not completely understood. A mutant in the abundant outer membrane protein FopA was identified through a competition assay as attenuated for internalization within macrophages compared to wild-type bacteria. Subsequent investigation determined that this strain had decreased levels of attachment to host cells, as well as decreased bacterial burden at later timepoints. Δ*fopA* bacteria colocalized at higher levels with the late endosomal marker LAMP1, suggesting that a defect in phagosomal escape may contribute to its attenuation. This mutant also elicited increased activation of NF-κB, implicating FopA in dampening of the immune response. However, because FopA is predicted to act as an anchor to stabilize the outer membrane, these phenotypes could also

reflect generalized membrane perturbations in the mutant strain. Subsequent studies determined that the Δ*fopA* mutant showed signs of membrane instability: Δ*fopA* mutant cell morphology was irregular and misshapen, Δ*fopA* bacteria grown in culture had fewer viable bacteria than wild-type during log phase growth, and mutant bacteria exhibited both increased sensitivity to detergents and release of antigens into the media. Overall, these data suggest that deletion of *fopA* results in membrane instability, bacterial death and antigen release, ultimately leading to induction of an immune response.

A.2: Introduction

Francisella tularensis is a Gram-negative bacterium and a facultative intracellular pathogen within the host. *Francisella* first attaches to host cells using surface adhesins such as the Type IV pilus or FsaP [254]. Uptake of attached bacteria is facilitated by host receptors such as the Fc receptor, Complement Receptor 3 (CR3), the Class A Scavenger Receptor 1, or the Mannose receptor [48, 49]. After uptake, bacteria reside within a phagosome but escape into the host cell cytosol within 30 minutes to two hours, with the kinetics of bacterial escape influenced by the receptor used for uptake [54]. Once the bacteria enter the cytosol, they are able to replicate to high numbers, ultimately leading to host cell lysis [52]. Infection with the virulent *F. tularensis* subspecies is associated with decreased immune detection at early timepoints as shown by delayed recruitment of neutrophils [26] and low levels of proinflammatory cytokine production [27, 73]. The dampened immune response to *F. tularensis* is partially due to impaired

bacterial recognition: *Francisella* LPS is not recognized by host TLR4 due to Lipid A modifications [67, 68]. In addition to an absence of recognition, decreased immune response to *Francisella* is also due to active suppression by the bacteria. Macrophages and dendritic cells infected with virulent *F. tularensis* Schu S4, but not avirulent species, are unable to respond to stimulation with *E. coli* LPS [252, 255, 256], suggesting that virulent strains are capable of suppressing the host immune response.

One potential mechanism of immune suppression is signaling crosstalk between TLRs and surface receptor interactions. Immune suppression can occur through direct interactions of bacterial proteins with host TLRs. Although the *Y. pestis* virulence factor LcrV directly interacts with TLR2, this interaction results in the production of anti-inflammatory cytokine IL-10 rather than the pro-inflammatory cytokine IL-12 [257]. Another mechanism of immune suppression relies on crosstalk between TLRs and surface receptors, where pathogen interactions with a host surface receptor results in inhibition of TLR inflammatory signaling. *M. tuberculosis* expression of ManLAM, a secreted cell wall component, has been implicated in inhibition of dendritic cell maturation and pro-inflammatory cytokine production. This process is dependent on interactions with dendritic cell receptors DC-SIGN [258] and the Mannose receptor [259], as production of cytokines is restored when interaction between these receptors and ManLAM is blocked. Crosstalk between host surface receptors and inflammatory signaling has also been observed in virulent *F. tularensis* species, as uptake of Schu S4 through CR3 results in decreased pro-inflammatory cytokine production due

to decreased phosphorylation of ERK1/2 and p38, signaling molecules that facilitate a proinflammatory response [50].This is due to activation of the MAPK phosphatase MKP-1 during Schu S4 uptake by CR3 but not by other receptors. This process was specific to the virulent Schu S4 strain, as *F. novicida* U112 was unable to suppress MAPK phosphorylation during CR3-mediated uptake.

Bacterial outer membrane proteins have many important contributions to bacterial survival, including membrane stability and passive solute transport [260]. OmpA is the most well characterized outer membrane protein, composed of an N-terminal eight β-strand barrel domain that is incorporated into the bacterial outer membrane and a C-terminal domain that is non-covalently associated with the peptidoglycan layer [261]. Association between OmpA and the peptidoglycan layer anchors the outer membrane, adding stability to the cell. The structure of the OmpA β-barrel forms a narrow pore allowing passive diffusion of ions and larger solutes [262, 263]. In addition to its role in membrane stability and passive transport, OmpA proteins can contribute to virulence in pathogenic bacteria. OmpA homologues in bacteria such as *E. coli*, *N. gonorrhea*, and *K. pneumoniae* have been implicated in adherence to mucosal epithelial cells [264-266]. OmpA from the meningitis-causing *E. coli* K1 strains also facilitates invasion of brain microvascular endothelial cells, allowing transversal past the blood-brain barrier [267]. OmpA homologs also contribute to host signaling: interactions between OmpA homologues and epithelial surface proteins can stimulate an immune response,

leading to MAPK and NF-κB activation and pro-inflammatory cytokine production [266, 268].

Francisella outer membrane protein A (FopA) is an OmpA family protein that was identified as a dominant immunoreactive protein in sera from *Francisella* infected patients [269-271]. Despite being an immunodominant antigen, antibodies against FopA are not protective against virulent *F. tularensis* challenge [272]. While FopA has been heavily investigated for its potential as a protective antigen [271-274] or as a marker for detection of *Francisella* by PCR [275-278], its contributions to virulence are not well understood. Cells infected with a U112 Δ*fopA* mutant strain exhibited higher levels of cell lysis than seen in wild-type infected cells, and this hypercytotoxicity was dependent on activation of the AIM2 inflammasome [279]. Elevated activation of the inflammasome may suggest increased release of bacterial products in the Δ*fopA* mutant and that FopA contributes to bacterial membrane integrity. FopA has also been shown to associate with DipA, a virulence factor required for intracellular growth and dissemination in Schu S4, and a Δ*fopA* mutant shared similar phenotype to a Δ*dipA* mutant in Schu S4 [280]. The FopA amino acid sequence is highly conserved (98% identity) between *Francisella* strains, suggesting that it may have a conserved function among *Francisella* species.

This work addresses the role of *fopA* in *Francisella* virulence. A U112 *fopA::*TN mutant was identified in a competition assay as attenuated in

internalization into host cells. Further investigation determined that this was due to a defect in attachment of the bacteria to host cells compared to wild-type. Macrophages infected with Δ*fopA* mutant in Schu S4 also showed decreased bacterial burdens at 24 hours post-infection compared to wild-type. Further investigation determined that Δ*fopA* mutant displays increased colocalization with the late phagosomal marker LAMP1 and increased activation of NF-κB, suggesting that this strain may be unable to dampen the host immune response. However, characterization of the Δ*fopA* strain determined that bacterial membranes were unstable, indicating that release of PAMPs and decreased bacterial viability explain these intracellular findings.

A.3: Disruption of *fopA* results in decreased attachment to and bacterial burden within host cells.

To identify *Francisella* genes that may contribute to surface interactions with the host, the *F. novicida* U112 genome was analyzed bioinformatically for predicted surface proteins based on signal sequence, number of predicted transmembrane domains, predicted homology to known proteins from other bacteria, and presence of homologs in the *F. tularensis* ssp. *tularensis* strain. Candidate genes were selected, and *F. novicida* transposon mutants in selected genes were utilized to screen for defects in internalization. Coinfections of J774A.1 cells were performed with a mix of wild-type and transposon mutant bacteria. After allowing internalization for two hours, bacteria were enumerated and compared to the number of input bacteria to calculate competitive indexes. Competition assays

were also performed using a *fipB*::TN mutant as a positive control for impaired competition with wild-type U112 [281]. A transposon mutant strain in the *fopA* gene was identified as being significantly less competitive than the wild-type strain at internalization within cells (Fig. A1), implicating FopA in either attachment or internalization of *Francisella* into host cells. A transposon mutant strain in FTN_0445, which encodes a DUF3573-containing protein and was also selected by the screening criteria, showed no difference in competition with wild-type.

While U112 is often used to identify virulence gene candidates, performing downstream experiments with virulent *Francisella* strains ensures that any results are relevant to human disease. To investigate whether FopA may contribute to internalization in the virulent *F. tularensis* ssp. *tularensis* strain, a Schu S4 Δ*fopA* mutant was generated using an allelic replacement technique previously described [98, 229]. To first address the decreased competition for internalization in the U112 *fopA*::TN mutant, attachment to J774A.1 macrophage-like cells was assayed. Wild-type and Δ*fopA* mutant bacteria were individually added to wells seeded with J774A.1 cells kept at 4° C to prevent actin-mediated internalization. After three hours, bacteria were enumerated and compared to input levels. Attachment of Δ*fopA* bacteria to J774A.1 cells was consistently decreased compared with wild-type, but this decrease did not meet statistical significance (Fig. A2A). The role of FopA in internalization and intracellular growth was also characterized. Bacterial colony counts of wild-type and Δ*fopA* bacteria were

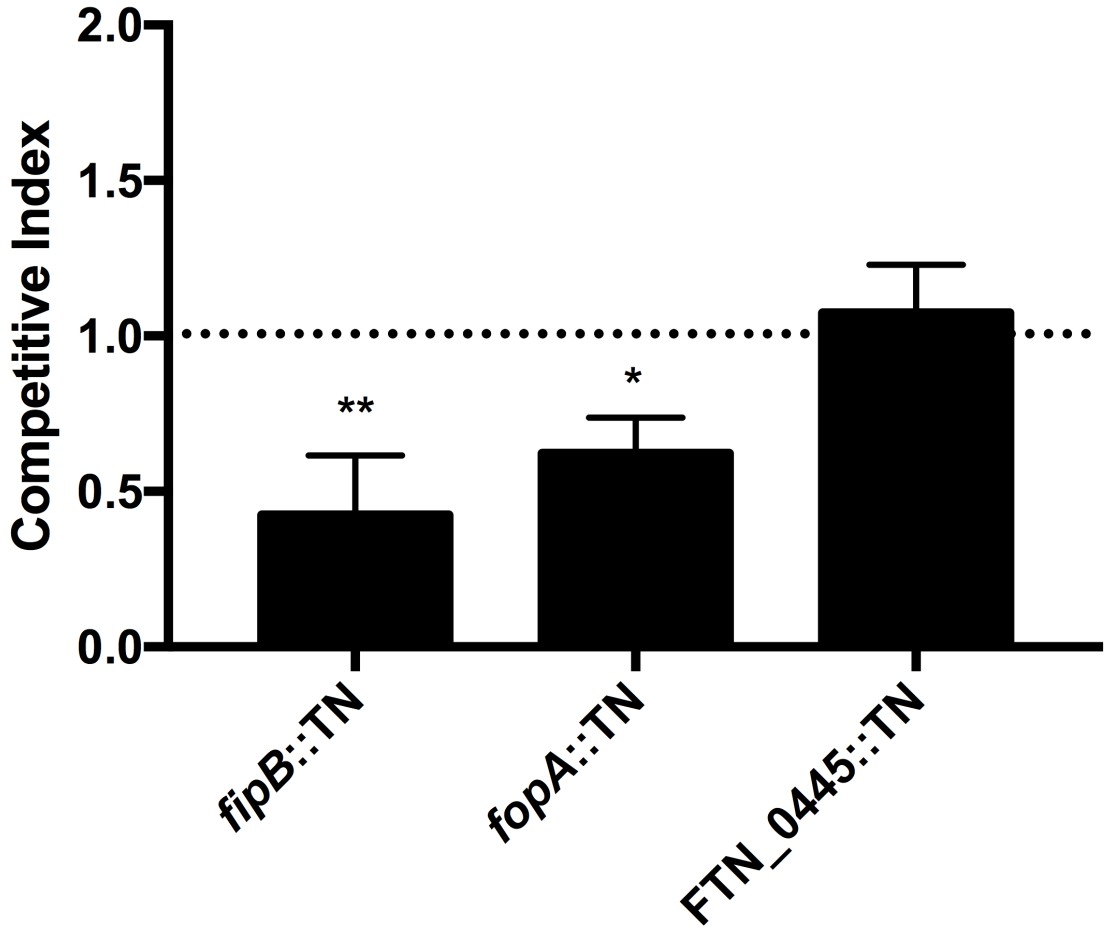
Competitive Index
2.0
1.5
1.0
0.5
0.0
**
*
fipB::TN
fopA::TN
FTN_0445::TN

Figure A1: *fopA*::TN is less competitive than wild-type U112 at internalization of J774A.1 cells. Competitive indexes (CIs) of *fopA*::TN and FTN_0445::TN with wild-type U112. Competition between wild-type and *fipB*::TN was used as a positive control for decreased bacterial competition. CIs were calculated by comparing the ratio of wild-type and mutant bacteria at two hours post-infection to the ratio of wild-type and mutant bacteria at the initial input. CIs greater than 1.0 represent increased competitiveness of the mutant compared to wild-type, while CIs less than 1.0 represent decreased competitiveness compared to wild-type. Statistical analysis was performed using a One way ANOVA with Dunnett's multiple comparison test to a reference value of 1.0. *, $p<0.05$; **, $p<0.01$

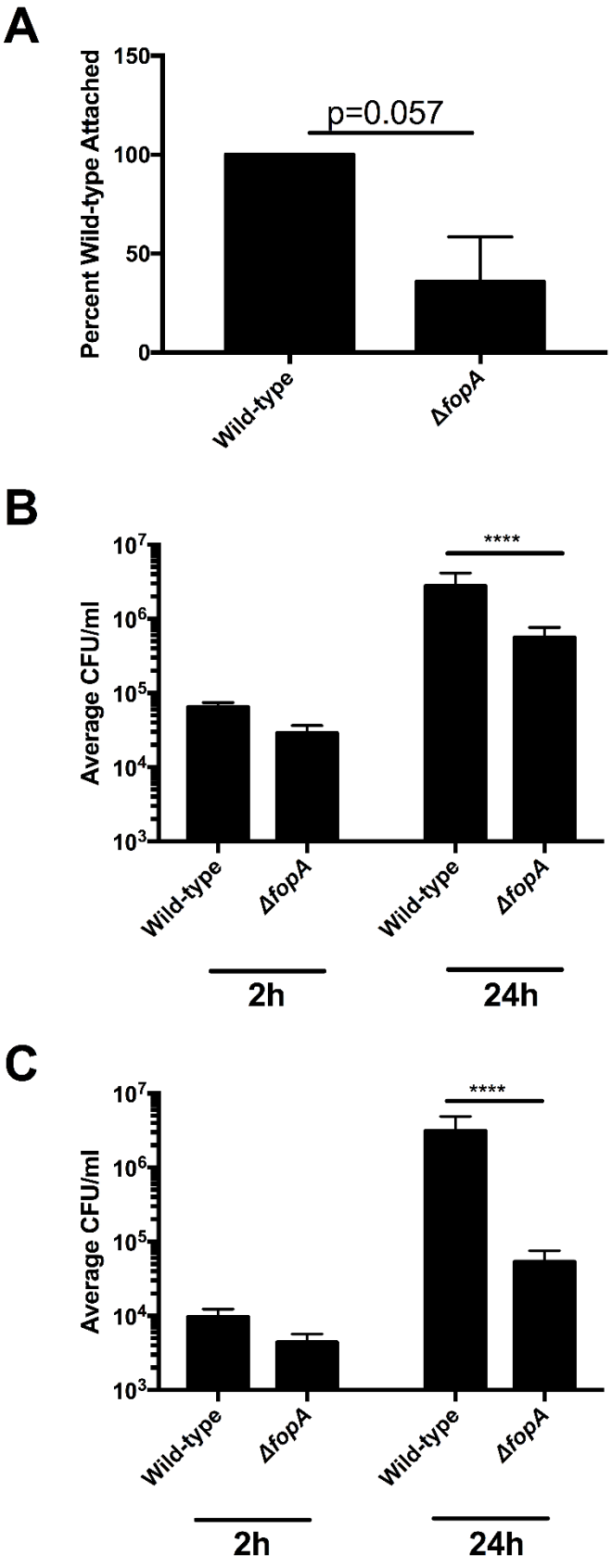
A
Percent Wild-type Attached
150
100
50
0
p=0.057
Wild-type
ΔfopA
B
Average CFU/ml
10^7
10^6
10^5
10^4
10^3
****
Wild-type
ΔfopA
Wild-type
ΔfopA
2h
24h
C
Average CFU/ml
10^7
10^6
10^5
10^4
10^3
****
Wild-type
ΔfopA
Wild-type
ΔfopA
2h
24h

Figure A2: Δ*fopA* intracellular burden is decreased compared to wild-type at 24 hours post-infection. (A) Attachment of wild-type and Δ*fopA* bacteria to J774A.1 cells after three hours at 4° C. Attachment is represented as percent of wild-type attached. No statistical difference was determined using a two-tailed Student's t test. (B-C) Bacterial burden of wild-type and Δ*fopA* bacteria at two and twenty-four hours post infection in either (B) J774A.1 macrophage-like cells or (C) bone marrow derived macrophages. Statistical analysis was performed using a One way ANOVA with Tukey's multiple comparison test. ****, $p<0.00001$

enumerated during infection within two macrophage cell types: the J774A.1 macrophage-like cell line and primary bone marrow derived macrophages (BMDMs). Bacterial burdens of the Δ*fopA* mutant were significantly lower in both cell types infected with Δ*fopA* bacteria at 24 hours post-infection (Fig. A2B-C). Although bacterial burdens at two hours trended lower in the Δ*fopA* mutant compared to wild-type, this difference was not significant, suggesting that the difference observed at 24 hours is not due to decreased internalization of the Δ*fopA* mutant. A much greater difference in bacterial burden between cells infected with wild-type and Δ*fopA* bacteria was observed in BMDMs than within J774s, consistent with published results [280].

A.4: The Δ*fopA* mutant exhibits delayed phagosomal escape and decreased bacterial burden within macrophages.

Differences in bacterial burden after 24 hours could be due to differences in bacterial growth within the cytosol or due to differences in the kinetics of phagosomal escape leading to delayed replication. Utilization of different receptors for uptake can result in differences in phagosomal escape kinetics, so FopA-mediated interactions with the host cell surface could potentially influence bacterial escape into the cytosol. To investigate the kinetics of phagosomal escape in the Δ*fopA* mutant, J774A.1 cells were infected with wild-type or Δ*fopA* Schu S4. As a control for retention within the phagosome, J774A.1 cells were also treated with wild-type Schu S4 that were heat killed prior to infection. After two hours,

cells were fixed and colocalization of bacteria with the late endosomal marker LAMP1 was investigated by fluorescence microscopy. Consistent with published data, wild-type bacteria displayed only limited colocalization with LAMP1, while heat killed bacteria were highly colocalized with LAMP1 containing vesicles [51]. Investigation of J774A.1 cells infected with Δ*fopA* bacteria determined that the Δ*fopA* mutant exhibited greater colocalization with LAMP1 than wild-type (Fig. A3), suggesting that the Δ*fopA* mutant is retained within the phagosome at higher numbers than wild-type.

A.5: The Δ*fopA* mutant stimulates increased NF-kB phosphorylation

Although Δ*fopA* bacteria colocalize with LAMP1-containing vesicles, it is unclear what causes this increased colocalization. It may represent differences in phagosomal escape kinetics, due to differences in signaling events in the absence of FopA. Alternatively, increased colocalization may indicate that FopA contributes to *Francisella* escape from the phagosome, and loss of this protein results in defective phagosomal escape in the Δ*fopA* mutant. Finally, increased colocalization may represent decreased bacterial viability in the Δ*fopA* mutant leading to retention of the bacteria within maturing phagosomes. The possibility of differences in phagosomal escape kinetics was first investigated by looking at differences in activation of downstream signaling pathways in J774A.1 cells infected with wild-type or Δ*fopA* bacteria. *F. tularensis* interacts with host surface receptors that can delay phagosomal escape and also result in differential

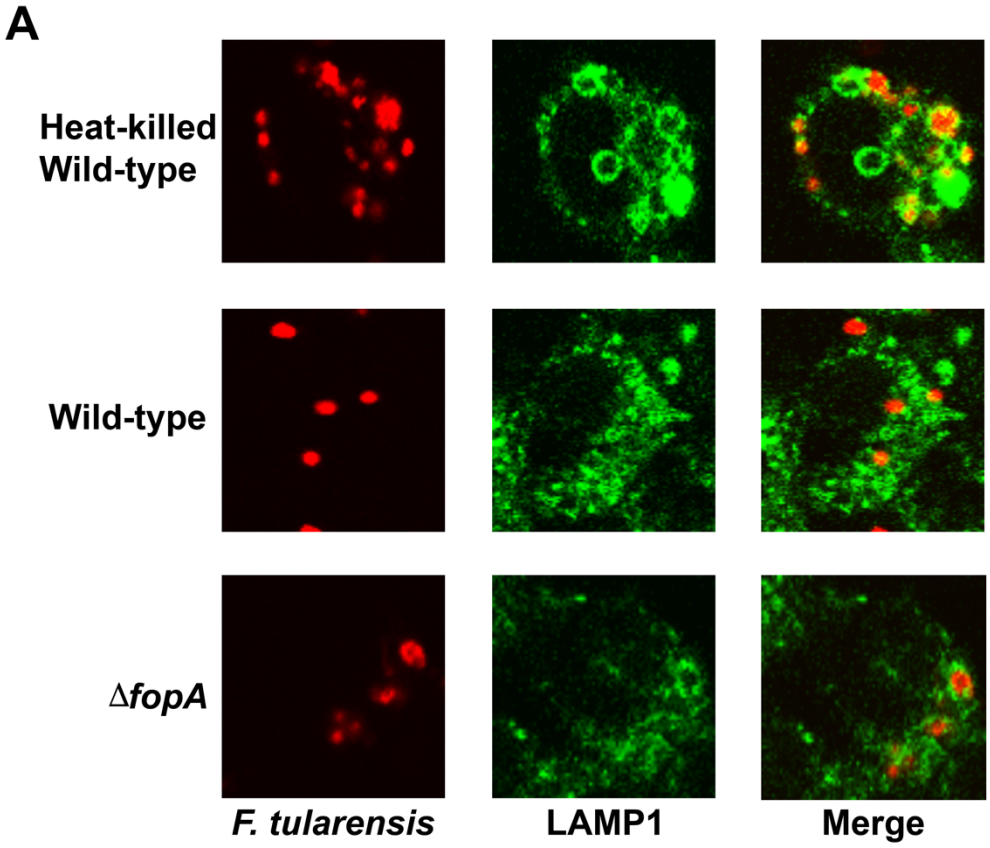
A
Heat-killed
Wild-type
Wild-type
ΔfopA
F. tularensis
LAMP1
Merge

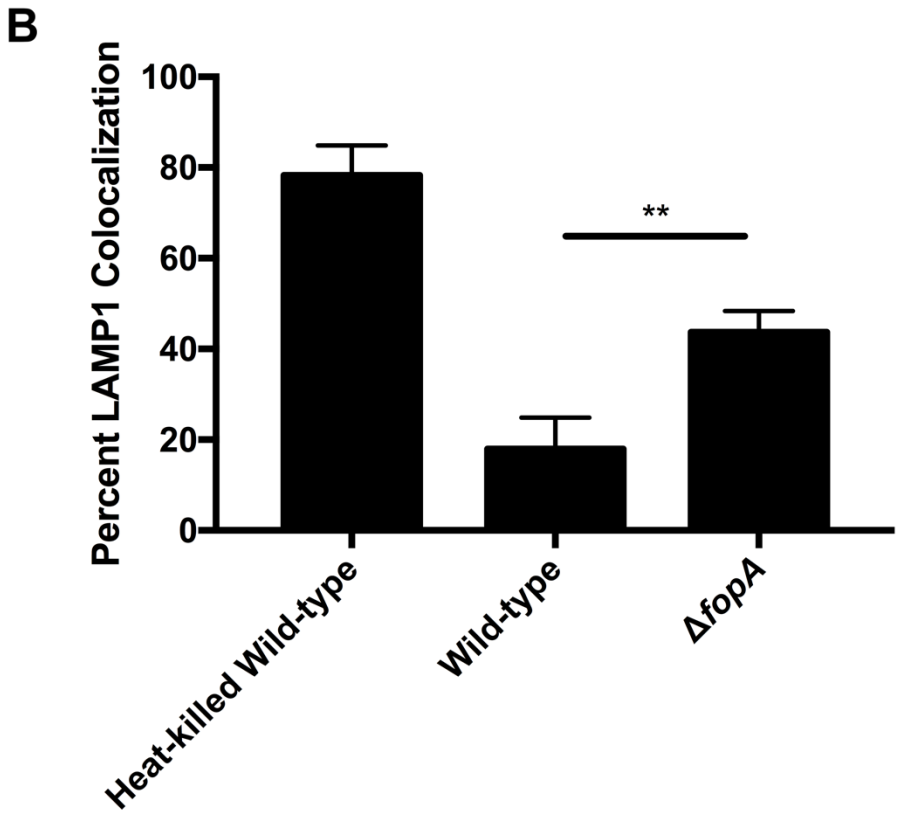
B
Percent LAMP1 Colocalization
100
80
60
40
20
0
**
Heat-killed Wild-type
Wild-type
ΔfopA

Figure A3: Schu S4 Δf*opA* bacteria display increased colocalization with LAMP1-positive vesicles. (A) Immunofluorescence images of wild-type or Δ*fopA* bacteria within J774A.1 macrophages at two hours post-infection, with heat-killed Schu S4 provided as a positive control for LAMP1 colocalization. *Francisella* bacteria are labeled in red, while LAMP1 is labeled in green. (B) Quantification of immunofluorescence results. Data is presented as the percent of total bacteria colocalized with LAMP1. Statistical analysis was performed using a One way ANOVA with Tukey's multiple comparison test. **, $p<0.01$

activation of proinflammatory pathways, such as NF-κB [50, 54]. To analyze if this pathway is differentially activated, whole cell lysates from J774A.1 cells infected with wild-type or Δ*fopA* bacteria were analyzed for phosphorylation of the p65 subunit of NF-κB. Cells infected with Δ*fopA* bacteria showed increased NF-κB p65 phosphorylation compared to cells infected with wild-type Schu S4 (Fig. A4A). No difference in actin protein levels were observed, suggesting that equivalent amounts of protein were loaded.

The extent of NF-κB activation during infection with the Δ*fopA* mutant was further investigated using a THP-1 human monocyte reporter cell line. This cell line contains a secreted alkaline phosphatase (SEAP) gene that is expressed upon NF-κB activation. THP-1 SEAP reporter cells were infected with wild-type or Δ*fopA* bacteria and media supernatant was collected and tested for SEAP activity at 24 hours post-infection. Media supernatant was also taken from PBS-treated cells as a negative control and cells treated with Pam3CSK4, a TLR2 agonist, as a positive control. Supernatants taken from cells infected with the Δ*fopA* mutant showed significantly higher levels of SEAP activity compared to supernatants from wild-type-infected cells (Fig. A4B), indicating higher levels of NF-κB activation. Taken together with the NF-κB p65 phosphorylation results, these data support the hypothesis that infection with Δ*fopA* mutant stimulates a higher level of immune activation that observed with wild-type Schu S4.

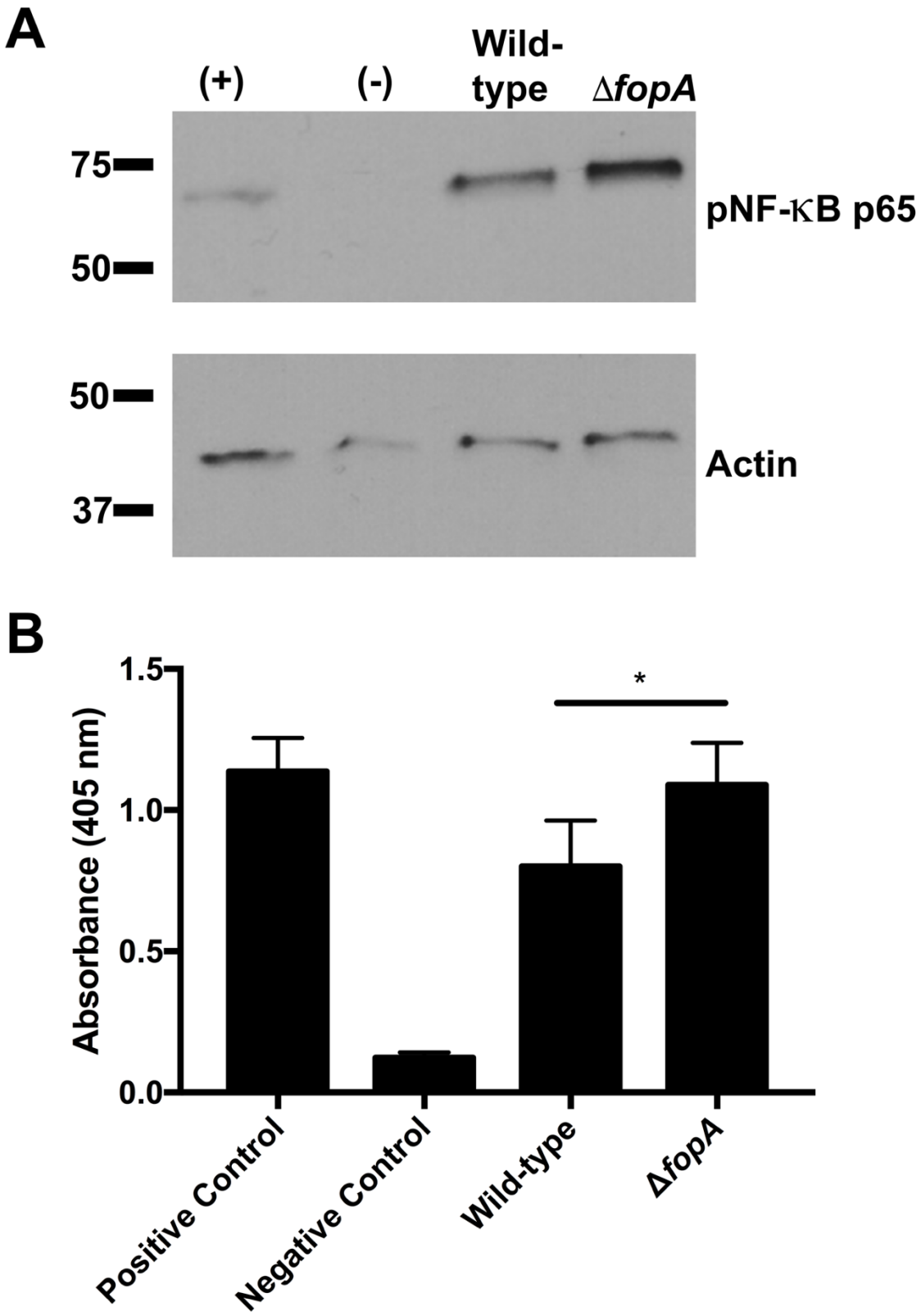
A
(+)
(-)
Wild-type
ΔfopA
75
50
pNF-κB p65
50
37
Actin
B
Absorbance (405 nm)
1.5
1.0
0.5
0.0
*
Positive Control
Negative Control
Wild-type
ΔfopA

Figure A4: NF-κB phosphorylation is increased in host cells infected with Δ*fopA* bacteria. (A) Western blot of whole cell lysates from J774A.1 cells infected from either wild-type or Δ*fopA* bacteria. J774A.1 cells treated with sterile PBS were used as a negative control (-) while cells treated with the TLR2 agonist Pam3CSK4 (100 ng/ml) were used as a positive control (+). Blots were incubated with antibodies against actin to confirm similar protein loading. (B) Alkaline phosphatase activity of media supernatant from SEAP reporter THP-1 cells infected with wild-type or Δ*fopA* bacteria. Cells treated with sterile PBS were used as a negative control (-) while cells treated with the TLR2 agonist Pam3CSK4 (100 ng/ml) were used as a positive control (+). Alkaline phosphatase activity was determined by detecting colorimetric changes after addition of p-Nitrophenyl Phosphate (pNPP) at 405 nm (OD_{405}). Statistical analysis was performed using a One way ANOVA with Tukey's multiple comparison test. *, $p<0.05$

A.6: Deletion of *fopA* results in impaired membrane integrity in the Δ*fopA* mutant.

The ability of the Δ*fopA* mutant to elicit increased activation of NF-κB may be due to direct or indirect effects. It is possible that FopA may interact directly with host cell surface proteins to dampen the immune response, and deletion of FopA prevents this interaction from occurring, increasing immune activation. However, it is also possible that this immune activation is due to indirect effects of the *fopA* deletion on the bacterial surface or structure. OmpA family proteins possess a conserved C-terminal domain which interacts with the peptidoglycan layer to increase membrane stability in Gram-negative bacteria [282, 283]. Deletion of these proteins results in compromised membrane integrity and increased release of PAMPs, which may lead to increased immune stimulation [279]. To test if the deletion of *fopA* compromised bacterial membrane integrity, release of bacterial proteins was determined by Western blot. Whole cell lysates and culture supernatants were obtained from overnight cultures of wild-type and Δ*fopA* strains. The Western blot was incubated with antibodies to the surface exposed protein FipB, as well as IglB and IglC, structural components of the *Francisella* Type Six Secretion system (T6SS), which should not be secreted during growth in vitro [284, 285]. While protein levels of FipB, IglB, and IglC were equivalent across strains in whole cell lysate samples, these proteins were absent from the culture supernatant in the wild-type strain but found at high levels in the Δ*fopA* mutant (Fig. A5A). These results support the hypothesis that the release of these proteins is due to membrane instability in the Δ*fopA* mutant.

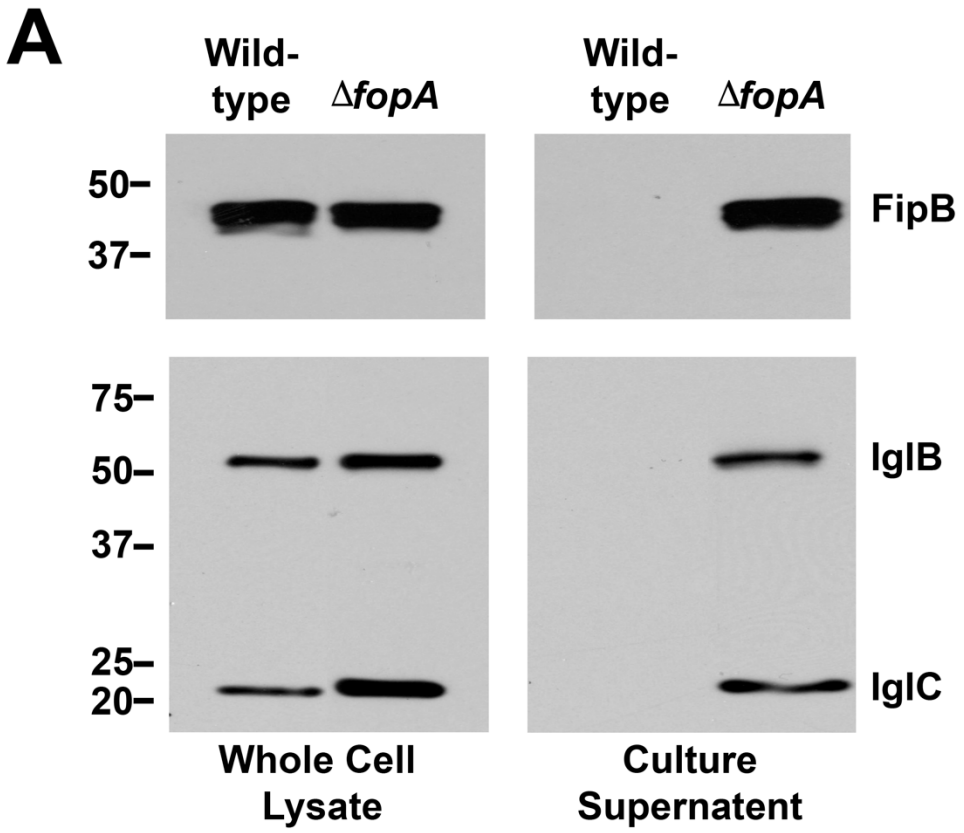
A
Wild-type
ΔfopA
Wild-type
ΔfopA
50–
37–
FipB
75–
50–
37–
25–
20–
IglB
IglC
Whole Cell Lysate
Culture Supernatent

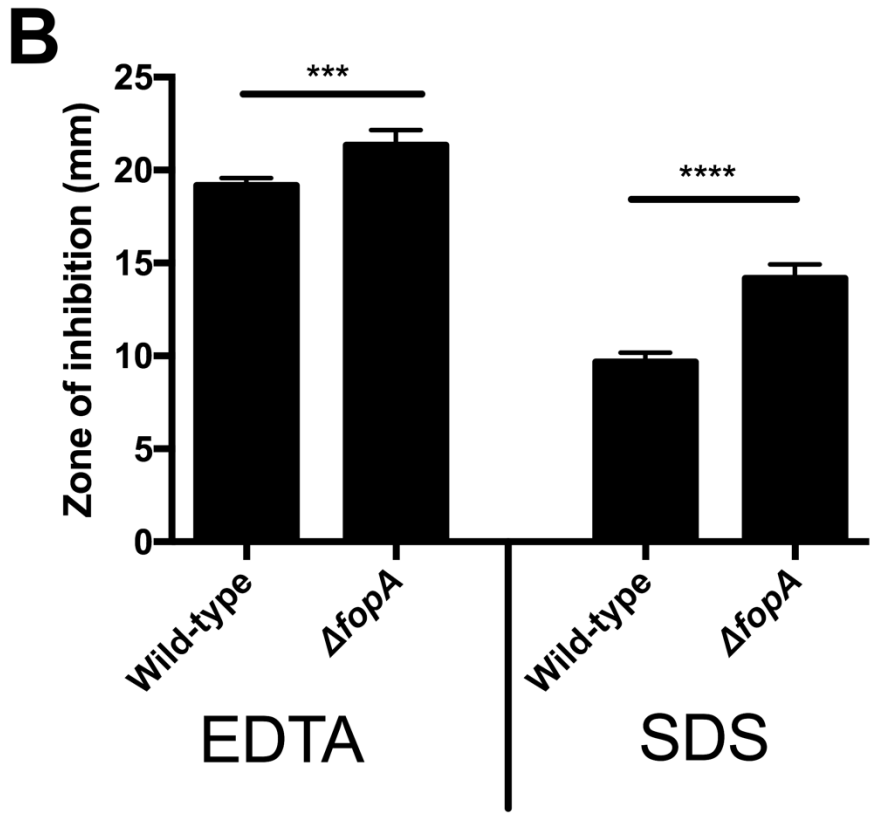
B
Zone of inhibition (mm)
25
20
15
10
5
0
***
****
Wild-type
ΔfopA
Wild-type
ΔfopA
EDTA
SDS

Figure A5: The Δ*fopA* mutant has disrupted membrane integrity. (A) Western blot of whole cell lysates and culture supernatants derived from overnight cultures of either wild-type or Δ*fopA* strains. Blots were incubated with antibodies against the outer membrane exposed protein FipB as well as structural components of the T6SS, IglB and IglC. (B) Sensitivity of wild-type and Δ*fopA* bacteria to treatment with different detergents using a disk diffusion assay. Data is represented as the average zone of inhibition in a confluent lawn of bacteria treated with a disk containing either 0.5M EDTA or 10% SDS. Statistical analysis was performed using an unpaired Student's t test. ***, $p<0.001$; ****, $p<0.0001$

Bacterial membrane integrity was also analyzed by comparing the sensitivity of wild-type and Δ*fopA* Schu S4 strains to different detergents. If the membrane of the Δ*fopA* mutant is unstable, this strain should be more sensitive to different antimicrobial compounds compared to wild-type. Confluent lawns of wild-type and Δ*fopA* bacteria were grown on MHA/c plates. Sensitivity of these strains to 10% SDS and 0.5 M EDTA was determined by placing solution-soaked disks onto the confluent bacteria and measuring the extent to which bacterial growth was inhibited. The Δ*fopA* mutant displayed increased susceptibility to both SDS and EDTA (Fig. A5B), further suggesting that the loss of FopA disrupts membrane integrity in the Δ*fopA* mutant.

A.7: Δ*fopA* bacteria are less viable than wild-type Schu S4 during growth *in vitro*.

A loss or decrease in membrane integrity can affect the viability of bacteria during growth. To characterize the impact of membrane instability on bacterial growth, growth of wild-type and Δ*fopA* bacteria in rich media was measured over time through optical density measurements as well as plating of viable bacteria. Growth curves of wild-type and Δ*fopA* bacteria showed no difference in bacterial growth by optical density (Fig. A6A). However, when log phase bacteria were plated onto MHA/c plates to test for viability, significantly fewer viable bacteria were obtained from Δ*fopA* mutant cultures than wild-type (Fig. A6B). To mimic the subpopulation of nonviable bacteria after overnight growth in the Δ*fopA*

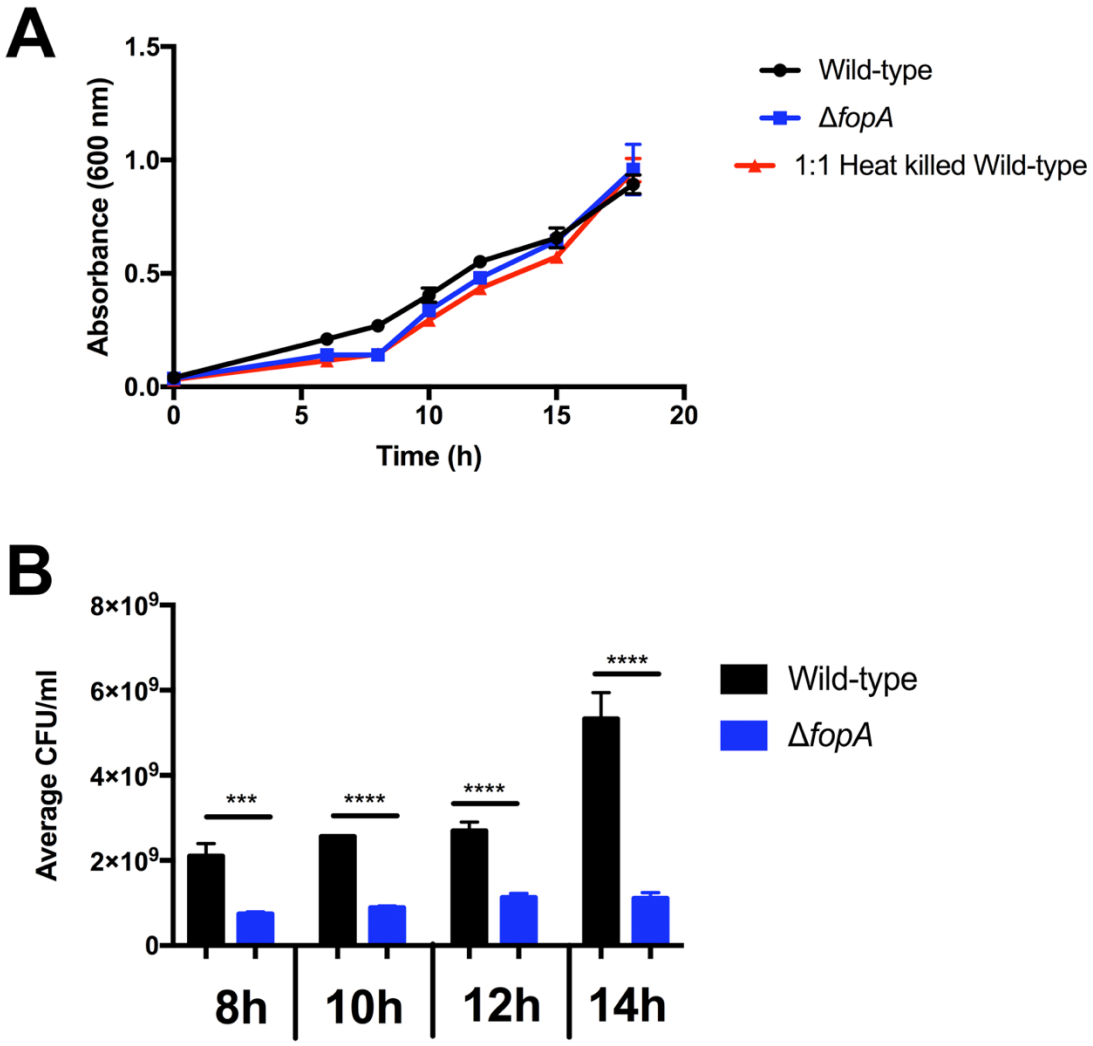
A
Absorbance (600 nm)
1.5
1.0
0.5
0.0
0
5
10
15
20
Time (h)
Wild-type
ΔfopA
1:1 Heat killed Wild-type
B
Average CFU/ml
8×10^9
6×10^9
4×10^9
2×10^9
0
***
****
****
****
8h
10h
12h
14h
Wild-type
ΔfopA

Figure A6: The Δ*fopA* mutant exhibits decreased viability during growth *in vitro* compared to wild-type. (A) Growth of wild-type (black), Δ*fopA* (blue) or an equal mix of live and heat killed wild-type (red) bacteria in TSB/c culture media was measured by taking optical density readings at 600 nm (OD_{600}) at specific timepoints. Data is the average of three biological replicates. (B) Average CFU/ml values for wild-type (black bars) and Δ*fopA* (blue bars) bacteria were enumerated by plating cultures at specified timepoints and performing colony counts. Statistical analysis was performed using a One way ANOVA with Tukey's multiple comparison test. ***, $p<0.001$; ****, $p<0.0001$.

mutant, wild-type bacteria were heat killed and mixed 1:1 with live bacteria before measuring growth. The 1:1 heat killed bacteria grew similarly to the Δ*fopA* mutant (Fig. A6A), supporting the hypothesis that while Δ*fopA* bacteria grow at a similar rate to that observed with wild-type, cultures hold fewer viable bacteria, which may indicate bacterial death due to membrane instability. If this were the case, Δ*fopA* bacteria should display altered cell morphology under these conditions. To confirm this, samples of culture-grown wild-type and Δ*fopA* bacteria were analyzed by fluorescence microscopy to identify differences in cell morphology. Bacteria were first fixed and then cell morphology was examined by fluorescence microscopy. Wild-type bacteria appeared uniform in size, but a subpopulation of Δ*fopA* mutant strains are enlarged and unusually shaped (Fig. A7), which is consistent with the loss of OmpA-mediated anchoring of the outer membrane to the peptidoglycan layer.

Overall, these data support the hypothesis that the attenuation observed in macrophages is due to bacterial membrane instability caused by deletion of *fopA* and not due to a specific interaction between FopA and the host surface. Decreased cell viability *in vitro*, abnormal cell shape, and release of proteins into the supernatant are all indicators of decreased membrane integrity and likely contribute to the phenotypes observed within macrophages: increased NF-κB activation, enhanced colocalization with LAMP1, and decreased viability at 24 hours post-infection.

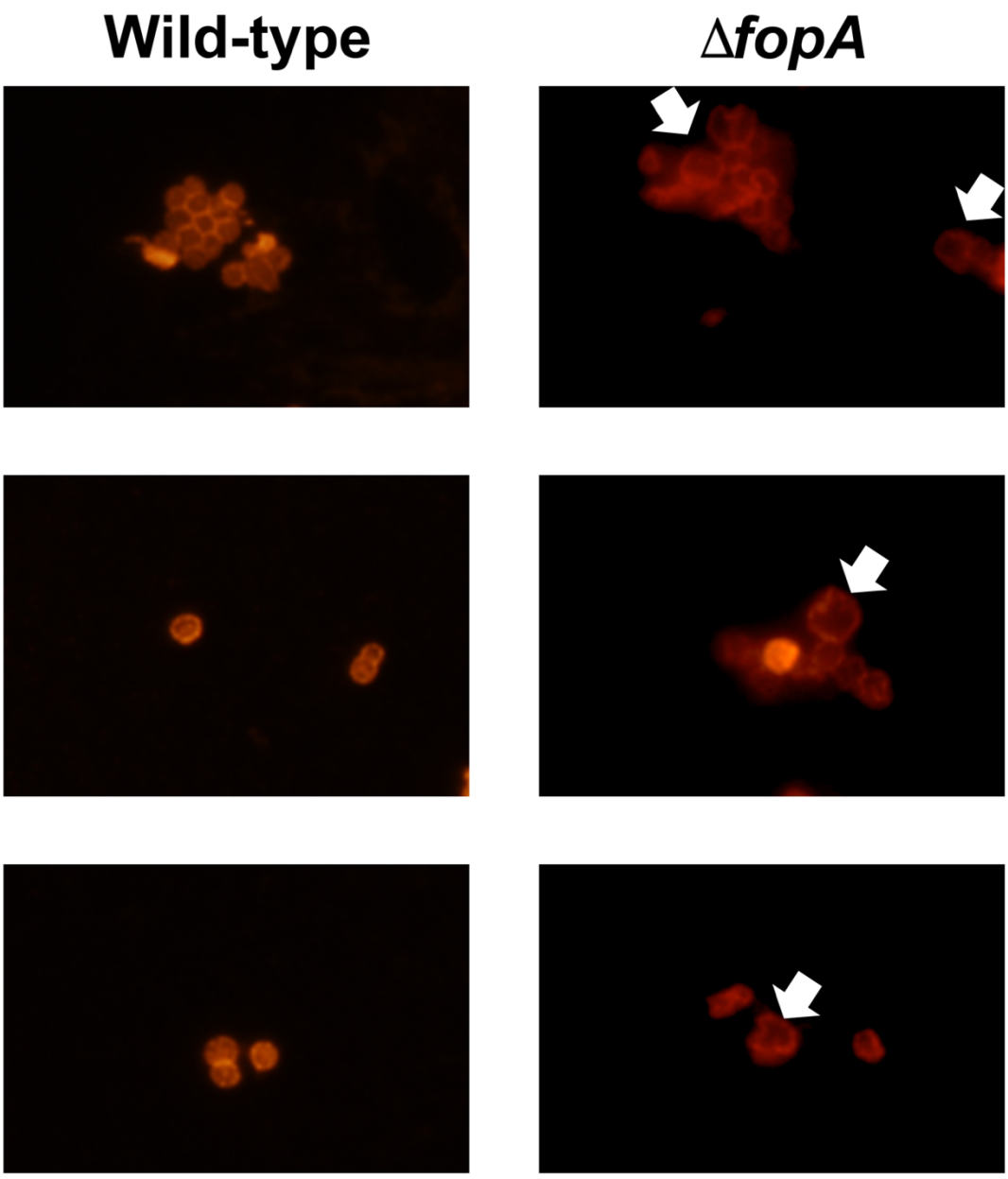
Wild-type
ΔfopA

Figure A7: The Δ*fopA* mutant exhibits altered cellular morphology.

Fluorescence microscopy images of culture grown wild-type or Δ*fopA* bacteria immunolabeled with a *Francisella* LPS-specific antibody to outline the outer membrane. Examples of misshapen bacteria are indicated with arrows.

A.8: Discussion

The specific role of FopA during interactions with the host cell is still unclear. This work initially identified the Δ*fopA* mutant as having a defect in attachment to host cells compared to wild-type. However, differences in bacterial attachment were determined by plating CFUs and determining viable cell counts, which cannot distinguish between differences in bacterial adhesion and differences in bacterial viability. OmpA family proteins contribute to attachment and internalization in other bacteria [264-266], so *Francisella* FopA may contribute in a similar manner. Decreased bacterial burden was also observed in the Δ*fopA* mutant at 24 hours post-infection. Differences in bacterial burdens were not compared between wild-type and *fopA*::TN U112 strains, but published results suggest that U112 *fopA*::TN exhibits a similar growth defect as observed in Schu S4 [279]. It is also possible that FopA interactions with the host cell have consequences on downstream host signaling, but this is also difficult to discriminate in a Δ*fopA* mutant due to the release of PAMPs and increased bacterial cell death in this strain. Although it is possible that FopA interactions with the host contribute to the dampened immune response, this effect is likely minimal; inhibition of the immune response is specific to virulent *F. tularensis* subspecies despite the FopA protein sequence being 98% identical among *Francisella* species, including *F. novicida*, which elicits a much greater proinflammatory response than virulent strains. Alternative approaches may be able to better discriminate FopA function. Fluorescence microscopy could be used to better discriminate between differences in attachment and bacterial viability. In

addition, the Δ*fopA* mutant could be complemented with a modified *fopA* gene encoding the beta barrel and peptidoglycan anchoring domains but lacking the extracellular loops to test for differences in intracellular growth or host cell signaling.

Δ*fopA* bacteria more frequently colocalized with LAMP1 than wild-type bacteria, indicating that they are retained within the phagosome. It is unclear whether these phagosomal bacteria were nonviable prior to phagocytosis or whether bacterial death occurred within the phagosome. Notably, Chong, *et al.* did not observe greater colocalization of a Δ*fopA* mutant with LAMP1 during infection with BMDMs [280]. The difference in LAMP1 colocalization observed this work may be due to differences between J774A.1 cells and BMDMs or due to differences in bacteria added during infection assays. Bacteria used for these experiments were derived from undiluted overnight bacterial cultures, which have a number of nonviable bacteria (Fig. A6B). It is likely that nonviable bacteria added to host macrophages will be phagocytosed and ultimately reside in mature phagosomes, so the increased colocalization of the Δ*fopA* mutant with LAMP1 may represent bacterial death during overnight growth rather than bacterial death within the phagosome. However, Δ*fopA* bacteria are likely more sensitive to phagosomal killing, as well, as the Δ*fopA* mutant is more sensitive to detergents such as SDS and EDTA. Despite increased colocalization with LAMP1, a subpopulation of Δ*fopA* bacteria did escape from the phagosome and replicate within the host

cytosol, indicating that intracellular infection may proceed normally with Δ*fopA* bacteria that remain viable despite membrane instability.

NF-κB activation was significantly increased in cells infected with the Δ*fopA* mutant compared to wild-type infected cells. Activation of the NF-κB pathway is likely due to the release of PAMPs on the bacterial surface due to membrane instability. One of the released bacterial proteins, FipB, is a known TLR2 agonist [286] and likely partially responsible for the increase in NF-κB activation. Retention of *F. tularensis* within the phagosome may also play a role in increased NF-κB activation, as other *Francisella* mutant strains that are unable to escape the phagosome led to increased TLR2-dependent proinflammatory gene expression [287]. It was previously observed that infection of murine BMDMs with a *F. novicida fopA::*TN mutant strain led to hypercytotoxicity of host cells during infection [288]. Hypercytotoxicity was dependent on detection of bacterial products by the AIM2 inflammasome, implicating the leaking of PAMPs from the *fopA* mutant. Although inflammasome activation was not investigated in this work, increased cytotoxicity was not observed in Δ*fopA* mutant-infected macrophages compared to wild-type-infected (Data not shown). Differences in inflammasome activation may be due to species specific differences, as *F. novicida* is known to activate the inflammasome during intracellular growth, while *F. tularensis* does not [81, 82]. However, it seems likely that the Δ*fopA* mutant would activate the inflammasome even in Schu S4 due to the release of PAMPs once bacteria become cytosolic. Active suppression of host immune activation

pathways may be sufficient to overcome release of PAMPs into the cytosol in a Δ*fopA* mutant. More sensitive measurements of inflammasome activation may be able to discern increases in activation in Δ*fopA* mutant-infected cells.

Initial observations determined that infection of host macrophages with Δ*fopA* bacteria results in decreased bacterial burden at 24 hours, increased phagosomal localization, and increased proinflammatory signaling activation. These data led to an initial hypothesis that FopA may contribute to *F. tularensis* virulence by engaging with host cell surface receptors, dampening immune signaling cascades. In the absence of FopA-host interactions, infection results in increased immune activation that ultimately leads to delayed phagosomal escape and decreased intracellular burden. However, characterization of bacterial morphology and viability in the absence of host cells determined that FopA significantly contributes to bacterial membrane stability and viability. In light of this data, a new model suggests that overnight growth of bacteria in culture is sufficient for a subpopulation of the culture to be nonviable. Infection of host cells with an overnight culture results in increased activation of inflammatory signaling pathways through increased release of PAMPs at the host cell surface or within the phagosome. While this may affect phagosomal escape kinetics, increased LAMP1 colocalization may also represent either uptake of nonviable bacteria or bacteria that are killed within the phagosome, leading to retention within the maturing phagosome. Increased Δ*fopA* mutant cell death also explains decreased bacterial burdens at 24 hours, which may be lower due to increased bacterial death

despite similar growth rates among viable wild-type and Δ*fopA* bacteria. Overall, these data highlight the importance of OmpA family proteins not only as virulence factors but also as fundamental structural proteins for maintaining cellular stability.

Chapter 6: Material and Methods

Bacterial Strains and Media

Francisella novicida U112 and *Francisella tularensis* subsp. *tularensis* Schu S4 strains were grown on cysteine supplemented Mueller Hinton Agar (MHA/c) plates. All experiments with the Schu S4 strain were performed in an approved Biosafety Level 3 laboratory. U112 single transposon mutants were obtained from the *F. novicida* transposon library [23]. For liquid growth, U112 and Schu S4 strains were grown in Tryptic Soy Broth supplemented with 10% cysteine (TSB/c) when zinc limitation was not required. For experiments with zinc mutant strains, bacteria were grown in complete Chamberlain's Defined Media (CDM) or Chelex®-treated CDM (Che-CDM) where specified. Che-CDM was prepared by treating complete CDM overnight with 10 g/L Chelex®-100 at 4°C. Che-CDM was then filter sterilized and supplemented with $FeSO_4$, $MgSO_4$, and $CaCl_2$. Acid-washed glassware was prepared by soaking glassware overnight in 10% metal-grade HNO_3 and then rinsing five times with MilliQ water. Plates and broth were supplemented with 200 μg/ml hygromycin or 15 μg/ml kanamycin when necessary for selection.

Generation of Mutant and Complemented Strains

U112 complemented strains were generated using the pEDL56 vector, a kind gift of Dr. Tom Kawula (Washington State University). Briefly, DNA was amplified by PCR using the Phusion PCR polymerase (Thermo Fisher) and gene-specific primers. PCR products and pEDL56 vector were digested using the

Table 4: Strains and plasmids used in this study

Name	Genotype	Comments	Source
F. novicida U112	Wild-type	*F. novicida*	BEI Resources
NR-3065	*F. novicida zur::*TN		[23]
NR-8039	*F. novicida zupT::*TN		[23]
NR-3063	*F. novicida znuA::*TN		[23]
NR-5336	*F. novicida fopA::*TN		[23]
NR-5341	*F. novicida* FTN_0445::TN		[23]
MFN245	U112 FTN_0710::TN, FTN_1155::TN, FTN_1487::TN, FTN_1698::TN	U112 strain transposon insertions into restriction system genes.	[290]
BJM3141	*F. novicida* wild-type, pEDL56	*F. novicida* wild-type vector control	This study
BJM3148	*zur::*TN, pEDL56	*zur::*TN strain containing the vector control	This study
BJM3142	*zur::*TN, pEDL56::*zur*	Episomal complement of *zur::*TN	This study
BJM3145	*zupT*::TN, pEDL56	*zupT*::TN strain containing the vector control	This study
BJM3143	*zupT::*TN, pEDL56::*zupT*	Episomal complement of *zupT::*TN	This study
BJM3150	*znuA*::TN, pEDL56	*znuA*::TN containing the vector control	This study
F. tularensis Schu S4	Wild-type	*F. tularensis* subsp. *tularensis*	CDC
BJM1213	Wild-type, pEDL56::*znuA*		This study
BJM1214	Δ*znuA*, pEDL56::*znuA*		This study
BJM1230	Wild-type, pEDL56::*znuA*-HA		This study

BJM1047	Δ*fopA*		[84]
pEDL56		TetR repressible expression vector	[230]
pBMBM363		U112 *zur* in pEDL56	This study
pBMBM361		U112 *zupT* in pEDL56	This study
pBMBM360		Schu S4 *znuA* in pEDL56	This study
pBMBM369		Schu S4 *znuA*+HA tag in pEDL56	This study
pGIR463		*sacB* suicide vector for genetic recombination	[98]
pBMBM353	pGIR463	Plasmid for genetic recombination of *znuA* gene	This study

Table 5: Oligonucleotides used in this study

Name	Sequence[a]	Source
zur complement 1-Fwd	TACAAAGGAGTAACTGCAGTTTGTTAATGAATAAAAAT	This study
zur complement 1-Rev	GTCATCGTCTTTGTAGTCGATTTCTAAACATTT	This study
zur complement 2-Fwd	ATTCACGCGTACAAAGGAGTAACTGCAGTT	This study
zur complement 2-Rev	AATTCCCGGGTTACTTGTCGTCATCGTCTTTGTA	This study
zupT complement Fwd	ATTCACGCGTACAAAGGAGTAACTGCAGTATGAGTAATTTTCAATTA	This study
zupT complement Rev	ATTACCCGGGCTACTTGTCGTCATCGTCTTTGTAGTCAGTCCAAATAGCAACTAT	This study
znuA pEDL56 Fwd	ATTCACGCGTACAAAGGAGTAACTGCAGTATGAAAAAATACATACTA	This study
znuA pEDL56 Rev	ACTGCCCGGGTTATTTTTGTACTTTATCCAA	This study
znuA suicide vector 1 Fwd	ACTATCCGGATTTGGTGGTGGATTTGCTATTCTATGTGC	This study
znuA suicide vector 1 Rev	AAGGAAGACATATGCCAAAGCTACAATAACAACAGCAGCTA	This study
znuA suicide vector 2 Fwd	ATCAACTGGCATATGGAAACATTACAAGCAACTGCTGTGG	This study
znuA suicide vector 2 Rev	GTTAGGCTCGAGGCAATAAGATTTATAGCAAGTTGCCC	This study
fopA qPCR Fwd	CATCTATCGCTGCAGGTTCA	This study
fopA qPCR Rev	TCCAGCTAGACCGTTAGCATC	This study
zur qPCR Fwd	GCCGCTAAAGAATTTTGTGAA	This study
zur qPCR Rev	AGCCAAAAGTCTATCGCTCTG	This study
zupT qPCR Fwd	GGTGAAGCTTTAGCGAGTGG	This study
zupT qPCR Rev	TTGCCTTTATTGCTCCTTGA	This study
FTN_0880 qPCR Fwd	AATGCTCGACGGCAGAAAAA	This study
FTN_0880 qPCR Rev	GTTTCCGGCACATGCTCTTT	This study

FTN_1758 qPCR Fwd	GCAATGTGTCCTCGTTTCCA	This study
FTN_1758 qPCR Rev	CCATAACCAGAGTTGCCTATCCA	This study
FTN_1759 qPCR Fwd	TGCACCTTCTAATGCTCCAAAA	This study
FTN_1759 qPCR Rev	GCTGCAAATGGGGCTACAAA	This study
FTN_0395 qPCR Fwd	TCCAAAAAGCTTTGGGAGATGA	This study
FTN_0395 qPCR Rev	GCCAGTTTAGCTGCTGCTGGT	This study
znuA qPCR Fwd	CCCAAACAACAAAAGGCAGT	This study
znuA qPCR Rev	CATCTGCTTCGGCTAAAAGC	This study

[a]Primer sequences are provide as 5′ to 3′

restriction enzymes MluI-HF and XmaI (New England Biolabs) and then ligated using T4 DNA ligase (New England Biolabs). Ligated plasmids were introduced into subcloning efficiency DH5α cells (Thermo Fisher) by chemical transformation and grown on LB plates supplemented with 200 μg/ml hygromycin to select for transformants. Plasmids were purified using the QIAprep Spin Miniprep Kit (Qiagen). Isolated plasmids were introduced by electroporation into electrocompetent *F. novicida* MFN245, a kind gift from Drs. Colin Manoil and Larry Gallagher (University of Washington), using a Gene Pulser II (Bio-Rad) at 1.5 kV, 400 ohms, 25 μF. Transformants were selected by growth on MHA/c plates supplemented with 200 μg/ml hygromycin. Plasmids were then isolated from MFN245 as described previously, and introduced into electrocompetent *F. novicida* U112 wild-type or select transposon mutants.

Construction of *znuA* deletion strain

Before deletion of the Schu S4 *znuA* gene (FTT0209) a pEDL56 vector containing the Schu S4 *znuA* gene was constructed as described above. The construct was introduced into electrocompetent wild-type Schu S4 using a Gene Pulser II at 2 kV, 400 ohms, 25 μF. Transformants were selected by growth on MHA/c plates supplemented with 200 μg/ml hygromycin. To construct an in-frame deletion of *znuA*, DNA sequences upstream and downstream of *znuA* were amplified by PCR and introduced into the *sacB* suicide vector pGIR463, a kind gift of Girija Ramakrishnan. This plasmid was introduced by electroporation into Schu

S4+pEDL56*znuA*, and integrant and single deletion strains were selected as previously described [40].

RNA Isolation from bacterial cultures

For RNA isolation, biological replicates of indicated strains were grown overnight in complete CDM at 37°C. Overnight cultures were diluted to an optical density (OD_{600} or OD_{595}) of 0.2 for RNA-seq experiments or 0.01 for quantitative PCR in 1 ml CDM and grown at 37°C until mid-log phase. Bacteria were pelleted by centrifugation and RNA was purified using the RNeasy kit (Qiagen). Genomic DNA contamination was removed using the Turbo DNase kit (Ambion). Total RNA concentration was then quantified using the Nanodrop 1000 Spectrophotometer (Thermo Scientific).

RNA Sequencing

RNA was isolated from 3 separate biological replicates of either wild-type U112 or *zur*::TN mutant. For TPEN RNA Sequencing, RNA was isolated from three separate biological replicates of untreated wild-type U112, TPEN-treated U112, untreated wild-type Schu S4, or TPEN-treated Schu S4. RNA quality for both experiments was confirmed using the Agilent Bioanalyzer at the Biomolecular Research Facility at UVA prior to sample submission. Total RNA was submitted to Hudson Alpha (Huntsville, Al) for *zur*::TN experiments or Genewiz (South Plainfield, NJ), where ribosomal reduction was performed to concentrate for

mRNA. Directional cDNA libraries were then generated and samples were sequenced in multiplex (50 PE reads) using the Illumina HiSeq v4 platform.

Data analysis for both experiments was performed by the UVA Bioinformatics Core. Briefly, gene reads were first aligned to reference genomes and read counts quantified using EDGE-pro software. The Deseq2 Bioconductor package was then used to normalize read counts and estimate dispersion for each gene. These data were then fit to a negative binomial model, which was used for differential expression analysis. Genes were considered differentially expressed between groups when adjusted p-values were below 0.05 for a given gene.

cDNA Generation and Quantitative PCR

500 ng of purified RNA was converted to first strand cDNA using the Moloney Murine Leukemia Virus (M-MLV) Reverse Transcriptase according to manufacturer's protocol. Briefly, a 20 μl reaction was set up with 500 ng purified RNA, 0.5 mM (each) dNTPs (New England Biolabs), 0.15 μg/μl random primers (Invitrogen), 10 mM DTT, 1x first-strand buffer (Invitrogen), and 200 units M-MLV (Invitrogen) in nuclease-free water. Reverse transcription was performed by incubating reaction mix at room temperature for 10 minutes, then at 37°C for 50 minutes, and then 70°C for 15 minutes. Samples were diluted to 100 μl total volume in nuclease-free water.

Quantitative PCR was performed using the SensiFAST SYBR and fluorescein kit (Bioline). Control reactions with no reverse transcriptase (No-RT) were used to ensure purity of each sample from genomic DNA contamination. Duplicate wells of three biological replicate samples were assayed for each gene and condition. Differential expression of each gene was calculated relative to the housekeeping gene *fopA* using the comparative C(T) method [289].

Bacterial growth

Bacterial strains were cultured on MHA/c plates from -80°C stocks. For bacterial growth assays, single colonies were inoculated into TSB/c, complete CDM or Che-CDM (whichever specified) and grown overnight at 37°C with shaking. For growth curves, overnight cultures were diluted to an optical density of 0.01 in indicated media. For zinc limitation experiments, overnight cultures were diluted to an optical density of 0.01 in CDM supplemented with 10 μM N,N,N′,N′-Tetrakis(2-pyridylmethyl)ethylenediamine (TPEN, Sigma) and grown overnight at 37°C with shaking to starve cultures. Overnight starved cultures were then diluted to an optical density of 0.01 in CDM that was either untreated, supplemented with 10 μM TPEN, or supplemented with 10 μM TPEN and 2 μM of either $ZnSO_4$ or $MnCl_2$ (Sigma). Bacterial absorbance was determined by taking the optical density of each bacterial culture at 600 nm (OD_{600}) using the Genesys 20 visible spectrophotometer (Thermo Scientific) or at 595 nm (OD_{595}) using the iMark Microplate Absorbace Reader (Bio-Rad).

Infection of J774A.1 macrophage-like cells with *F. tularensis* subsp. *tularensis*

Overnight cultures of Schu S4 pEDL56*znuA* or the Δ*znuA* pEDL56*znuA* mutant were grown in Che-CDM. Bacteria were diluted to an OD_{595} of 0.01 in Che-CDM that was either untreated or supplemented with 100 ng/ml ATc and grown for 24 hours. Bacteria were diluted in DMEM culture medium and added to J774A.1 macrophage-like cells seeded into a 24 well plate at a multiplicity of infection (MOI) of 50. Plates were centrifuged at 800 X g, 4°C for 10 minutes to bring bacteria in contact with J774A.1 cells and synchronize infections. Plates were then incubated at 37°C, 5% CO_2 for 50 minutes to allow for phagocytosis. Cells were washed three times with PBS and then incubated with DMEM supplemented with 50 μg/ml gentamicin for one hour to kill extracellular bacteria. After one hour, cells were washed with PBS and incubated in complete DMEM at 37°C, 5% CO_2 with complete DMEM. At indicated time points, J774A.1 cells were lysed by treatment with 0.1% saponin for 5 minutes. Serial dilutions of the lysate were grown on MHA/c plates, incubated at 37°C, and bacterial colonies counted after two days of incubation to enumerate bacteria.

For RNA isolation, total RNA was recovered from infected cells at one hour and eight hours post-infection by aspirating off media and adding 250 μl TRIzol reagent to each well of the plate. Four replicate wells were pooled per sample. RNA was extracted by chloroform phase separation, and the aqueous layer was

further purified using the RNeasy Mini kit (Qiagen) and Turbo Dnase kit (Ambion) as previously described.

Competition Assay

Wild-type U112 and individual transposon mutant strains were grown overnight in TSB/c at 37° C with shaking. Overnight growth was quantified by taking optical density readings at 595 nm. Wild-type and individual mutants were mixed in a 1:1 ratio based on OD_{595} readings and added to J774A.1 cells as described above. Wild-type and transposon mutant bacterial burdens were quantified at input as well as at two hours post-infection by serially diluting bacteria on MHA/c plates that were untreated or supplemented with 50 μg/ml kanamycin. As the transposon insertion has a kanamycin resistance gene, growth on kanamycin plates was used to represent mutant bacterial burden, and growth on total plates minus growth on kanamycin plates was used to assay wild-type bacterial burden. Competitive indexes were calculated by dividing the ratio of mutant to wild-type after infection by the ratio of mutant to wild-type in the initial inoculum.

Bacterial Protein Release Assay

Whole cell lysate was prepared by mix equal amount of overnight bacterial culture (OD=1.0) grown in TSB/c with 2x SDS-PAGE buffer. Culture supernatant was obtained from 10 ml of overnight culture (OD=1.0). Culture was centrifuged at 3000, 5000, and 8000 rpm for 30 minutes respectively, discarding bacterial pellet each time. Supernatant was then filtered with 0.22 μm syringe filter followed by

10% TCA precipitation. Protein pellets were resuspended in 100 µl of 1x SDS-PAGE buffer. Whole cell lysates and culture supernatants were analyzed by Western blot.

Western Blot

Whole cell lysates were boiled and pelleted by centrifugation, after which 20 µl of sample supernatant was loaded into wells of a pre-cast polyacrylamide gel and run at 150 V for 1 hour, 10 minutes. Samples were transferred from the gel onto a nitrocellulose membrane for 2 hours at 50 V. After transfer, membranes were blocked overnight at 4° C in PBS containing 5% milk. Blocked membranes were then blocked with PBS containing primary antibodies of interest at room temperature for 1 hour with shaking, then washed 3 times for 5 minutes each. After washing, membranes were incubated with PBS containing secondary antibodies of interest conjugated to horse radish peroxidase (HRP) at room temperature for 1 hour with shaking before being washed as before. Blots were visualized with the Pierce ECL Western blot detection kit (Thermo Scientific).

Fluorescence Microscopy

Either Schu S4 bacteria in culture or host cells infected with Schu S4 bacteria were prepared for microscopy. For bacteria, 100 µl of mid-log phase cultures were brought into contact with poly-L-lysine coated coverslips by centrifugation. For host cells, cells were seeded onto glass coverslips and then infected with Schu S4 according to infection protocol. At indicated timepoints, cover slips were

prepared. Coverslips with either bacteria or infected cells were fixed in 4% paraformaldehyde for 30 minutes at room temperature. After fixation, cover slips were washed twice with sterile PBS and then transferred to a sterile 24 well plate and transported out of the BSL3.

To prepare samples for fluorescence microscopy, coverslips were first treated overnight in PBS supplemented with 5% natural goat serum to block nonspecific antibody binding. Labeling of Schu S4 was accomplished by incubating coverslips with PBS containing 1:1000 mouse anti-*F. tularensis* antibodies for 1 hour with shaking and then, following 3 five minute washes, PBS containing 1:1000 goat anti-mouse Alexa 546 antibodies for 1 hour with shaking. To label bacteria within infected host cells, 0.1% saponin was added to antibody solutions. For host cells, LAMP1 was labeled by incubating coverslips with PBS containing 1:250 rat anti-LAMP1 for 1 hour with shaking and then following 3 five minute washes, PBS containing goat anti-rat Alexa 488 antibodies for 1 hour with shaking. After labeling, coverslips were washed 3 times for five minutes each and mounted onto glass slides with 1.5 ul Fluoromount G. Slides were observed using the Olympus BX51 microscope and images captured with an Olympus DP70 digital camera.

NF-κB Reporter Cell Assay

THP-1 cells containing an alkaline phosphatase gene under the NF-κB promoter (Invitrogen) were differentiated with 10 ng/ml Phorbol 12-myristate 13-acetate (PMA) and seeded at $2.5x10^5$ cells per well in a 24 well plate. After 24 hours, cells were washed with PBS and incubated in media without PMA for 48 hours. After 48 hours, cells were infected according to infection protocol. Twenty-four hours post-infection, 50 μl of cell supernatant was removed and added to 50 μl p-Nitrophenyl Phosphate (pNPP) for 30 minutes in a 96 well plated. Optical density of samples was read at 405 nm.

Disk Diffusion Assay

Bacterial lawns were generated by streaking a bacterial lawn onto MHA/c plates. Paper disks were placed in triplicate onto each bacterial plate, and 10 μl of 0.5 M EDTA or 10% SDS was added onto each disk. Plates were incubated for 37° C for 48 hours. Growth inhibition was determined by measuring the diameter of the zone of inhibition around each disk.

Statistical Analysis

Statistical Analysis for RNA-Seq is described above. For other experiments, data were analyzed with either a One-way analysis of variance (ANOVA) or a two-tailed Student's t test using Prism software (Graphpad Software, Inc., San Diego, CA).

References

1. Oyston, P.C., A. Sjostedt, and R.W. Titball, *Tularaemia: bioterrorism defence renews interest in Francisella tularensis.* Nat Rev Microbiol, 2004. **2**(12): p. 967-78.
2. Dennis, D.T., et al., *Tularemia as a biological weapon: medical and public health management.* Jama, 2001. **285**(21): p. 2763-2773.
3. Evans, M.E., et al., *Tularemia: a 30-year experience with 88 cases.* Medicine (Baltimore), 1985. **64**(4): p. 251-69.
4. Helvaci, S., et al., *Tularemia in Bursa, Turkey: 205 cases in ten years.* Eur J Epidemiol, 2000. **16**(3): p. 271-6.
5. *Possession, use, and transfer of select agents and toxins; biennial review. Final rule.* Fed Regist, 2012. **77**(194): p. 61083-115.
6. McCrumb, F.R., *AEROSOL INFECTION OF MAN WITH PASTEURELLA TULARENSIS.* Bacteriol Rev, 1961. **25**(3): p. 262-7.
7. Dienst, F.T., Jr., *Tularemia: a perusal of three hundred thirty-nine cases.* J La State Med Soc, 1963. **115**: p. 114-27.
8. Harris, S., *Japanese biological warfare research on humans: a case study of microbiology and ethics.* Ann N Y Acad Sci, 1992. **666**: p. 21-52.
9. Christopher, G.W., et al., *Biological warfare. A historical perspective.* Jama, 1997. **278**(5): p. 412-7.
10. World Health, O., *Health aspects of chemical and biological weapons. Report of a WHO Group of Consultants*. 1970, Geneva.

11. Kaufmann, A.F., M.I. Meltzer, and G.P. Schmid, *The economic impact of a bioterrorist attack : are prevention and postattack intervention programs justifiable?* 1997, [Emmitsburg, MD]: [National Emergency Training Center].

12. Oyston, P.C. and J.E. Quarry, *Tularemia vaccine: past, present and future.* Antonie Van Leeuwenhoek, 2005. **87**(4): p. 277-81.

13. Forsman, M., G. Sandstrom, and A. Sjostedt, *Analysis of 16S ribosomal DNA sequences of Francisella strains and utilization for determination of the phylogeny of the genus and for identification of strains by PCR.* Int J Syst Bacteriol, 1994. **44**(1): p. 38-46.

14. Larson, M.A., et al., *Reclassification of Wolbachia persica as Francisella persica comb. nov. and emended description of the family Francisellaceae.* Int J Syst Evol Microbiol, 2016. **66**(3): p. 1200-5.

15. Foley, J.E. and N.C. Nieto, *Tularemia.* Vet Microbiol, 2010. **140**(3-4): p. 332-8.

16. Sjostedt, A., *Tularemia: history, epidemiology, pathogen physiology, and clinical manifestations.* Ann N Y Acad Sci, 2007. **1105**: p. 1-29.

17. Akimana, C. and Y.A. Kwaik, *Francisella-arthropod vector interaction and its role in patho-adaptation to infect mammals.* Front Microbiol, 2011. **2**: p. 34.

18. Hesselbrock, W. and L. Foshay, *The Morphology of Bacterium tularense.* J Bacteriol, 1945. **49**(3): p. 209-31.

19. Eigelsbach, H.T., W. Braun, and R.D. Herring, *Studies on the variation of Bacterium tularense.* J Bacteriol, 1951. **61**(5): p. 557-69.

20. Kingry, L.C. and J.M. Petersen, *Comparative review of Francisella tularensis and Francisella novicida.* Front Cell Infect Microbiol, 2014. **4**: p. 35.

21. Brett, M.E., et al., *Outbreak of Francisella novicida bacteremia among inmates at a louisiana correctional facility.* Clin Infect Dis, 2014. **59**(6): p. 826-33.

22. Larson, C.L., W. Wicht, and W.L. Jellison, *A new organism resembling P. tularensis isolated from water.* Public Health Reports, 1955. **70**(3): p. 253-258.

23. Gallagher, L.A., et al., *A comprehensive transposon mutant library of Francisella novicida, a bioweapon surrogate.* Proc Natl Acad Sci U S A, 2007. **104**(3): p. 1009-14.

24. Huber, B., et al., *Description of Francisella hispaniensis sp. nov., isolated from human blood, reclassification of Francisella novicida (Larson et al. 1955) Olsufiev et al. 1959 as Francisella tularensis subsp. novicida comb. nov. and emended description of the genus Francisella.* Int J Syst Evol Microbiol, 2010. **60**(Pt 8): p. 1887-96.

25. Johansson, A., et al., *Objections to the transfer of Francisella novicida to the subspecies rank of Francisella tularensis.* International Journal of Systematic and Evolutionary Microbiology, 2010. **60**(8): p. 1717-1718.

26. Hall, J.D., et al., *Infected-host-cell repertoire and cellular response in the lung following inhalation of Francisella tularensis Schu S4, LVS, or U112.* Infect Immun, 2008. **76**(12): p. 5843-52.

27. Cremer, T.J., et al., *MiR-155 induction by F. novicida but not the virulent F. tularensis results in SHIP down-regulation and enhanced pro-inflammatory cytokine response.* PLoS One, 2009. **4**(12): p. e8508.

28. Petersen, J.M., et al., *Direct isolation of Francisella spp. from environmental samples.* Lett Appl Microbiol, 2009. **48**(6): p. 663-7.

29. Rohmer, L., et al., *Comparison of Francisella tularensis genomes reveals evolutionary events associated with the emergence of human pathogenic strains.* Genome Biol, 2007. **8**(6): p. R102.

30. Larsson, P., et al., *The complete genome sequence of Francisella tularensis, the causative agent of tularemia.* Nat Genet, 2005. **37**(2): p. 153-9.

31. Svensson, K., et al., *Evolution of subspecies of Francisella tularensis.* J Bacteriol, 2005. **187**(11): p. 3903-8.

32. Conlan, J.W., et al., *Experimental tularemia in mice challenged by aerosol or intradermally with virulent strains of Francisella tularensis: bacteriologic and histopathologic studies.* Microb Pathog, 2003. **34**(5): p. 239-48.

33. Horzempa, J., et al., *Francisella tularensis DeltapyrF mutants show that replication in nonmacrophages is sufficient for pathogenesis in vivo.* Infect Immun, 2010. **78**(6): p. 2607-19.

34. Andersson, H., et al., *Transcriptional profiling of host responses in mouse lungs following aerosol infection with type A Francisella tularensis.* J Med Microbiol, 2006. **55**(Pt 3): p. 263-71.

35. Mares, C.A., et al., *Initial delay in the immune response to Francisella tularensis is followed by hypercytokinemia characteristic of severe sepsis and correlating with upregulation and release of damage-associated molecular patterns.* Infect Immun, 2008. **76**(7): p. 3001-10.

36. Abplanalp, A.L., et al., *TLR-dependent control of Francisella tularensis infection and host inflammatory responses.* PLoS One, 2009. **4**(11): p. e7920.

37. Russo, B.C., M.J. Brown, and G.J. Nau, *MyD88-dependent signaling prolongs survival and reduces bacterial burden during pulmonary infection with virulent Francisella tularensis.* Am J Pathol, 2013. **183**(4): p. 1223-32.

38. Forestal, C.A., et al., *Francisella tularensis has a significant extracellular phase in infected mice.* J Infect Dis, 2007. **196**(1): p. 134-7.

39. Twine, S., et al., *A mutant of Francisella tularensis strain SCHU S4 lacking the ability to express a 58-kilodalton protein is attenuated for virulence and is an effective live vaccine.* Infect Immun, 2005. **73**(12): p. 8345-52.

40. Qin, A., et al., *Identification of an essential Francisella tularensis subsp. tularensis virulence factor.* Infect Immun, 2009. **77**(1): p. 152-61.

41. Broms, J.E., et al., *DotU and VgrG, core components of type VI secretion systems, are essential for Francisella LVS pathogenicity.* PLoS One, 2012. **7**(4): p. e34639.

42. Schwartz, J.T., et al., *Natural IgM mediates complement-dependent uptake of Francisella tularensis by human neutrophils via complement receptors 1 and 3 in nonimmune serum.* J Immunol, 2012. **189**(6): p. 3064-77.

43. Ben Nasr, A., et al., *Critical role for serum opsonins and complement receptors CR3 (CD11b/CD18) and CR4 (CD11c/CD18) in phagocytosis of Francisella tularensis by human dendritic cells (DC): uptake of Francisella leads to activation of immature DC and intracellular survival of the bacteria.* J Leukoc Biol, 2006. **80**(4): p. 774-86.

44. Craven, R.R., et al., *Francisella tularensis invasion of lung epithelial cells.* Infect Immun, 2008. **76**(7): p. 2833-42.

45. Melillo, A., et al., *Identification of a Francisella tularensis LVS outer membrane protein that confers adherence to A549 human lung cells.* FEMS Microbiol Lett, 2006. **263**(1): p. 102-8.

46. Bradburne, C.E., et al., *Temporal transcriptional response during infection of type II alveolar epithelial cells with Francisella tularensis live vaccine strain (LVS) supports a general host suppression and bacterial uptake by macropinocytosis.* J Biol Chem, 2013. **288**(15): p. 10780-91.

47. Law, H.T., et al., *Francisella tularensis uses cholesterol and clathrin-based endocytic mechanisms to invade hepatocytes.* Sci Rep, 2011. **1**: p. 192.

48. Balagopal, A., et al., *Characterization of the receptor-ligand pathways important for entry and survival of Francisella tularensis in human macrophages.* Infect Immun, 2006. **74**(9): p. 5114-25.

49. Pierini, L.M., *Uptake of serum-opsonized Francisella tularensis by macrophages can be mediated by class A scavenger receptors.* Cell Microbiol, 2006. **8**(8): p. 1361-70.

50. Dai, S., et al., *Fine tuning inflammation at the front door: macrophage complement receptor 3-mediates phagocytosis and immune suppression for Francisella tularensis.* PLoS Pathog, 2013. **9**(1): p. e1003114.

51. Checroun, C., et al., *Autophagy-mediated reentry of Francisella tularensis into the endocytic compartment after cytoplasmic replication.* Proc Natl Acad Sci U S A, 2006. **103**(39): p. 14578-83.

52. Chong, A., et al., *The early phagosomal stage of Francisella tularensis determines optimal phagosomal escape and Francisella pathogenicity island protein expression.* Infect Immun, 2008. **76**(12): p. 5488-99.

53. Clemens, D.L., B.Y. Lee, and M.A. Horwitz, *Virulent and avirulent strains of Francisella tularensis prevent acidification and maturation of their phagosomes and escape into the cytoplasm in human macrophages.* Infect Immun, 2004. **72**(6): p. 3204-17.

54. Geier, H. and J. Celli, *Phagocytic receptors dictate phagosomal escape and intracellular proliferation of Francisella tularensis.* Infect Immun, 2011. **79**(6): p. 2204-14.

55. Clemens, D.L., B.Y. Lee, and M.A. Horwitz, *Francisella tularensis phagosomal escape does not require acidification of the phagosome.* Infect Immun, 2009. **77**(5): p. 1757-73.

56. Edwards, J.A., et al., *Restricted cytosolic growth of Francisella tularensis subsp. tularensis by IFN-gamma activation of macrophages.* Microbiology, 2010. **156**(Pt 2): p. 327-39.

57. Steele, S., et al., *Trogocytosis-associated cell to cell spread of intracellular bacterial pathogens.* Elife, 2016. **5**.

58. Takeda, K., T. Kaisho, and S. Akira, *Toll-Like Receptors.* Annual Review of Immunology, 2003. **21**(1): p. 335-376.

59. Ishii, K.J., et al., *Host innate immune receptors and beyond: making sense of microbial infections.* Cell Host Microbe, 2008. **3**(6): p. 352-63.

60. Man, S.M., R. Karki, and T.D. Kanneganti, *AIM2 inflammasome in infection, cancer, and autoimmunity: Role in DNA sensing, inflammation, and innate immunity.* Eur J Immunol, 2016. **46**(2): p. 269-80.

61. Tschopp, J. and K. Schroder, *NLRP3 inflammasome activation: The convergence of multiple signalling pathways on ROS production?*, in *Nat Rev Immunol*. 2010: England. p. 210-5.

62. Netea, M.G., et al., *Differential requirement for the activation of the inflammasome for processing and release of IL-1beta in monocytes and macrophages.* Blood, 2009. **113**(10): p. 2324-35.

63. Bergsbaken, T., S.L. Fink, and B.T. Cookson, *Pyroptosis: host cell death and inflammation.* Nat Rev Microbiol, 2009. **7**(2): p. 99-109.

64. Miao, E.A., et al., *Caspase-1-induced pyroptosis is an innate immune effector mechanism against intracellular bacteria.* Nat Immunol, 2010. **11**(12): p. 1136-42.

65. Katz, J., et al., *Toll-like receptor 2 is required for inflammatory responses to Francisella tularensis LVS.* Infect Immun, 2006. **74**(5): p. 2809-16.

66. Chen, W., et al., *Toll-like receptor 4 (TLR4) does not confer a resistance advantage on mice against low-dose aerosol infection with virulent type A Francisella tularensis.* Microb Pathog, 2004. **37**(4): p. 185-91.

67. Hajjar, A.M., et al., *Lack of in vitro and in vivo recognition of Francisella tularensis subspecies lipopolysaccharide by Toll-like receptors.* Infect Immun, 2006. **74**(12): p. 6730-8.

68. Llewellyn, A.C., et al., *NaxD is a deacetylase required for lipid A modification and Francisella pathogenesis.* Mol Microbiol, 2012. **86**(3): p. 611-27.

69. Wang, X., et al., *Attenuated virulence of a Francisella mutant lacking the lipid A 4'-phosphatase.* Proc Natl Acad Sci U S A, 2007. **104**(10): p. 4136-41.

70. Kanistanon, D., et al., *A Francisella mutant in lipid A carbohydrate modification elicits protective immunity.* PLoS Pathog, 2008. **4**(2): p. e24.

71. Kieffer, T.L., et al., *Francisella novicida LPS has greater immunobiological activity in mice than F. tularensis LPS, and contributes to F. novicida murine pathogenesis.* Microbes Infect, 2003. **5**(5): p. 397-403.

72. Butchar, J.P., et al., *Francisella tularensis induces IL-23 production in human monocytes.* J Immunol, 2007. **178**(7): p. 4445-54.

73. Butchar, J.P., et al., *Microarray analysis of human monocytes infected with Francisella tularensis identifies new targets of host response subversion.* PLoS One, 2008. **3**(8): p. e2924.

74. Fernandes-Alnemri, T., et al., *The AIM2 inflammasome is critical for innate immunity to Francisella tularensis.* Nat Immunol, 2010. **11**(5): p. 385-93.

75. Belhocine, K. and D.M. Monack, *Francisella infection triggers activation of the AIM2 inflammasome in murine dendritic cells.* Cell Microbiol, 2012. **14**(1): p. 71-80.

76. Ghonime, M.G., et al., *Inflammasome priming is similar for francisella species that differentially induce inflammasome activation.* PLoS One, 2015. **10**(5): p. e0127278.

77. Mariathasan, S., et al., *Cryopyrin activates the inflammasome in response to toxins and ATP.* Nature, 2006. **440**(7081): p. 228-32.

78. Weiss, D.S., T. Henry, and D.M. Monack, *Francisella tularensis: activation of the inflammasome.* Ann N Y Acad Sci, 2007. **1105**: p. 219-37.

79. Dotson, R.J., et al., *Repression of inflammasome by Francisella tularensis during early stages of infection.* J Biol Chem, 2013. **288**(33): p. 23844-57.

80. Meunier, E., et al., *Guanylate-binding proteins promote activation of the AIM2 inflammasome during infection with Francisella novicida.* Nat Immunol, 2015. **16**(5): p. 476-484.

81. Lai, X.H. and A. Sjostedt, *Delineation of the molecular mechanisms of Francisella tularensis-induced apoptosis in murine macrophages.* Infect Immun, 2003. **71**(8): p. 4642-6.

82. Wickstrum, J.R., et al., *Francisella tularensis induces extensive caspase-3 activation and apoptotic cell death in the tissues of infected mice.* Infect Immun, 2009. **77**(11): p. 4827-36.

83. Santic, M., et al., *The Francisella tularensis pathogenicity island protein IglC and its regulator MglA are essential for modulating phagosome biogenesis and subsequent bacterial escape into the cytoplasm.* Cell Microbiol, 2005. **7**(7): p. 969-79.

84. Qin, A., et al., *Components of the type six secretion system are substrates of Francisella tularensis Schu S4 DsbA-like FipB protein.* Virulence, 2016. **7**(8): p. 882-894.

85. Brodmann, M., et al., *Francisella requires dynamic type VI secretion system and ClpB to deliver effectors for phagosomal escape.* Nat Commun, 2017. **8**: p. 15853.

86. Meyer, L., et al., *Microinjection of Francisella tularensis and Listeria monocytogenes reveals the importance of bacterial and host factors for successful replication.* Infect Immun, 2015. **83**(8): p. 3233-42.

87. Nano, F.E., et al., *A Francisella tularensis pathogenicity island required for intramacrophage growth.* J Bacteriol, 2004. **186**(19): p. 6430-6.

88. McDonough, M.A. and J.R. Butterton, *Spontaneous tandem amplification and deletion of the shiga toxin operon in Shigella dysenteriae 1.* Mol Microbiol, 1999. **34**(5): p. 1058-69.

89. Wehrly, T.D., et al., *Intracellular biology and virulence determinants of Francisella tularensis revealed by transcriptional profiling inside macrophages.* Cell Microbiol, 2009. **11**(7): p. 1128-50.

90. Gesbert, G., et al., *Asparagine assimilation is critical for intracellular replication and dissemination of Francisella.* Cell Microbiol, 2014. **16**(3): p. 434-49.

91. Gesbert, G., et al., *Importance of branched-chain amino acid utilization in Francisella intracellular adaptation.* Infect Immun, 2015. **83**(1): p. 173-83.

92. Steele, S., et al., *Francisella tularensis harvests nutrients derived via ATG5-independent autophagy to support intracellular growth.* PLoS Pathog, 2013. **9**(8): p. e1003562.

93. Brissac, T., et al., *Gluconeogenesis, an essential metabolic pathway for pathogenic Francisella.* Mol Microbiol, 2015. **98**(3): p. 518-34.

94. Bent, Z.W., et al., *Use of a capture-based pathogen transcript enrichment strategy for RNA-Seq analysis of the Francisella tularensis LVS transcriptome during infection of murine macrophages.* PLoS One, 2013. **8**(10): p. e77834.

95. Thomas-Charles, C.A., et al., *FeoB-mediated uptake of iron by Francisella tularensis.* Infect Immun, 2013. **81**(8): p. 2828-37.

96. Kiss, K., et al., *Characterization of fig operon mutants of Francisella novicida U112.* FEMS Microbiol Lett, 2008. **285**(2): p. 270-7.

97. Deng, K., et al., *Identification of Francisella tularensis genes affected by iron limitation.* Infect Immun, 2006. **74**(7): p. 4224-36.

98. Ramakrishnan, G., A. Meeker, and B. Dragulev, *fslE is necessary for siderophore-mediated iron acquisition in Francisella tularensis Schu S4.* J Bacteriol, 2008. **190**(15): p. 5353-61.

99. Perez, N.M. and G. Ramakrishnan, *The reduced genome of the Francisella tularensis live vaccine strain (LVS) encodes two iron acquisition systems essential for optimal growth and virulence.* PLoS One, 2014. **9**(4): p. e93558.

100. Wu, X., et al., *FmvB: A Francisella tularensis Magnesium-Responsive Outer Membrane Protein that Plays a Role in Virulence.* PLoS One, 2016. **11**(8): p. e0160977.

101. Hambleton, P., et al., *Changes in whole blood and serum components during Francisella tularensis and rabbit pox infections of rabbits.* Br J Exp Pathol, 1977. **58**(6): p. 644-52.

102. Liuzzi, J.P., et al., *Interleukin-6 regulates the zinc transporter Zip14 in liver and contributes to the hypozincemia of the acute-phase response.* Proc Natl Acad Sci U S A, 2005. **102**(19): p. 6843-8.

103. Paranavitana, C., et al., *Transcriptional profiling of Francisella tularensis infected peripheral blood mononuclear cells: a predictive tool for tularemia.* FEMS Immunol Med Microbiol, 2008. **54**(1): p. 92-103.

104. Pekarek, R.S., *Humoral and cellular immune responses in zinc deficient rats.* Nutrition reports international, 1977. **v. 16**(no. 3): p. pp. 267-276-1977 v.16 no.3.

105. Melillo, A.A., et al., *Identification of Francisella tularensis live vaccine strain CuZn superoxide dismutase as critical for resistance to extracellularly generated reactive oxygen species.* J Bacteriol, 2009. **191**(20): p. 6447-56.

106. Auld, D.S., *The ins and outs of biological zinc sites.* Biometals, 2009. **22**(1): p. 141-8.

107. Vallee, B.L. and D.S. Auld, *Cocatalytic zinc motifs in enzyme catalysis.* Proc Natl Acad Sci U S A, 1993. **90**(7): p. 2715-8.

108. Fillat, M.F., *The FUR (ferric uptake regulator) superfamily: diversity and versatility of key transcriptional regulators.* Arch Biochem Biophys, 2014. **546**: p. 41-52.

109. Cousins, R.J., *Metal elements and gene expression.* Annu Rev Nutr, 1994. **14**: p. 449-69.

110. Andreini, C., et al., *Zinc through the three domains of life.* J Proteome Res, 2006. **5**(11): p. 3173-8.

111. Pan, H. and D.B. Wigley, *Structure of the zinc-binding domain of Bacillus stearothermophilus DNA primase.* Structure, 2000. **8**(3): p. 231-9.

112. Katayama, A., et al., *Systematic search for zinc-binding proteins in Escherichia coli.* Eur J Biochem, 2002. **269**(9): p. 2403-13.

113. Anzellotti, A.I. and N.P. Farrell, *Zinc metalloproteins as medicinal targets.* Chem Soc Rev, 2008. **37**(8): p. 1629-51.

114. Gaballa, A. and J.D. Helmann, *Identification of a zinc-specific metalloregulatory protein, Zur, controlling zinc transport operons in Bacillus subtilis.* J Bacteriol, 1998. **180**(22): p. 5815-21.

115. Althaus, E.W., et al., *The ferric uptake regulation (Fur) repressor is a zinc metalloprotein.* Biochemistry, 1999. **38**(20): p. 6559-69.

116. Massova, I. and S. Mobashery, *Kinship and diversification of bacterial penicillin-binding proteins and beta-lactamases.* Antimicrob Agents Chemother, 1998. **42**(1): p. 1-17.

117. Piddington, D.L., et al., *Cu,Zn superoxide dismutase of Mycobacterium tuberculosis contributes to survival in activated macrophages that are generating an oxidative burst.* Infect Immun, 2001. **69**(8): p. 4980-7.

118. Oggioni, M.R., et al., *Pneumococcal zinc metalloproteinase ZmpC cleaves human matrix metalloproteinase 9 and is a virulence factor in experimental pneumonia.* Mol Microbiol, 2003. **49**(3): p. 795-805.

119. Andreini, C., I. Bertini, and A. Rosato, *Metalloproteomes: a bioinformatic approach.* Acc Chem Res, 2009. **42**(10): p. 1471-9.

120. Maret, W., *Zinc and the zinc proteome.* Met Ions Life Sci, 2013. **12**: p. 479-501.

121. Lander, E.S., et al., *Initial sequencing and analysis of the human genome.* Nature, 2001. **409**(6822): p. 860-921.

122. Hershfinkel, M., et al., *A zinc-sensing receptor triggers the release of intracellular Ca2+ and regulates ion transport.* Proc Natl Acad Sci U S A, 2001. **98**(20): p. 11749-54.

123. Kitamura, H., et al., *Toll-like receptor-mediated regulation of zinc homeostasis influences dendritic cell function.* Nat Immunol, 2006. **7**(9): p. 971-7.

124. Yamasaki, S., et al., *Zinc is a novel intracellular second messenger.* J Cell Biol, 2007. **177**(4): p. 637-45.

125. Aydemir, T.B., et al., *Zinc transporter ZIP8 (SLC39A8) and zinc influence IFN-gamma expression in activated human T cells.* J Leukoc Biol, 2009. **86**(2): p. 337-48.

126. Yamasaki, S., et al., *A novel role of the L-type calcium channel alpha1D subunit as a gatekeeper for intracellular zinc signaling: zinc wave.* PLoS One, 2012. **7**(6): p. e39654.

127. McDevitt, C.A., et al., *A molecular mechanism for bacterial susceptibility to zinc.* PLoS Pathog, 2011. **7**(11): p. e1002357.

128. Watjen, W., et al., *Induction of apoptosis in mammalian cells by cadmium and zinc.* Environ Health Perspect, 2002. **110 Suppl 5**: p. 865-7.

129. Kambe, T., A. Hashimoto, and S. Fujimoto, *Current understanding of ZIP and ZnT zinc transporters in human health and diseases.* Cell Mol Life Sci, 2014. **71**(17): p. 3281-95.

130. Roohani, N., et al., *Zinc and its importance for human health: An integrative review.* J Res Med Sci, 2013. **18**(2): p. 144-57.

131. Colvin, R.A., et al., *Insights into Zn2+ homeostasis in neurons from experimental and modeling studies.* Am J Physiol Cell Physiol, 2008. **294**(3): p. C726-42.

132. Krezel, A. and W. Maret, *Zinc-buffering capacity of a eukaryotic cell at physiological pZn.* J Biol Inorg Chem, 2006. **11**(8): p. 1049-62.

133. Hijova, E., *Metallothioneins and zinc: their functions and interactions.* Bratisl Lek Listy, 2004. **105**(5-6): p. 230-4.

134. Rahman, M.T. and M.M. Karim, *Metallothionein: a Potential Link in the Regulation of Zinc in Nutritional Immunity.* Biol Trace Elem Res, 2017.

135. Krezel, A. and W. Maret, *Dual nanomolar and picomolar Zn(II) binding properties of metallothionein.* J Am Chem Soc, 2007. **129**(35): p. 10911-21.

136. Krezel, A. and W. Maret, *Thionein/metallothionein control Zn(II) availability and the activity of enzymes.* J Biol Inorg Chem, 2008. **13**(3): p. 401-9.

137. Costello, L.C., C.C. Fenselau, and R.B. Franklin, *Evidence for operation of the direct zinc ligand exchange mechanism for trafficking, transport, and reactivity of zinc in mammalian cells.* J Inorg Biochem, 2011. **105**(5): p. 589-99.

138. Lichten, L.A. and R.J. Cousins, *Mammalian zinc transporters: nutritional and physiologic regulation.* Annu Rev Nutr, 2009. **29**: p. 153-76.

139. Kozlowski, H., et al., *Specific metal ion binding sites in unstructured regions of proteins.* Coordination Chemistry Reviews, 2013. **257**(19): p. 2625-2638.

140. Bin, B.H., et al., *Biochemical characterization of human ZIP13 protein: a homo-dimerized zinc transporter involved in the spondylocheiro dysplastic Ehlers-Danlos syndrome.* J Biol Chem, 2011. **286**(46): p. 40255-65.

141. Kambe, T., *Molecular architecture and function of ZnT transporters.* Curr Top Membr, 2012. **69**: p. 199-220.

142. Ohana, E., et al., *Identification of the Zn2+ binding site and mode of operation of a mammalian Zn2+ transporter.* J Biol Chem, 2009. **284**(26): p. 17677-86.

143. Kimura, T. and T. Kambe, *The Functions of Metallothionein and ZIP and ZnT Transporters: An Overview and Perspective.* Int J Mol Sci, 2016. **17**(3): p. 336.

144. Potter, B.M., et al., *The six zinc fingers of metal-responsive element binding transcription factor-1 form stable and quasi-ordered structures with relatively small differences in zinc affinities.* J Biol Chem, 2005. **280**(31): p. 28529-40.

145. Gunther, V., U. Lindert, and W. Schaffner, *The taste of heavy metals: gene regulation by MTF-1.* Biochim Biophys Acta, 2012. **1823**(9): p. 1416-25.

146. Lichten, L.A., et al., *MTF-1-mediated repression of the zinc transporter Zip10 is alleviated by zinc restriction.* PLoS One, 2011. **6**(6): p. e21526.

147. Zheng, D., et al., *Regulation of ZIP and ZnT zinc transporters in zebrafish gill: zinc repression of ZIP10 transcription by an intronic MRE cluster.* Physiol Genomics, 2008. **34**(2): p. 205-14.

148. Wang, F., et al., *Zinc-stimulated endocytosis controls activity of the mouse ZIP1 and ZIP3 zinc uptake transporters.* J Biol Chem, 2004. **279**(23): p. 24631-9.

149. Bhutia, D.T., *Protein energy malnutrition in India: the plight of our under five children.* J Family Med Prim Care, 2014. **3**(1): p. 63-7.

150. Bonaventura, P., et al., *Zinc and its role in immunity and inflammation.* Autoimmun Rev, 2015. **14**(4): p. 277-85.

151. Fraker, P.J., et al., *Interrelationships between zinc and immune function.* Fed Proc, 1986. **45**(5): p. 1474-9.

152. Ripa, S. and R. Ripa, *Zinc and immune function.* Minerva Med, 1995. **86**(7-8): p. 315-8.

153. Turvey, S.E. and D.H. Broide, *Innate immunity.* J Allergy Clin Immunol, 2010. **125**(2 Suppl 2): p. S24-32.

154. Ibs, K.H. and L. Rink, *Zinc-altered immune function.* J Nutr, 2003. **133**(5 Suppl 1): p. 1452s-6s.

155. Hujanen, E.S., S.T. Seppa, and K. Virtanen, *Polymorphonuclear leukocyte chemotaxis induced by zinc, copper and nickel in vitro.* Biochim Biophys Acta, 1995. **1245**(2): p. 145-52.

156. Sheikh, A., et al., *Zinc influences innate immune responses in children with enterotoxigenic Escherichia coli-induced diarrhea.* J Nutr, 2010. **140**(5): p. 1049-56.

157. Hasegawa, H., et al., *Effects of zinc on the reactive oxygen species generating capacity of human neutrophils and on the serum opsonic activity in vitro.* Luminescence, 2000. **15**(5): p. 321-7.

158. Mayer, L.S., et al., *Differential impact of zinc deficiency on phagocytosis, oxidative burst, and production of pro-inflammatory cytokines by human monocytes.* Metallomics, 2014. **6**(7): p. 1288-95.

159. Fuchs, T.A., et al., *Novel cell death program leads to neutrophil extracellular traps.* J Cell Biol, 2007. **176**(2): p. 231-41.

160. Hasan, R., L. Rink, and H. Haase, *Zinc signals in neutrophil granulocytes are required for the formation of neutrophil extracellular traps.* Innate Immun, 2013. **19**(3): p. 253-64.

161. Brieger, A., L. Rink, and H. Haase, *Differential regulation of TLR-dependent MyD88 and TRIF signaling pathways by free zinc ions.* J Immunol, 2013. **191**(4): p. 1808-17.

162. King, L.E., et al., *Chronic zinc deficiency in mice disrupted T cell lymphopoiesis and erythropoiesis while B cell lymphopoiesis and myelopoiesis were maintained.* J Am Coll Nutr, 2005. **24**(6): p. 494-502.

163. Prasad, A.S., *Effects of zinc deficiency on Th1 and Th2 cytokine shifts.* J Infect Dis, 2000. **182 Suppl 1**: p. S62-8.

164. Afshari, M., et al., *Oral treatment with zinc sulfate increases the expression of Th1 cytokines mRNA in BALB/c mice infected with Leishmania major.* Cytokine, 2016. **81**: p. 71-6.

165. Spellberg, B. and J.E. Edwards, Jr., *Type 1/Type 2 immunity in infectious diseases.* Clin Infect Dis, 2001. **32**(1): p. 76-102.

166. Allendoerfer, R., G.P. Biovin, and G.S. Deepe, Jr., *Modulation of immune responses in murine pulmonary histoplasmosis.* J Infect Dis, 1997. **175**(4): p. 905-14.

167. Kehl-Fie, T.E. and E.P. Skaar, *Nutritional immunity beyond iron: a role for manganese and zinc.* Curr Opin Chem Biol, 2010. **14**(2): p. 218-24.

168. Ravasi, T., et al., *Probing the S100 protein family through genomic and functional analysis.* Genomics, 2004. **84**(1): p. 10-22.

169. Brodersen, D.E., J. Nyborg, and M. Kjeldgaard, *Zinc-binding site of an S100 protein revealed. Two crystal structures of Ca2+-bound human psoriasin (S100A7) in the Zn2+-loaded and Zn2+-free states.* Biochemistry, 1999. **38**(6): p. 1695-704.

170. Korndorfer, I.P., F. Brueckner, and A. Skerra, *The crystal structure of the human (S100A8/S100A9)2 heterotetramer, calprotectin, illustrates how conformational changes of interacting alpha-helices can determine specific association of two EF-hand proteins.* J Mol Biol, 2007. **370**(5): p. 887-98.

171. Glaser, R., et al., *Antimicrobial psoriasin (S100A7) protects human skin from Escherichia coli infection.* Nat Immunol, 2005. **6**(1): p. 57-64.

172. Zackular, J.P., W.J. Chazin, and E.P. Skaar, *Nutritional Immunity: S100 Proteins at the Host-Pathogen Interface.* J Biol Chem, 2015. **290**(31): p. 18991-8.

173. Corbin, B.D., et al., *Metal chelation and inhibition of bacterial growth in tissue abscesses*. Science, 2008. **319**(5865): p. 962-5.

174. Ghavami, S., et al., *S100A8/A9 at low concentration promotes tumor cell growth via RAGE ligation and MAP kinase-dependent pathway.* J Leukoc Biol, 2008. **83**(6): p. 1484-92.

175. Vogl, T., et al., *Mrp8 and Mrp14 are endogenous activators of Toll-like receptor 4, promoting lethal, endotoxin-induced shock.* Nat Med, 2007. **13**(9): p. 1042-9.

176. Subramanian Vignesh, K., et al., *Granulocyte macrophage-colony stimulating factor induced Zn sequestration enhances macrophage superoxide and limits intracellular pathogen survival.* Immunity, 2013. **39**(4): p. 697-710.

177. Botella, H., et al., *Metallobiology of host-pathogen interactions: an intoxicating new insight.* Trends Microbiol, 2012. **20**(3): p. 106-12.

178. Botella, H., et al., *Mycobacterial p(1)-type ATPases mediate resistance to zinc poisoning in human macrophages.* Cell Host Microbe, 2011. **10**(3): p. 248-59.

179. Subramanian Vignesh, K. and G.S. Deepe, Jr., *Immunological orchestration of zinc homeostasis: The battle between host mechanisms and pathogen defenses.* Arch Biochem Biophys, 2016. **611**: p. 66-78.

180. Haas, C.E., et al., *A subset of the diverse COG0523 family of putative metal chaperones is linked to zinc homeostasis in all kingdoms of life.* BMC Genomics, 2009. **10**: p. 470.

181. Nairn, B.L., et al., *The Response of Acinetobacter baumannii to Zinc Starvation.* Cell Host Microbe, 2016. **19**(6): p. 826-36.

182. Paulsen, I.T., et al., *A family of gram-negative bacterial outer membrane factors that function in the export of proteins, carbohydrates, drugs and heavy metals from gram-negative bacteria.* FEMS Microbiol Lett, 1997. **156**(1): p. 1-8.

183. Palmgren, M.G. and P. Nissen, *P-Type ATPases.* Annual Review of Biophysics, 2011. **40**(1): p. 243-266.

184. Banci, L., et al., *A new zinc-protein coordination site in intracellular metal trafficking: solution structure of the Apo and Zn(II) forms of ZntA(46-118).* J Mol Biol, 2002. **323**(5): p. 883-97.

185. Watly, J., S. Potocki, and M. Rowinska-Zyrek, *Zinc Homeostasis at the Bacteria/Host Interface-From Coordination Chemistry to Nutritional Immunity.* Chemistry, 2016. **22**(45): p. 15992-16010.

186. Hudek, L., et al., *Functional characterization of the twin ZIP/SLC39 metal transporters, NpunF3111 and NpunF2202 in Nostoc punctiforme.* Appl Microbiol Biotechnol, 2013. **97**(19): p. 8649-62.

187. Grass, G., et al., *The metal permease ZupT from Escherichia coli is a transporter with a broad substrate spectrum.* J Bacteriol, 2005. **187**(5): p. 1604-11.

188. Karlinsey, J.E., et al., *The phage shock protein PspA facilitates divalent metal transport and is required for virulence of Salmonella enterica sv. Typhimurium.* Mol Microbiol, 2010. **78**(3): p. 669-85.

189. Taudte, N. and G. Grass, *Point mutations change specificity and kinetics of metal uptake by ZupT from Escherichia coli.* Biometals, 2010. **23**(4): p. 643-56.

190. Cerasi, M., et al., *The ZupT transporter plays an important role in zinc homeostasis and contributes to Salmonella enterica virulence.* Metallomics, 2014. **6**(4): p. 845-53.

191. Sabri, M., S. Houle, and C.M. Dozois, *Roles of the extraintestinal pathogenic Escherichia coli ZnuACB and ZupT zinc transporters during urinary tract infection.* Infection and immunity, 2009. **77**(3): p. 1155-1164.

192. Dawson, R.J. and K.P. Locher, *Structure of a bacterial multidrug ABC transporter.* Nature, 2006. **443**(7108): p. 180-5.

193. Wilkens, S., *Structure and mechanism of ABC transporters.* F1000Prime Rep, 2015. **7**: p. 14.

194. Claverys, J.P., *A new family of high-affinity ABC manganese and zinc permeases.* Res Microbiol, 2001. **152**(3-4): p. 231-43.

195. Hantke, K., *Bacterial zinc uptake and regulators.* Curr Opin Microbiol, 2005. **8**(2): p. 196-202.

196. Li, H. and G. Jogl, *Crystal structure of the zinc-binding transport protein ZnuA from Escherichia coli reveals an unexpected variation in metal coordination.* J Mol Biol, 2007. **368**(5): p. 1358-66.

197. Wei, B., et al., *Possible regulatory role for the histidine-rich loop in the zinc transport protein, ZnuA.* Biochemistry, 2007. **46**(30): p. 8734-43.

198. Castelli, S., et al., *Zinc ion coordination as a modulating factor of the ZnuA histidine-rich loop flexibility: a molecular modeling and fluorescence spectroscopy study.* Biochem Biophys Res Commun, 2013. **430**(2): p. 769-73.

199. Petrarca, P., et al., *The Zur-regulated ZinT protein is an auxiliary component of the high-affinity ZnuABC zinc transporter that facilitates metal recruitment during severe zinc shortage.* J Bacteriol, 2010. **192**(6): p. 1553-64.

200. Stork, M., et al., *Zinc piracy as a mechanism of Neisseria meningitidis for evasion of nutritional immunity.* PLoS Pathog, 2013. **9**(10): p. e1003733.

201. Stork, M., et al., *An outer membrane receptor of Neisseria meningitidis involved in zinc acquisition with vaccine potential.* PLoS Pathog, 2010. **6**: p. e1000969.

202. Hood, M.I., et al., *Identification of an Acinetobacter baumannii zinc acquisition system that facilitates resistance to calprotectin-mediated zinc sequestration.* PLoS Pathog, 2012. **8**(12): p. e1003068.

203. Bobrov, A.G., et al., *The Yersinia pestis siderophore, yersiniabactin, and the ZnuABC system both contribute to zinc acquisition and the development of lethal septicaemic plague in mice.* Mol Microbiol, 2014. **93**(4): p. 759-75.

204. Lhospice, S., et al., *Pseudomonas aeruginosa zinc uptake in chelating environment is primarily mediated by the metallophore pseudopaline.* Sci Rep, 2017. **7**(1): p. 17132.

205. Citiulo, F., et al., *Candida albicans scavenges host zinc via Pra1 during endothelial invasion.* PLoS Pathog, 2012. **8**(6): p. e1002777.

206. Ammendola, S., et al., *High-affinity Zn2+ uptake system ZnuABC is required for bacterial zinc homeostasis in intracellular environments and contributes to the virulence of Salmonella enterica.* Infect Immun, 2007. **75**(12): p. 5867-76.

207. Yang, X., et al., *Deletion of znuA virulence factor attenuates Brucella abortus and confers protection against wild-type challenge.* Infect Immun, 2006. **74**(7): p. 3874-9.

208. Liu, J.Z., et al., *Zinc sequestration by the neutrophil protein calprotectin enhances Salmonella growth in the inflamed gut.* Cell Host Microbe, 2012. **11**(3): p. 227-39.

209. Choi, S. and A.J. Bird, *Zinc'ing sensibly: controlling zinc homeostasis at the transcriptional level.* Metallomics, 2014. **6**(7): p. 1198-215.

210. Ma, Z., S.E. Gabriel, and J.D. Helmann, *Sequential binding and sensing of Zn(II) by Bacillus subtilis Zur.* Nucleic Acids Res, 2011. **39**(21): p. 9130-8.

211. Gilston, B.A., et al., *Structural and mechanistic basis of zinc regulation across the E. coli Zur regulon.* PLoS Biol, 2014. **12**(11): p. e1001987.

212. Shin, J.H. and J.D. Helmann, *Molecular logic of the Zur-regulated zinc deprivation response in Bacillus subtilis.* Nat Commun, 2016. **7**: p. 12612.

213. Shin, J.H., et al., *Graded expression of zinc-responsive genes through two regulatory zinc-binding sites in Zur.* Proc Natl Acad Sci U S A, 2011. **108**(12): p. 5045-50.

214. Shin, J.H., et al., *The zinc-responsive regulator Zur controls a zinc uptake system and some ribosomal proteins in Streptomyces coelicolor A3(2).* J Bacteriol, 2007. **189**(11): p. 4070-7.

215. Mortensen, B.L., et al., *Acinetobacter baumannii response to host-mediated zinc limitation requires the transcriptional regulator Zur.* J Bacteriol, 2014. **196**(14): p. 2616-26.

216. Sheehan, L.M., et al., *Coordinated zinc homeostasis is essential for the wild-type virulence of Brucella abortus.* J Bacteriol, 2015. **197**(9): p. 1582-91.

217. Campoy, S., et al., *Role of the high-affinity zinc uptake znuABC system in Salmonella enterica serovar typhimurium virulence.* Infect Immun, 2002. **70**(8): p. 4721-5.

218. Nanamiya, H., et al., *Zinc is a key factor in controlling alternation of two types of L31 protein in the Bacillus subtilis ribosome.* Mol Microbiol, 2004. **52**(1): p. 273-83.

219. Makarova, K.S. and N.V. Grishin, *The Zn-peptidase superfamily: functional convergence after evolutionary divergence.* J Mol Biol, 1999. **292**(1): p. 11-7.

220. Osman, D. and J.S. Cavet, *Bacterial metal-sensing proteins exemplified by ArsR-SmtB family repressors.* Nat Prod Rep, 2010. **27**(5): p. 668-80.

221. McWilliam, H., et al., *Analysis Tool Web Services from the EMBL-EBI.* Nucleic Acids Res, 2013. **41**(Web Server issue): p. W597-600.

222. Pawlik, M.C., et al., *The zinc-responsive regulon of Neisseria meningitidis comprises 17 genes under control of a Zur element.* J Bacteriol, 2012. **194**(23): p. 6594-603.

223. Chillappagari, S., et al., *Copper stress affects iron homeostasis by destabilizing iron-sulfur cluster formation in Bacillus subtilis.* J Bacteriol, 2010. **192**(10): p. 2512-24.

224. Yagi, T., *Bacterial NADH-quinone oxidoreductases.* J Bioenerg Biomembr, 1991. **23**(2): p. 211-25.

225. Perez, N., et al., *Two parallel pathways for ferric and ferrous iron acquisition support growth and virulence of the intracellular pathogen Francisella tularensis Schu S4.* Microbiologyopen, 2016. **5**(3): p. 453-68.

226. Perkins, J. and J. Pero, *Bacillus subtilis and its relatives: from genes to cells*. 2001, American Society for Microbiology, Washington, DC.

227. Fontecave, M. and S. Ollagnier-de-Choudens, *Iron-sulfur cluster biosynthesis in bacteria: Mechanisms of cluster assembly and transfer*. Arch Biochem Biophys, 2008. **474**(2): p. 226-37.

228. Champion, M.D., et al., *Comparative genomic characterization of Francisella tularensis strains belonging to low and high virulence subspecies.* PLoS Pathog, 2009. **5**(5): p. e1000459.

229. LoVullo, E.D., L.A. Sherrill, and M.S. Pavelka, Jr., *Improved shuttle vectors for Francisella tularensis genetics.* FEMS Microbiol Lett, 2009. **291**(1): p. 95-102.

230. LoVullo, E.D., et al., *TetR-based gene regulation systems for Francisella tularensis.* Appl Environ Microbiol, 2012. **78**(19): p. 6883-9.

231. Liu, M.J., et al., *ZIP8 regulates host defense through zinc-mediated inhibition of NF-kappaB.* Cell Rep, 2013. **3**(2): p. 386-400.

232. Crossley, R.A., et al., *Riboflavin biosynthesis is associated with assimilatory ferric reduction and iron acquisition by Campylobacter jejuni.* Appl Environ Microbiol, 2007. **73**(24): p. 7819-25.

233. Sigdel, T.K., J.A. Easton, and M.W. Crowder, *Transcriptional response of Escherichia coli to TPEN.* J Bacteriol, 2006. **188**(18): p. 6709-13.

234. Anderegg, G., et al., *Pyridinderivate als Komplexbildner. XI. Die Thermodynamik der Metallkomplexbildung mit Bis-, Tris-und Tetrakis [(2-pyridyl) methyl]-aminen.* Helvetica Chimica Acta, 1977. **60**(1): p. 123-140.

235. Panina, E.M., A.A. Mironov, and M.S. Gelfand, *Comparative genomics of bacterial zinc regulons: enhanced ion transport, pathogenesis, and rearrangement of ribosomal proteins.* Proceedings of the National Academy of Sciences, 2003. **100**(17): p. 9912-9917.

236. Kohler, S., et al., *The analysis of the intramacrophagic virulome of Brucella suis deciphers the environment encountered by the pathogen inside the macrophage host cell.* Proc Natl Acad Sci U S A, 2002. **99**(24): p. 15711-6.

237. Mohapatra, N.P., et al., *Identification of an orphan response regulator required for the virulence of Francisella spp. and transcription of pathogenicity island genes.* Infect Immun, 2007. **75**(7): p. 3305-14.

238. Twine, S.M., et al., *In vivo proteomic analysis of the intracellular bacterial pathogen, Francisella tularensis, isolated from mouse spleen.* Biochem Biophys Res Commun, 2006. **345**(4): p. 1621-33.

239. Schmidt, C., et al., *FurC regulates expression of zupT for the central zinc importer ZupT of Cupriavidus metallidurans.* J Bacteriol, 2014. **196**(19): p. 3461-71.

240. Grass, G., et al., *ZupT is a Zn(II) uptake system in Escherichia coli.* J Bacteriol, 2002. **184**(3): p. 864-6.

241. Patzer, S.I. and K. Hantke, *The ZnuABC high-affinity zinc uptake system and its regulator Zur in Escherichia coli.* Mol Microbiol, 1998. **28**(6): p. 1199-210.

242. Wilcox, D.E., *Isothermal titration calorimetry of metal ions binding to proteins: An overview of recent studies.* Inorganica Chimica Acta, 2008. **361**(4): p. 857-867.

243. Pasquali, P., et al., *Attenuated Salmonella enterica serovar Typhimurium lacking the ZnuABC transporter confers immune-based protection against challenge infections in mice.* Vaccine, 2008. **26**(27-28): p. 3421-6.

244. Shen, H., W. Chen, and J.W. Conlan, *Mice sublethally infected with Francisella novicida U112 develop only marginal protective immunity against systemic or aerosol challenge with virulent type A or B strains of F. tularensis.* Microbial Pathogenesis, 2004. **37**(2): p. 107-110.

245. Ilari, A., et al., *Salmonella enterica serovar Typhimurium growth is inhibited by the concomitant binding of Zn(II) and a pyrrolyl-hydroxamate to ZnuA, the soluble component of the ZnuABC transporter.* Biochim Biophys Acta, 2016. **1860**(3): p. 534-41.

246. Crosa, L.M., J.H. Crosa, and F. Heffron, *Iron transport in Francisella in the absence of a recognizable TonB protein still requires energy generated by the proton motive force.* Biometals, 2009. **22**(2): p. 337-44.

247. Wang, T., et al., *Type VI Secretion System Transports Zn2+ to Combat Multiple Stresses and Host Immunity.* PLoS Pathog, 2015. **11**(7): p. e1005020.

248. Larsson, P., et al., *Molecular evolutionary consequences of niche restriction in Francisella tularensis, a facultative intracellular pathogen.* PLoS Pathog, 2009. **5**(6): p. e1000472.

249. Jeffares, D.C., et al., *A Beginners Guide to Estimating the Non-synonymous to Synonymous Rate Ratio of all Protein-Coding Genes in a Genome*, in *Parasite Genomics Protocols*, C. Peacock, Editor. 2015, Springer New York: New York, NY. p. 65-90.

250. Qin, A., D.W. Scott, and B.J. Mann, *Francisella tularensis subsp. tularensis Schu S4 disulfide bond formation protein B, but not an RND-type efflux pump, is required for virulence.* Infect Immun, 2008. **76**(7): p. 3086-92.

251. Mortensen, B.L., et al., *Effects of the putative transcriptional regulator IclR on Francisella tularensis pathogenesis.* Infect Immun, 2010. **78**(12): p. 5022-32.

252. Telepnev, M., et al., *Francisella tularensis inhibits Toll-like receptor-mediated activation of intracellular signalling and secretion of TNF-alpha and IL-1 from murine macrophages.* Cell Microbiol, 2003. **5**(1): p. 41-51.

253. Kikuchi, K., K. Komatsu, and T. Nagano, *Zinc sensing for cellular application.* Current Opinion in Chemical Biology, 2004. **8**(2): p. 182-191.

254. Moreau, G.B. and B.J. Mann, *Adherence and uptake of Francisella into host cells.* Virulence, 2013. **4**(8): p. 826-32.

255. Bosio, C.M., H. Bielefeldt-Ohmann, and J.T. Belisle, *Active suppression of the pulmonary immune response by Francisella tularensis Schu4.* J Immunol, 2007. **178**(7): p. 4538-47.

256. Walters, K.A., et al., *Prior infection with Type A Francisella tularensis antagonizes the pulmonary transcriptional response to an aerosolized Toll-like receptor 4 agonist.* BMC Genomics, 2015. **16**: p. 874.

257. Sing, A., et al., *Yersinia V-antigen exploits toll-like receptor 2 and CD14 for interleukin 10-mediated immunosuppression.* J Exp Med, 2002. **196**(8): p. 1017-24.

258. Geijtenbeek, T.B., et al., *Mycobacteria target DC-SIGN to suppress dendritic cell function.* J Exp Med, 2003. **197**(1): p. 7-17.

259. Nigou, J., et al., *Mannosylated lipoarabinomannans inhibit IL-12 production by human dendritic cells: evidence for a negative signal delivered through the mannose receptor.* J Immunol, 2001. **166**(12): p. 7477-85.

260. Confer, A.W. and S. Ayalew, *The OmpA family of proteins: roles in bacterial pathogenesis and immunity.* Vet Microbiol, 2013. **163**(3-4): p. 207-22.

261. Reusch, R.N., *Insights into the structure and assembly of Escherichia coli outer membrane protein A.* Febs j, 2012. **279**(6): p. 894-909.

262. Sugawara, E. and H. Nikaido, *Pore-forming activity of OmpA protein of Escherichia coli.* J Biol Chem, 1992. **267**(4): p. 2507-11.

263. Zakharian, E. and R.N. Reusch, *Outer membrane protein A of Escherichia coli forms temperature-sensitive channels in planar lipid bilayers.* FEBS Lett, 2003. **555**(2): p. 229-35.

264. Torres, A.G. and J.B. Kaper, *Multiple elements controlling adherence of enterohemorrhagic Escherichia coli O157:H7 to HeLa cells.* Infect Immun, 2003. **71**(9): p. 4985-95.

265. Serino, L., et al., *Identification of a new OmpA-like protein in Neisseria gonorrhoeae involved in the binding to human epithelial cells and in vivo colonization.* Mol Microbiol, 2007. **64**(5): p. 1391-403.

266. Pichavant, M., et al., *Outer membrane protein A from Klebsiella pneumoniae activates bronchial epithelial cells: implication in neutrophil recruitment.* J Immunol, 2003. **171**(12): p. 6697-705.

267. Prasadarao, N.V., *Identification of Escherichia coli outer membrane protein A receptor on human brain microvascular endothelial cells.* Infect Immun, 2002. **70**(8): p. 4556-63.

268. Krull, M., et al., *Mechanisms of Chlamydophila pneumoniae-mediated GM-CSF release in human bronchial epithelial cells.* Am J Respir Cell Mol Biol, 2006. **34**(3): p. 375-82.

269. Bevanger, L., J.A. Maeland, and A.I. Naess, *Agglutinins and antibodies to Francisella tularensis outer membrane antigens in the early diagnosis of disease during an outbreak of tularemia.* J Clin Microbiol, 1988. **26**(3): p. 433-7.

270. Nano, F.E., *Identification of a heat-modifiable protein of Francisella tularensis and molecular cloning of the encoding gene.* Microb Pathog, 1988. **5**(2): p. 109-19.

271. Post, D.M.B., et al., *Characterization of Inner and Outer Membrane Proteins from Francisella tularensis Strains LVS and Schu S4 and Identification of Potential Subunit Vaccine Candidates.* MBio, 2017. **8**(5).

272. Fulop, M., R. Manchee, and R. Titball, *Role of two outer membrane antigens in the induction of protective immunity against Francisella tularensis strains of different virulence.* FEMS Immunol Med Microbiol, 1996. **13**(3): p. 245-7.

273. Hickey, A.J., et al., *Identification of Francisella tularensis outer membrane protein A (FopA) as a protective antigen for tularemia.* Vaccine, 2011. **29**(40): p. 6941-7.

274. Savitt, A.G., et al., *Francisella tularensis infection-derived monoclonal antibodies provide detection, protection, and therapy.* Clin Vaccine Immunol, 2009. **16**(3): p. 414-22.

275. Fulop, M., D. Leslie, and R. Titball, *A rapid, highly sensitive method for the detection of Francisella tularensis in clinical samples using the polymerase chain reaction.* Am J Trop Med Hyg, 1996. **54**(4): p. 364-6.

276. Versage, J.L., et al., *Development of a multitarget real-time TaqMan PCR assay for enhanced detection of Francisella tularensis in complex specimens.* J Clin Microbiol, 2003. **41**(12): p. 5492-9.

277. Emanuel, P.A., et al., *Detection of Francisella tularensis within infected mouse tissues by using a hand-held PCR thermocycler.* J Clin Microbiol, 2003. **41**(2): p. 689-93.

278. Turingan, R.S., et al., *Rapid focused sequencing: a multiplexed assay for simultaneous detection and strain typing of Bacillus anthracis, Francisella tularensis, and Yersinia pestis.* PLoS One, 2013. **8**(2): p. e56093.

279. Peng, K., et al., *Elevated AIM2-mediated pyroptosis triggered by hypercytotoxic Francisella mutant strains is attributed to increased intracellular bacteriolysis.* Cell Microbiol, 2011. **13**(10): p. 1586-600.

280. Chong, A., et al., *Structure-Function Analysis of DipA, a Francisella tularensis Virulence Factor Required for Intracellular Replication.* PLoS One, 2013. **8**(6): p. e67965.

281. Qin, A., et al., *Requirement of the CXXC motif of novel Francisella infectivity potentiator protein B FipB, and FipA in virulence of F. tularensis subsp. tularensis.* PLoS One, 2011. **6**(9): p. e24611.

282. De Mot, R. and J. Vanderleyden, *The C-terminal sequence conservation between OmpA-related outer membrane proteins and MotB suggests a common function in both gram-positive and gram-negative bacteria, possibly in the interaction of these domains with peptidoglycan.* Mol Microbiol, 1994. **12**(2): p. 333-4.

283. Cascales, E., et al., *Pal lipoprotein of Escherichia coli plays a major role in outer membrane integrity.* J Bacteriol, 2002. **184**(3): p. 754-9.

284. Clemens, D.L., et al., *Atomic structure of T6SS reveals interlaced array essential to function.* Cell, 2015. **160**(5): p. 940-951.

285. Qin, A., et al., *FipB, an essential virulence factor of Francisella tularensis subsp. tularensis, has dual roles in disulfide bond formation.* J Bacteriol, 2014. **196**(20): p. 3571-81.

286. Thakran, S., et al., *Identification of Francisella tularensis lipoproteins that stimulate the toll-like receptor (TLR) 2/TLR1 heterodimer.* J Biol Chem, 2008. **283**(7): p. 3751-60.

287. Cole, L.E., et al., *Macrophage proinflammatory response to Francisella tularensis live vaccine strain requires coordination of multiple signaling pathways.* J Immunol, 2008. **180**(10): p. 6885-91.

288. Lai, X.H., et al., *Mutations of Francisella novicida that alter the mechanism of its phagocytosis by murine macrophages.* PLoS One, 2010. **5**(7): p. e11857.

289. Schmittgen, T.D. and K.J. Livak, *Analyzing real-time PCR data by the comparative C(T) method.* Nat Protoc, 2008. **3**(6): p. 1101-8.